SEISMIC FRAGILITY ESTIMATES AND SENSITIVITY ANALYSES FOR CORRODING REINFORCED CONCRETE BRIDGES

A Dissertation

by

DO-EUN CHOE

Submitted to the Office of Graduate Studies of
Texas A&M University
in partial fulfillment of the requirements for the degree of

DOCTOR OF PHILOSOPHY

December 2007

Major Subject: Civil Engineering

SEISMIC FRAGILITY ESTIMATES AND SENSITIVITY ANALYSES FOR CORRODING REINFORCED CONCRETE BRIDGES

A Dissertation

by

DO-EUN CHOE

Submitted to the Office of Graduate Studies of
Texas A&M University
in partial fulfillment of the requirements for the degree of

DOCTOR OF PHILOSOPHY

Approved by:

Chair of Committee,	Paolo Gardoni
Committee Members,	David V. Rosowsky
	Joseph M. Bracci
	Michael Sherman
Head of Department,	David V. Rosowsky

December 2007

Major Subject: Civil Engineering

ABSTRACT

Seismic Fragility Estimates and Sensitivity Analyses for Corroding Reinforced Concrete Bridges. (December 2007)

Do-Eun Choe, B.S., Inha University; M.S., Inha University

Chair of Advisory Committee: Dr. Paolo Gardoni

The objective of this study is to develop methodologies to estimate and predict the fragility of deteriorating reinforced concrete (RC) bridges, and to identify the effect of design and construction parameters on the reliability of RC bridges over time to assist in the design and construction process.

To accurately estimate the fragility of deteriorating bridge, probabilistic capacity and demand models are developed. In addition, to simplify the calculation cost maintaining accuracy, fragility increment functions are developed. The proposed fragilities account for model uncertainties in the structural capacity, demand models, corrosion models. Furthermore, proper account is made of the uncertainties in the environmental conditions, material properties, and structural geometry. To identify the effect of design and construction parameters on the reliability of RC bridges, a sensitivity and importance analysis is conducted. Sensitivity analysis for an example bridge subject to corrosion is carried out to identify which parameters have the largest impact on the reliability over time. This dissertation considers different combinations of chloride exposure condition, environmental oxygen availability, water-to-cement ratios,

and curing conditions, which affect the reliability of bridges over time. The developed models are applicable to both existing and new RC bridges and may be employed for the prediction of service-life and life-cycle cost analysis of RC bridges.

DEDICATION

To my husband Sanyun Shim

ACKNOWLEDGEMENTS

I would like to thank my committee chair, Dr. Gardoni and my committee member Dr. Rosowsky, who have advised and supported throughout the course of this research. I would like to thank my committee members, Dr. Sherman and Dr. Bracci for their guidance and support.

Thanks also go to my friends and colleagues and the department faculty and staff for making my time at Texas A&M University a great experience. I also want to extend my gratitude to Dr. Haukaas who supported developing computational works.

Finally, thanks to my mother and father for their encouragement and to my husband for his patience and love.

TABLE OF CONTENTS

Page

Page

Page

LIST OF FIGURES

Page

Page

Page

Page

LIST OF TABLES

Page

Page

CHAPTER I

INTRODUCTION

Overview

Reinforced concrete (RC) structures in the United States are aging and deteriorating due to harsh environmental exposure conditions. Throughout their life cycle, reinforced concrete structures are affected by corrosion more than by any other natural phenomenon including earthquakes and hurricanes. Even when corrosion does not lead to the direct failure of a structure, it may weaken a structure, making it significantly more vulnerable to earthquakes. A structure originally designed meeting code specifications may not meet them once corrosion starts.

In particular, bridges are among the structures most vulnerable to corrosion. De-icing and anti-icing salts can cause or accelerate corrosion in the deck while exposure to marine water is a common cause of corrosion of columns and the area underneath the deck. Approximately 60,000 bridges are considered structurally deficient due to corrosion of the reinforcement and the annual direct costs to repair these deficient bridges are estimated to be billions (Koch et al., 2001). The indirect costs to the user, such as traffic delays and lost productivity, are estimated to be up to 10 times the direct cost. Similar, but more alarming, estimates are given by other authors (Aktan et al., 1996; Dunker and Rabbat, 1993; Armaghani and Bloomquist, 1993). As a specific

---

This dissertation follows the style and form of *Journal of Engineering Mechanics*, *ASCE.*

example, the cost of repairing corrosion-related damage to a 10-year old bridge in the Florida Keys was nearly 25% as much as the original construction cost. The magnitude of the problem has also been emphasized by the federal government, FHWA, and other agencies, encouraging the development of new solutions (Dunker and Rabbat, 1993; Clinton and Gore, 1993).

An accurate assessment of the seismic performance of corroding structures will protect public safety as well as save the nation several billion dollars. By predicting the reliability over time, bridge owners will have the ability to make an informed decision to retrofit deteriorating bridges by implementing retrofitting strategies and/or corrosion protection strategies such as chloride extraction (Marcotte, Hansson, and Hope, 1999a,b; Ihekwaba, Hope and Hansson, 1996), protective coatings (Babei and Hawkins, 1988), and cathodic protection (Berkeley and Pathmanaban, 1990).

However, it has been difficult to predict the seismic vulnerability of deteriorating RC bridges due to the uncertainties in the corrosion process, the structural properties, and the demands on the structures due to an impending earthquake.

Scope

This research develops probabilistic capacity and demand models given an earthquake ground motion for deteriorating RC bridges. The models employ a probabilistic corrosion initiation model for the reinforcement and a time-dependent corrosion rate function. It is emphasized that the deterioration models incorporate uncertainties both in

the structural properties and the material deterioration processes. This is significant because of the presence of considerable uncertainty in these constituents.

The increasing fragility over time of corroding reinforced concrete (RC) bridge columns is modeled as a function of time using fragility increment functions for given deformation and shear demands. Seismic increment functions are developed for deteriorating RC bridges given an earthquake spectral acceleration. These functions can be applied to various environmental and material conditions by means of controlling parameters that corresponds to the specific conditions. The developed increment function accounts for the effects of the time-dependent uncertainties that are present in the corrosion model as well as in the structural capacity models.

Background and Objectives

Gardoni et al. (2002) developed probabilistic capacity models for pristine RC columns with circular cross section using a Bayesian updating framework (Box and Tiao, 1992). The models properly account for all the prevailing uncertainties, including model error arising from potential inaccuracies in the model form and potentially missing variables, as well as measurement errors and statistical uncertainty. In this study, the models developed by Gardoni et al. (2002) are updated using newly available data to extend the range of applicability of the models. In addition, closed-forms of the probabilistic models are derived to reduce computational costs.

In recent decades, significant research efforts have been devoted to the quantification and inclusion of corrosion in design, construction and maintenance of RC

structures. Tuutti (1982) and Liu and Weyers (1998) suggested deterministic corrosion models for RC reinforcement, while Thoft-Christensen *et al*. (1997) and Dura-Crete (2000) presented probabilistic models for the deterioration process. Stewart and Rosowsky (1998), Vu and Stewart (2000), Enright and Frangopol (1998a, 1998b) developed probabilistic corrosion models for bridge slabs, beams and girders by extending commonly employed RC capacity models. This dissertation further extends these developments by constructing deterioration models that incorporate both probabilistic models for the drift and shear capacity of RC columns and probabilistic models for the deterioration process.

Gardoni et al. (2003) developed probabilistic demand models for pristine (not corroding) bridges by employing deterministic demand models used in practice as a starting point. For this study, probabilistic demand models of deteriorating RC bridge systems are developed based on the previous models by Gardoni et al. (2003). Seismic fragility estimation and sensitivity analysis for deteriorating RC bridge systems are carried out, combining the new demand models for deteriorated RC bridge systems with the developed capacity models.

Several studies tried to assess the reliability of deteriorating bridges. Clifton and Knab (1989) suggested a deterioration function to model the material deterioration of underground concrete structures. Mori and Ellingwood (1993) used the material deterioration function developed by Clifton and Knab (1989) and introduced a function that describes the loss of structural capacity to compute the time-varying reliability of RC bridges. However, while introducing the concept of a deterioration function, they

did not assess its parameters. Enright and Frangopol (1998a) assessed a deterioration function for the loss of flexural strength due to corrosion for a specific set of environmental and material conditions. However, the formulation cannot be used for different environmental and material conditions and the parameters are specific to the considered structure. The developed model was used by Enright and Frangopol (1998b) to investigate the effects of the structural deterioration on the time-variant reliability of bridge beams. However, their formulation does not account for the increasing uncertainty over time that is accounted for in this research. Li and Melchers (2005) developed a deterioration function as a stochastic process with a mean function and a coefficient of variation function. While considering the increasing uncertainty of the capacity degradation over time, the reliability analysis neglected the increasing uncertainty. Furthermore, the function developed by Li and Melchers is still limited to specific material and environmental conditions. For this study, fragility increment functions for deteriorating RC structure given demands are developed. In addition, it provides the fragility increment functions given earthquakes intensity, S_a. The functions consider the growing uncertainties with corrosion propagation, and are applicable to different environmental and material conditions. The function considers increasing uncertainties both in capacity and demand models with corrosion process.

Organization of Dissertation

The dissertation is composed of the following four chapters, each containing a journal paper. Each of the following chapters contains one of the journal papers.

In Chapter II, a model updating and sensitivity analysis for pristine RC columns is conducted. This study is performed to first update existing capacity models for pristine bridge developed by Gardoni et al. (2002) with new data. Also an importance and sensitivity analyses is conducted to understand the contribution of each variable. The title of the corresponding paper is "Closed-form Fragility Estimates Parameter Sensitivity and Bayesian Updating for RC Columns" and was published in the *Journal of Engineering Mechanics ASCE*, 133 (7).

In Chapter III, probabilistic capacity models for deteriorating RC bridge columns are developed. The updated capacity models for pristine columns in Chapter 2 are used to develop new models for deteriorating RC column using a probabilistic model of the corrosion initiation time and propagation. The corresponding paper titled "Probabilistic Capacity Models and Seismic Fragility Estimates for RC Columns Subject to Corrosion" was published online in the journal *Reliability Engineering & System Safety*, (doi:10.1016/j.ress.2006.12.015.).

In Chapter IV, probabilistic demand models for deteriorating RC bridges are developed for given earthquake intensity. The developed capacity and demand models are combined to assess the fragility of corroding RC bridges. The corresponding paper titled "Seismic Fragility Estimates for Reinforced Concrete Bridges Subject to Corrosion" was submitted to *Structural Safety.*

In Chapter V, fragility increment functions for deteriorating RC bridge columns are developed using the fragility data obtained by the capacity models presented in

Chapter III. The corresponding paper titled “Fragility Increment Function of Corroding Reinforced Concrete Bridge Columns” is currently under preparation for submission.

Chapter VI contains the overall summary and conclusions of the report.

CHAPTER II*

CLOSED-FORM FRAGILITY ESTIMATES, PARAMETER SENSITIVITY AND BAYESIAN UPDATING FOR RC COLUMNS

Reinforced concrete (RC) columns are the most critical components in bridges under seismic excitation. In this chapter, a simple closed-form formulation to estimate the fragility of RC columns is developed. The formulation is used to estimate the conditional probability of failure of an example column for given shear and deformation demands. The estimated fragilities are as accurate as more sophisticated estimates (i.e., predictive fragilities) and do not require any reliability software. A sensitivity analysis is carried out to identify to which parameter(s) the reliability of the example column is most sensitive. The closed-form formulation uses probabilistic capacity models. A Bayesian procedure is presented to updated existing probabilistic models with new data. The model updating process can incorporate different types of information, including laboratory test data, field observations, and subjective engineering judgment, as they become available.

Introduction

Fragility curves can be used to quantify the seismic vulnerability of structures in terms of the conditional probability of attaining or exceeding a specified damage state for a

* Reprinted with permission from "Closed-form Fragility Estimates Parameter Sensitivity and Bayesian Updating for RC Columns" by Choe, D., Gardoni, P., and Rosowsky, D., 2007. Journal of Engineering Mechanics ASCE, 133 (7), 833-843, Copyright [2007] ASCE.

given set of demand variables. In this chapter, I (a) develop approximate closed-form estimates of the fragilities of RC columns subjected to shear and deformation demands; (b) carry out a sensitivity analysis to identify to which parameter(s) the reliability of an example column is most sensitive; (c) present a Bayesian formulation that can be used to update existing probabilistic models with newly available data.

An approach to estimate fragility curves must be both accurate and easily applied to both existing and new structures. The proposed closed-form approximations are as accurate as more sophisticated estimates (i.e., predictive fragilities) and can be conveniently used in practice without the need for any specialized reliability software. As an application, I develop fragility curves for an example RC column with geometry and material properties that are representative of RC highway bridge columns currently built in California (Naito, 2000). A sensitivity analysis is carried out to identify to which parameter(s) the reliability of the example column is most sensitive. Measures of sensitivity can be used for optimal design and resource allocation, and provide insight into the physics of the problem.

Key inputs in the proposed formulation are probabilistic capacity models. In this chapter, I present a Bayesian formulation that can be used to update existing models with newly available data. In principle, a probabilistic model is applicable only within the ranges of the data used to assess the model. The range of applicability of an updated model may be expanded if any of the new data fall outside the original ranges. In addition, the statistical uncertainty in the estimated values of the model parameters can

be reduced by using more data to estimate the model parameter. This model updating process can incorporate different types of information as they become available.

In this chapter, I use this Bayesian approach to update probabilistic models for shear and deformation capacity. The updated models can be conveniently used in practice, are unbiased, and account for the most relevant uncertainties including those that are aleatory and those that are epistemic in nature. The updated models are used to estimate the fragility of the example RC column.

Probabilistic Capacity Models

In this research, a "model" is a mathematical expression that relates one or more quantities of interest, e.g., the capacities of a structural component, to a set of measurable variables $\mathbf{x} = (x_1, x_2, \ldots)$, e.g., material property constants, member dimensions, imposed boundary conditions. I use models to predict the quantities of interest based on the deterministic or random values of the variables $\mathbf{x}$. I call a model uni-variate when only one quantity is to be predicted (e.g., only shear or only deformation capacity) and bi-variate when two quantities are to be predicted (e.g., shear and deformation capacity).

A uni-variate capacity model has the general form

$$C = C(\mathbf{x}, \boldsymbol{\Theta}) \tag{2-1}$$

where $\boldsymbol{\Theta}$ denotes a set of parameters introduced to fit the model to observed data and C is the capacity quantity of interest. The function $C(\mathbf{x}, \boldsymbol{\Theta})$ can have a general form involving algebraic expressions, integrals or differentials. Ideally, it should be derived

from first principles, e.g., the rules of mechanics. In order to facilitate the use of probabilistic models in practice, Gardoni *et al.* (2002) suggest developing $C(\mathbf{x},\boldsymbol{\Theta})$ based on commonly accepted deterministic models and an additive correction term. Accordingly, the general form of a uni-variate model can be written as

$$C(\mathbf{x},\boldsymbol{\Theta}) = \hat{c}(\mathbf{x}) + \gamma(\mathbf{x},\boldsymbol{\theta}) + \sigma\varepsilon \tag{2-2}$$

where $\boldsymbol{\Theta} = (\boldsymbol{\theta},\sigma)$ denotes the set of unknown model parameters, $\boldsymbol{\theta} = (\theta_1,\theta_2,\ldots)$, $\hat{c}(\mathbf{x})$ is a selected deterministic model, $\gamma(\mathbf{x},\boldsymbol{\theta})$ (Greek gamma) is a correction term for the bias inherent in the deterministic model that is expressed as a function of the variables $\mathbf{x}$ and parameters $\boldsymbol{\theta}$, ε is a random variable with zero mean and unit variance, and σ represents the standard deviation of the model error. Note that for given $\mathbf{x}$, $\boldsymbol{\theta}$ and σ, I have $\mathrm{Var}[C(\mathbf{x},\boldsymbol{\Theta})] = \sigma^2$ as the variance of the model.

In formulating the model, it is convenient to use a suitable transformation of the physical quantity of interest to justify the following assumptions: (a) the model variance σ^2 is independent of $\mathbf{x}$ (homoskedasticity assumption), and (b) ε follows a normal distribution (normality assumption). One can explore which transformation is most appropriate by checking diagnostic plots of the data or the residuals against model predictors or individual regresses (Rao and Toutenburg, 1997).

The true form of the correction term $\gamma(\mathbf{x},\boldsymbol{\theta})$ is in general unknown. In order to explore the potential sources of bias in $\hat{c}(\mathbf{x})$, I select a suitable set of p "explanatory" basis functions $h_i(\mathbf{x})$, $i = 1,\ldots,p$, and express the bias correction term as

$$\gamma(\mathbf{x},\boldsymbol{\theta}) = \sum_{i=1}^{p} \theta_i h_i(\mathbf{x}) \tag{2-3}$$

Note that in this expression $\gamma(\mathbf{x},\boldsymbol{\theta})$ is a linear function in the parameters θ_i, but not necessarily linear in the basic variables $\mathbf{x}$. To facilitate the use in practice of the probabilistic model, $\gamma(\mathbf{x},\boldsymbol{\theta})$ needs to have as few parameters θ_i as possible. Also, from a statistical standpoint, a parsimonious parameterization helps avoid (a) loss of precision of the estimates and of the model due to inclusion of unimportant predictors and (b) overfit of the data. I can identify which explanatory function is significant in correcting the deterministic model by examining the posterior statistics of the unknown parameters θ_i.

Similarly to Eq. (2-2), a bi-variate capacity models can be formulated as

$$C_k(\mathbf{x},\boldsymbol{\theta}_k,\boldsymbol{\Sigma}) = \hat{c}_k(\mathbf{x}) + \gamma_k(\mathbf{x},\boldsymbol{\theta}_k) + \sigma_k\varepsilon_k, \qquad k = 1, 2 \tag{2-4}$$

where

$$\gamma_k(\mathbf{x},\boldsymbol{\theta}_k) = \sum_{i=1}^{p_k} \theta_{ki} h_{ki}(\mathbf{x}), \qquad k = 1, 2 \tag{2-5}$$

In the above expressions $\boldsymbol{\Sigma}$ denotes the covariance matrix of the variables $\sigma_k\varepsilon_k$, $k = 1, 2$, and all other entries have the same definitions as for the uni-variate model. The set of unknown parameters of the bi-variate model is $\boldsymbol{\Theta} = (\boldsymbol{\theta}, \boldsymbol{\Sigma})$, where $\boldsymbol{\theta} = (\boldsymbol{\theta}_1, \boldsymbol{\theta}_2)$ and $\boldsymbol{\theta}_k = (\theta_{k1}, \ldots, \theta_{kp_k})$. Considering symmetry, $\boldsymbol{\Sigma}$ includes two unknown variances σ_k^2, $k = 1, 2$, and one unknown correlation coefficient ρ.

Gardoni *et al.* (2002) use the formulation described above to develop three probabilistic models: a uni-variate deformation capacity model, a uni-variate shear

capacity model, and a bi-variate deformation-shear capacity model. The probabilistic models are assessed using data from 106 experimental tests on RC columns under the effect of repeated cyclic loading. Based on the posterior statistics of the unknown parameters, the most parsimonious form of the deformation capacity model is

$$\ln[d(\mathbf{x},\boldsymbol{\Theta}_d)] = \ln[\hat{d}(\mathbf{x})] + \gamma_d(\mathbf{x},\boldsymbol{\theta}_d) + \sigma_d\varepsilon_d \tag{2-6}$$

where $d = \Delta / H$ is the drift ratio capacity, Δ is the displacement capacity, H is the clear column height, and $\boldsymbol{\Theta}_d = (\boldsymbol{\theta}_d, \sigma_d)$, where $\boldsymbol{\theta}_d = (\theta_{d1}, \theta_{d7}, \theta_{d11})$. The deterministic model $\hat{d}(\mathbf{x})$ is defined following common practice (e.g., Priestley *et al.*, 1996) by decomposing the displacement capacity into two components: the elastic component due to the onset of yield, and the inelastic component due to the plastic flow.

Similarly, the most parsimonious form of the shear capacity model is

$$\ln[v(\mathbf{x},\boldsymbol{\Theta}_v)] = \ln[\hat{v}(\mathbf{x})] + \gamma_v(\mathbf{x},\boldsymbol{\theta}_v) + \sigma_v\varepsilon_v \tag{2-7}$$

where $v = V/(A_g f_t')$ (lower case vee) is the normalized shear capacity, V is the shear capacity, A_g is the gross cross-sectional area, $f_t' = 0.5\sqrt{f_c'}$ is the tensile strength of concrete in units of MPa, f_c' is the compressive strength of concrete in units of MPa, and $\boldsymbol{\Theta}_v = (\boldsymbol{\theta}_v, \sigma_v)$, where $\boldsymbol{\theta}_v = (\theta_{v2}, \theta_{v4})$. The deterministic model $\hat{v}(\mathbf{x})$ is taken to be a refinement of the FEMA 273 (1997) model proposed by Moehle *et al.* (1999, 2000). This model accounts for the reduction in the shear strength due to the effects of flexural stress and redistribution of internal forces as cracking develops. The bi-variate model

uses the same explanatory functions but also accounts for the correlation between ε_d and ε_v.

Table 2-1. Ranges of the variables from the database considered in Gardoni et al. (2002, ASCE) (A) and when including the new additional data (B)

Variable	Symbol	Range (A)	Range (B)
Compressive strength of concrete [MPa]	f_c'	18.9 – 42.2	18.9 – 69.6
Yield stress of longitudinal steel [MPa]	f_y	240 – 508	240 – 565
Ultimate strength of longitudinal steel [MPa]	f_{su}	360 – 761	360 – 821
Yield stress of transverse steel [MPa]	f_{yh}	207 – 607	200 – 692
Longitudinal reinforcement ratio [%]	ρ_l	0.530 – 5.50	0.530 – 5.50
Volumetric transverse reinforcement ratio [%]	ρ_s	0.170 – 3.23	0.098 – 3.23
Slenderness ratio	H / D_g	1.09 – 10.0	1.09 – 10.0
Ratio of gross to core diameters	D_g / D_c	1.07 – 1.34	1.07 – 1.41
Axial load ratio	$4P / \pi D_g^2 f_c'$	0.000 – 0.700	0.000 – 0.700

Limitations of the Probabilistic Capacity Models

Probabilistic models are in principle applicable only within the ranges of the data used to assess the models or, at least, within the ranges of the explanatory functions $h_i(\mathbf{x})$ used

to correct for the bias. Table 2-1 lists the ranges of the important variables for the columns considered in Gardoni *et al.* (2002). In this table, P represents the applied constant axial load, and D_g and D_c are the gross and core column diameters, respectively.

Table 2-2. Ranges of the explanatory functions based on the data from the database considered (A) and when including the new additional data (B)

Description		Symbol		Range
Deformation Model	Effect of idealized elastic-perfectly plastic shear force	$h_{d,7} = 4V_I/(\pi D_g^2 f')$	(A)	0.114 – 2.05
			(B)	0.114 – 2.05
	Effect of confining transverse reinforcement and core size	$h_{d,8} = \rho_s (f_{yh}/f_c')(D_c/D_g)$	(A)	0.020 – 0.344
			(B)	0.008 – 0.344
	Effect of ultimate longitudinal compressive strain	$h_{d,11} = \varepsilon_{cu}$	(A)	0.008 – 0.049
			(B)	0.006 – 0.049
Shear Model	Contribution of longitudinal steel	$h_{v,2} = \rho_l$	(A)	0.005 – 0.055
			(B)	0.005 – 0.055
	Contribution from the transverse steel	$h_{v,4} = A_v f_{yh} D_g/(A_g f_t' S)$	(A)	0.129 – 2.44
			(B)	0.052 – 2.44

Table 2-2 lists the ranges of all the explanatory functions that are used to correct for the bias in the probabilistic capacity models. In this table, $V_I = M_I/H$ is the idealized elastic-perfectly plastic shear force, A_v is the total area in a layer of the

transverse reinforcement in the direction of the shear force, and S is the longitudinal spacing of the hoops or spirals.

In addition, the accuracy of the estimates of the model parameters $\boldsymbol{\Theta}$ depends on the sample size of observations used to assess the model. The smaller is the sample size, the larger is the uncertainty in the estimated values of the parameters. This type of uncertainty, called *statistical uncertainty*, can be measured in terms of the estimated variances of the parameters. Statistical uncertainty is epistemic in nature and can be reduced by using more data to estimate the model parameters.

Bayesian Model Updating

In this section, I present a Bayesian formulation to update existing probabilistic models with newly acquired data. As an application, I update the models previously developed by Gardoni *et al*. (2002) using additional data.

In the Bayesian approach, the unknown parameters $\boldsymbol{\Theta}$ are estimated by use of the updating rule (Box and Tiao, 1992)

$$f(\boldsymbol{\Theta}) = \kappa L(\boldsymbol{\Theta}|\mathbf{y})\, p(\boldsymbol{\Theta}) \tag{2-8}$$

where $p(\boldsymbol{\Theta})$ is the prior distribution reflecting our state of knowledge about $\boldsymbol{\Theta}$ based on our past experience, engineering judgment or previous models, $L(\boldsymbol{\Theta}\,|\,\mathbf{y})$ is the likelihood function representing the objective information on $\boldsymbol{\Theta}$ contained in a set of observations $\mathbf{y}$, $\kappa = [\int L(\boldsymbol{\Theta}\,|\,\mathbf{y})\, p(\boldsymbol{\Theta})\, d\boldsymbol{\Theta}]^{-1}$ (Greek kappa) is a normalizing factor, and $f(\boldsymbol{\Theta})$ is the posterior distribution representing our updated state of knowledge about $\boldsymbol{\Theta}$. The

distribution $f(\boldsymbol{\Theta})$ incorporates both the previous information about $\boldsymbol{\Theta}$ included in $p(\boldsymbol{\Theta})$ and the new data included in $L(\boldsymbol{\Theta} \mid \mathbf{y})$. Once the posterior distribution of $\boldsymbol{\Theta}$ is determined, I can compute its mean vector, $\mathbf{M}_{\boldsymbol{\Theta}}$, and covariance matrix, $\boldsymbol{\Sigma}_{\boldsymbol{\Theta}\boldsymbol{\Theta}}$.

Application of the rule in Eq. (2-8) can be repeated to update our present state of knowledge every time new knowledge becomes available. For example, if an initial sample of observations, $\mathbf{y}_1$, is originally available, Eq. (2-8) can be written as

$$p\left(\boldsymbol{\Theta}|\mathbf{y}_1\right) \propto p\left(\boldsymbol{\Theta}\right) L\left(\boldsymbol{\Theta}|\mathbf{y}_1\right) \tag{2-9}$$

If a second sample of observations, $\mathbf{y}_2$, distributed independently of the first sample, becomes available, I can update $p(\boldsymbol{\Theta} \mid \mathbf{y}_1)$ with the new information using Eq. (2-8) where $p(\boldsymbol{\Theta} \mid \mathbf{y}_1)$ is now the prior distribution

$$\begin{aligned} p\left(\boldsymbol{\Theta}|\mathbf{y}_1,\mathbf{y}_2\right) &\propto p\left(\boldsymbol{\Theta}\right) L\left(\boldsymbol{\Theta}|\mathbf{y}_1\right) L\left(\boldsymbol{\Theta}|\mathbf{y}_2\right) \\ &\propto p\left(\boldsymbol{\Theta}|\mathbf{y}_1\right) L\left(\boldsymbol{\Theta}|\mathbf{y}_2\right) \end{aligned} \tag{2-10}$$

From Eq. (2-10) follows that the posterior distribution $p(\boldsymbol{\Theta} \mid \mathbf{y}_1, \mathbf{y}_2)$ does not depend on the order in which $\mathbf{y}_1$ and $\mathbf{y}_2$ are collected. If $\mathbf{y}_2$ is observed before $\mathbf{y}_1$, the posterior distribution $p(\boldsymbol{\Theta} \mid \mathbf{y}_1, \mathbf{y}_2)$ is the same as if $\mathbf{y}_1$ is observed before $\mathbf{y}_2$ and as if $\mathbf{y}_1$ and $\mathbf{y}_2$ are observed both at the same time.

The same updating process can be repeated any number of times. If I have m independent samples of observations, the posterior distribution can be updated after each new sample becomes available. The likelihood associated with the q-th sample updates

the posterior distribution of $\boldsymbol{\Theta}$ that accounts for the information content of the previous $q-1$ samples. Mathematically, I can write

$$p\left(\boldsymbol{\Theta}\middle|\mathbf{y}_1,\ldots,\mathbf{y}_q\right) \propto p\left(\boldsymbol{\Theta}\middle|\mathbf{y}_1,\ldots,\mathbf{y}_{q-1}\right) L\left(\boldsymbol{\Theta}\middle|\mathbf{y}_q\right) \qquad q=2,\ldots,m \tag{2-11}$$

where $p(\boldsymbol{\Theta}\,|\,\mathbf{y}_1)$ is given as in Eq. (2-9). Repeated applications of Bayes' theorem can then be seen as a learning process, where our present knowledge about the unknown parameters $\boldsymbol{\Theta}$ is updated, as new data become available.

Additional Experimental Data

As an application of this Bayesian formulation, I update the models previously developed by Gardoni *et al*. (2002) using additional data. The new data are available at the World Wide Web site http://www.ce.washington.edu/~peera1/, where references to the original publications for each tested column are listed. Among the available data, I consider the experiments on the following 26 columns: 136-138, 141-145, 147-155, 157-158, 160, 161, 164, and 165. Columns 136, 137, 141, 142, 147, 149-152, and 158 provide lower bound data (also called censored data) where the observed capacities are lower bounds to the true capacities. Columns 138, 143-145, 148, 153-157, 160, 161, 164, and 165 provide equality data; the observed capacities are measured at the instant when the columns fail. Formulations of the likelihood function based on equality and lower bound data can be found in Gardoni *et al.* (2002).

Table 1-1 shows a comparison between the ranges of the basic variables used in Gardoni *et al.* (2002) and the new updated ranges based on the new and the old data sets.

Table 2-2 shows a similar comparison for the explanatory functions used in the deformation and shear models.

Updated Models

Table 2-3 lists the updated posterior statistics of the parameters $\boldsymbol{\Theta}_d = (\theta_{d1}, \theta_{d2}, \theta_{d11}, \sigma_d)$ for the deformation capacity model. The estimates now include the information content of the new additional data. The updated posterior means of θ_{d1}, θ_{d2}, and θ_{d11} are similar to the ones estimated based on the original dataset. The posterior variances are smaller, indicating a reduction of the statistical uncertainty in the model. The updated standard deviation of the model error ($\sigma = 0.402$) is higher than the one based on the original 106 data points ($\sigma = 0.383$) due to the fact that the model has the same flexibility to fit the data (same number of parameters) but 26 more data points to accommodate.

Table 2-3. Updated posterior statistics of the parameters in the deformation model

$\boldsymbol{\Theta}_d$	Mean	Standard deviation	Correlation coefficient			
			θ_{d1}	θ_{d7}	θ_{d11}	σ_d
θ_{d1}	0.675	0.105	1			
θ_{d7}	0.631	0.133	–0.27	1		
θ_{d11}	–57.5	10.1	–0.65	–0.39	1	
σ_d	0.400	0.045	0.39	–0.06	–0.13	1

Similarly, Table 2-4 lists the updated posterior statistics of the parameters $\boldsymbol{\Theta}_v = (\theta_{v2}, \theta_{v4}, \sigma_v)$ for the shear capacity model. As noted for the updated deformation models, the updated posterior means of θ_{v2}, and θ_{v4} are similar to the ones estimated based on the original dataset, the posterior variances are smaller, and the updated standard deviation of the model error ($\sigma = 0.185$) is higher than the one based on the original 106 data points ($\sigma = 0.153$).

Table 2-4. Updated posterior statistics of the parameters in the shear model

$\boldsymbol{\Theta}_v$	Mean	Standard deviation	Correlation coefficient		
			θ_{v2}	θ_{v4}	σ_v
θ_{v2}	18.3	1.45	1		
θ_{v4}	–0.470	0.078	–0.87	1	
σ_v	0.185	0.018	–0.04	–0.02	1

Table 2-5 lists the updated posterior statistics of the parameters $\boldsymbol{\Theta} = (\boldsymbol{\theta}_d, \sigma_d, \boldsymbol{\theta}_v, \sigma_v, \rho)$. As expected, the estimates of $\boldsymbol{\theta}_d$, $\boldsymbol{\theta}_v$, σ_d, and σ_v are nearly the same as the corresponding estimates for the individual models. The negative sign of the posterior estimate of ρ shows that the error terms in the deformation and shear capacities are negatively correlated. This means that when the error in the deformation model is positive, the shear model tends to have a negative error term, and vice versa.

Table 2-5. Updated posterior statistics of the parameters in the bi-variate deformation-shear model

	θ_{d1}	θ_{d7}	θ_{d11}	σ_d	θ_{v2}	θ_{v4}	σ_v	ρ
Mean	0.597	0.787	–56.437	0.415	17.039	–0.446	0.196	–0.463
Standard deviation	0.116	0.179	11.071	0.048	1.519	0.081	0.019	0.152
				Correlation coefficients				
θ_{d7}	–0.40							
θ_{d11}	–0.60	–0.34						
σ_d	–0.02	0.17	0.09					
θ_{v2}	0.00	–0.02	0.04	–0.05				
θ_{v4}	0.06	–0.14	0.03	0.05	–0.84			
σ_v	0.09	0.03	–0.11	0.15	–0.12	0.12		
ρ	0.15	–0.22	0.03	–0.09	0.13	0.00	–0.10	

Fig. 2-1 shows a comparison between the measured and predicted values of the drift ratio capacities for the test columns based on the deterministic (left chart) and the probabilistic models (right chart). For the probabilistic model, I show the median predictions ($\varepsilon = 0$). The failure data are shown as dots and the censored data are shown as triangles. For a perfect model, the failure data should line up along the 1:1 dashed line and the censored data should lie above it. The deterministic model on the left is strongly biased on the conservative side since most of the failure and many of the censored data lie below the 1:1 line. The probabilistic model on the right clearly corrects this bias. Using the median prediction from the probabilistic model, most of the censored data are above the 1:1 line (with the exception of a few of them that lie close to it) and the failure data are more equally distributed around the 1:1 line (approximately

half above and half below).

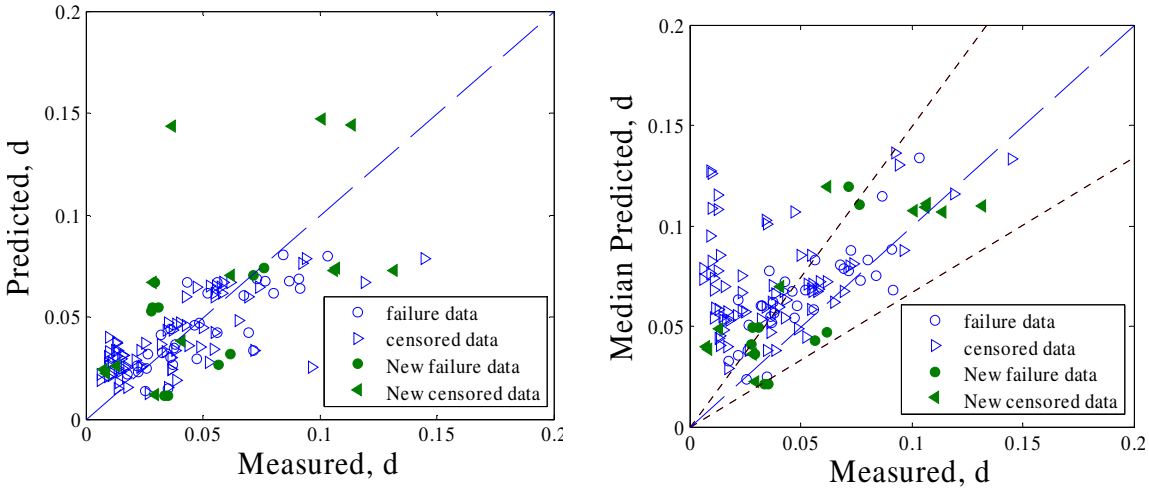

Fig. 2-1. Comparison between measured and predicted drift ratio capacities based on deterministic (left) and probabilistic (right) models

The dotted lines in the right figure delimit the region within 1 standard deviation of the median. I note that the majority of the failure data points fall within 1 standard deviation limits and that most of the censored data points are above the 1:1 line. While the conservatism inherent in the deterministic deformation capacity model might be appropriate for a traditional design approach, in order to assess the vulnerability of a structure I need unbiased estimates of the capacity. The constructed probabilistic model is unbiased and properly accounts for all the prevailing uncertainties.

Fig. 2-2 shows a comparison between the measured and predicted values of the normalized shear capacities for the test columns based on the deterministic (left chart) and probabilistic (right chart) shear capacity models. The same definitions as in Fig. 2-1

apply. I can see that the deterministic model on the left is strongly biased on the conservative side. The probabilistic model on the right corrects this bias.

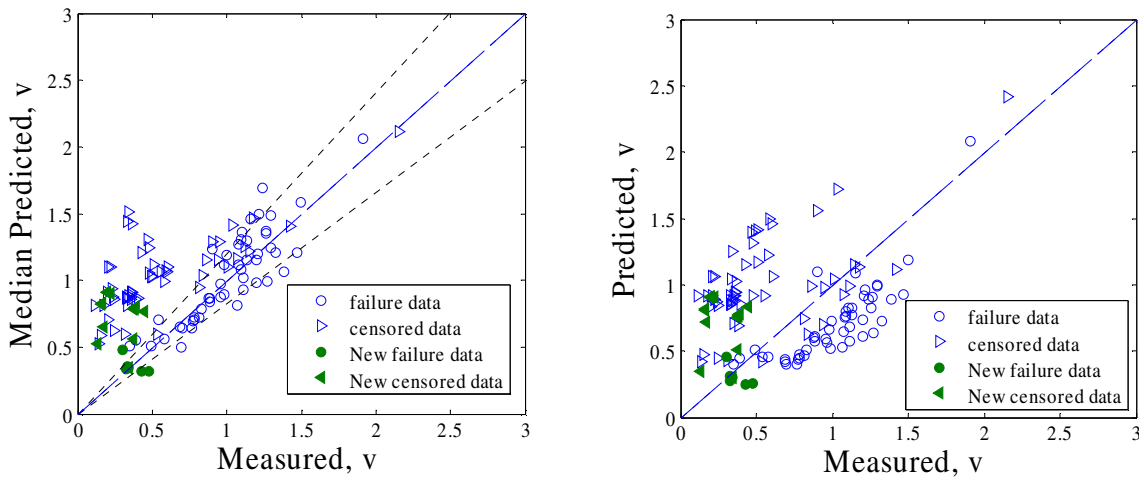

Fig. 2-2. Comparison between measured and predicted shear capacities based on deterministic (left) and probabilistic (right) models

Component Fragility and Measures of Sensitivity and Importance

With the updated capacity models I can estimate the deformation fragility, shear fragility, and deformation-shear fragility functions for RC circular columns. For a structural component, fragility is defined as the conditional probability of attaining or exceeding prescribed *limit states* for a given set of boundary variables. Following the conventional notation in structural reliability theory (e.g., Ditlevsen and Madsen, 1996), I can define a *limit state function* $g_k(\mathbf{x},\boldsymbol{\Theta})$ such that the event $\{g_k(\mathbf{x},\boldsymbol{\Theta}) \le 0\}$ denotes

the attainment or exceedance of the *k*-th limit state by the structural component. As in the previous sections, $\mathbf{x}$ denotes a vector of measurable variables and $\boldsymbol{\Theta}$ denotes a vector of model parameters. Usually $\mathbf{x}$ can be partitioned in a vector of material and geometrical variables, $\mathbf{x}_\mathrm{r}$, and in a vector of demand variables such as boundary forces or deformations, $\mathbf{x}_\mathrm{s}$. In this case $\mathbf{x}$ can be written as $\mathbf{x} = (\mathbf{x}_\mathrm{r}, \mathbf{x}_\mathrm{s})$.

Using the capacity models described earlier, $g_k(\mathbf{x}, \boldsymbol{\Theta})$ can be formulated as

$$g_k\left(\mathbf{x}_\mathrm{r}, \mathbf{x}_\mathrm{s}, \boldsymbol{\Theta}\right) = C_k\left(\mathbf{x}_\mathrm{r}, \mathbf{x}_\mathrm{s}, \boldsymbol{\Theta}\right) - D_k\left(\mathbf{x}_\mathrm{r}, \mathbf{x}_\mathrm{s}\right) \qquad k = 1, \ldots, q \tag{2-12}$$

where $D_k(\mathbf{x}_\mathrm{r}, \mathbf{x}_\mathrm{s})$ denotes the demand for the *k*-th failure mode. For example, for failure in shear of a reinforced concrete column, $C_k(\mathbf{x}_\mathrm{r}, \mathbf{x}_\mathrm{s}, \boldsymbol{\Theta})$ is the maximum shear force that the column can sustain, whereas $D_k(\mathbf{x}_\mathrm{r}, \mathbf{x}_\mathrm{s})$ is the maximum applied shear force. Note that the functions $C_k(\mathbf{x}_\mathrm{r}, \mathbf{x}_\mathrm{s}, \boldsymbol{\Theta})$ and $D_k(\mathbf{x}_\mathrm{r}, \mathbf{x}_\mathrm{s})$ generally could include both $\mathbf{x}_r$ and $\mathbf{x}_s$ as arguments. The fragility of a structural component can be written as

$$F\left(\mathbf{x}_\mathrm{s}, \boldsymbol{\Theta}\right) = \mathrm{P}\left[\bigcup_k \left\{ g_k\left(\mathbf{x}_\mathrm{r}, \mathbf{x}_\mathrm{s}, \boldsymbol{\Theta}\right) \le 0 \right\} \middle| \, \mathbf{x}_\mathrm{s}, \boldsymbol{\Theta}\right] \tag{2-13}$$

where $\mathrm{P}[A \mid \mathbf{x}_\mathrm{s}]$ denotes the conditional probability of event *A* for the given values of variables $\mathbf{x}_\mathrm{s}$. The uncertainty in the event for given $\mathbf{x}_\mathrm{s}$ arises from the inherent randomness in the capacity variables $\mathbf{x}_\mathrm{r}$, the inexact nature of the limit state model $g_k(\mathbf{x}_\mathrm{r}, \mathbf{x}_\mathrm{s}, \boldsymbol{\Theta})$ (or its sub-models), and the uncertainty inherent in the model parameters $\boldsymbol{\Theta}$.

Predictive Estimates of Fragility

A predictive estimate of fragility, $\tilde{F}(\mathbf{x}_s)$, incorporates the uncertainties in the model parameters $\boldsymbol{\Theta}$, by considering $\boldsymbol{\Theta}$ as random variables and taking the expected value of $F(\mathbf{x}_s, \boldsymbol{\Theta})$ over the posterior distribution of $\boldsymbol{\Theta}$, i.e.,

$$\tilde{F}(\mathbf{x}_s) = \int F(\mathbf{x}_s, \boldsymbol{\Theta}) f(\boldsymbol{\Theta}) d\boldsymbol{\Theta} \tag{2-14}$$

This estimate of fragility incorporates the epistemic uncertainties in an average sense and does not distinguish between the different natures of the aleatory and epistemic uncertainties.

Figs. 2-3 and 2-4 compare the predictive fragilities in Gardoni *et al.* (2002) (dashed lines) and the predictive fragility based on the updated probabilistic capacity models (solid lines) for the deformation and shear modes, respectively. The fragility estimates are computed using the reliability module of the software framework OpenSees (Haukaas and Der Kiureghian, 2004) for an example column with geometry and material properties that are representative of currently constructed highway bridge columns in California (Naito, 2000). The column has the longitudinal reinforcement ratio $\rho_l = 1.99\%$, gross diameter $D_g = 1520$ mm, ratio of gross to core diameter $D_g / D_c = 1.07$, and clear height $H = 9140$ mm. To account for material variability, the compressive strength of concrete f_c' is lognormally distributed with mean 35.8 MPa and 10% coefficient of variation (COV), the yield stress of longitudinal reinforcement f_y is lognormal with mean 475 MPa and 5% COV, and the volumetric transverse

reinforcement f_{yh} is lognormal with mean 493 MPa and 5% COV. To account for variability in the axial load, P is normally distributed with mean 4450 kN (corresponding to 7% of the axial capacity based on the gross cross-sectional area) and 25% COV. Finally, to account for variability in construction, the effective moment of inertia I_e is lognormal with mean 2.126×10^{11} mm^4 and 10% COV, and the cover is lognormal with mean 59 mm and 10% COV.

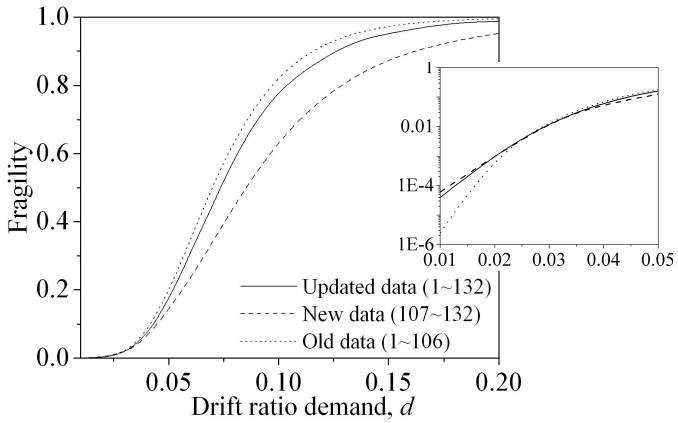

Fig. 2-3. Comparison between predictive fragilities for deformation in Gardoni *et al.* (2002, ASCE) (dotted lines) and based on the updated probabilistic capacity model (solid lines)

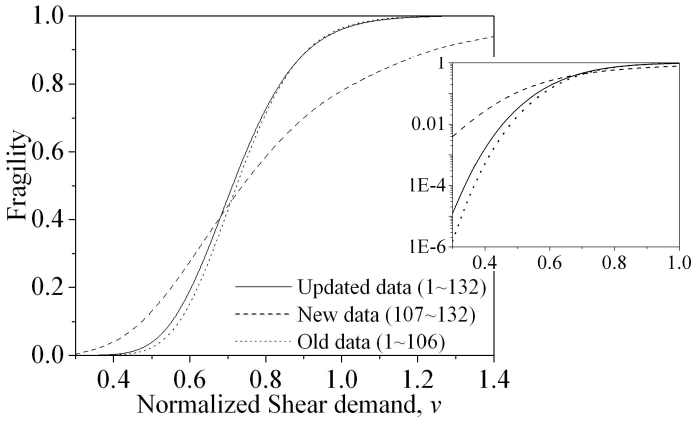

Fig. 2-4. Comparison between predictive fragilities for shear (dotted lines) and based on the updated probabilistic capacity model (solid lines)

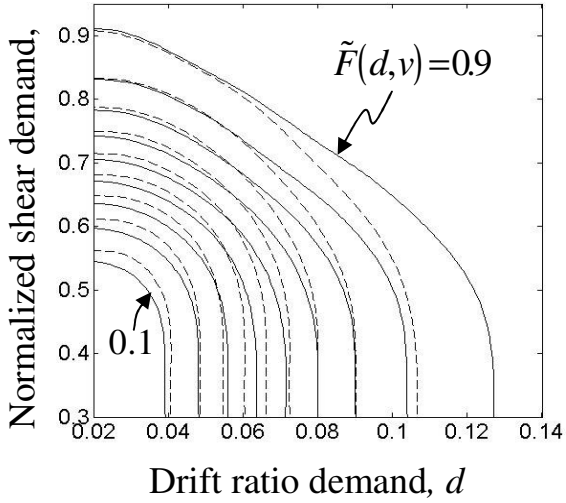

Fig. 2-5. Comparison between predictive deformation shear fragilities in Gardoni *et al.* (2002, ASCE) (dashed lines) and based on the updated probabilistic capacity model (solid lines)

In Figs. 2-3 and 2-4, I see that the updated fragility curves (solid lines) are close to the ones previously developed (dotted lines). In particular, incorporating the new data set marginally reduces the fragility for the deformation mode especially for higher values of the demand, *d*. On the contrary, the updated shear fragility is marginally higher especially for lower values of the demand, *v*. Fragility estimates developed using only the new 26 data are also shown for comparison (dashed lines). These fragility estimates have a higher degree of statistical uncertainty (due to the limited number of data used), which leads to flatter S-shaped curves. Fig. 2-5 shows a comparison between the contour lines of the predictive bi-variate fragility based on the original database and the updated one. Each contour line in this figure connects pairs of values of the demands d and v that are associated with a given level of fragility in the range 0.1–0.9. Consistently with the uni-variate fragilities, I see that the updated bi-variate fragility is lower than the one previously developed in the range $0.05 \le d \le 0.12$ and $0.0 \le v \le 0.7$. The main differences for all the fragilities are that (a) the updated ones can be used for a wider range of columns than the original ones and that (b) they have less statistical uncertainty.

Bounds on Fragility

For the updated fragility curves, I want to explicitly show the effect of the epistemic uncertainty in the model parameters $\boldsymbol{\Theta}$. To do this, I use approximate confidence bounds obtained by first-order analysis (Gardoni *et al.*, 2002). These bounds approximately correspond to 15% and 85% probability levels. This can be written as

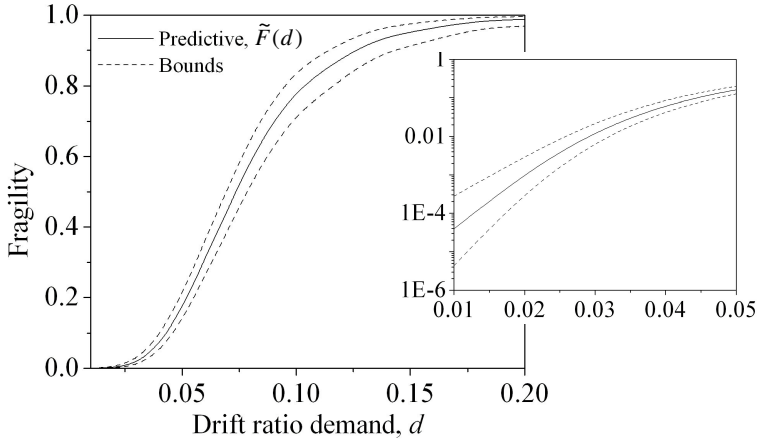

Fig. 2-6. Updated fragility estimate and confidence bounds for deformation failure of example RC column

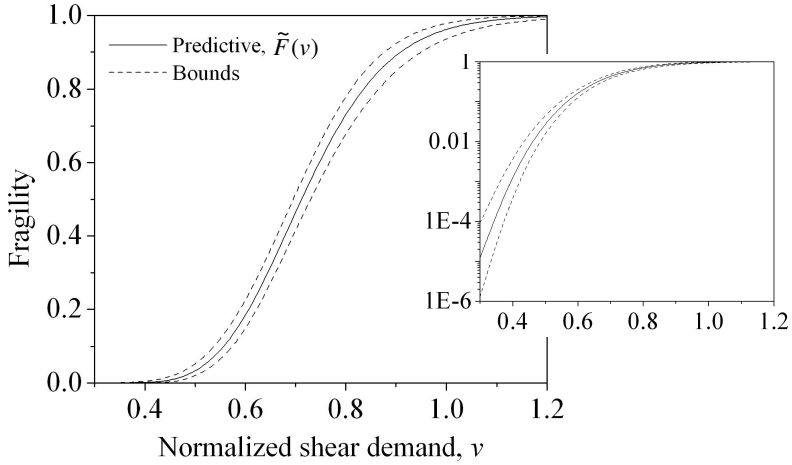

Fig. 2-7. Updated fragility estimate and confidence bounds for shear failure of example RC column

$$\left\{ \Phi\left[-\tilde{\beta}(\mathbf{x}_s)-\sigma_\beta(\mathbf{x}_s)\right],\ \Phi\left[-\tilde{\beta}(\mathbf{x}_s)+\sigma_\beta(\mathbf{x}_s)\right] \right\} \tag{2-15}$$

where $\Phi(\cdot)$ denotes the standard normal cumulative distribution function, $\tilde{\beta}(\mathbf{x}_s)=\Phi^{-1}[1-\tilde{F}(\mathbf{x}_s)]$ is the reliability index corresponding to the predictive fragility $\tilde{F}(\mathbf{x}_s)$, $\sigma_\beta(\mathbf{x}_s)$ is the standard deviation of $\beta(\mathbf{x}_s,\boldsymbol{\Theta})=\Phi^{-1}[1-F(\mathbf{x}_s,\boldsymbol{\Theta})]$, and $-\tilde{\beta}(\mathbf{x}_s)\pm\sigma_\beta(\mathbf{x}_s)$ denotes the mean ± 1 standard deviation bounds on the reliability index.

Figs. 2-6 and 2-7, respectively, show the uni-variate fragility curves with respect to drift ratio demand, d , and normalized shear demand, v . The solid lines represent the predictive fragilities $\tilde{F}(d)$ and $\tilde{F}(v)$ for the updated capacity model and the dashed lines indicate the 15 and 85% confidence bounds. The dispersion indicated by the slope of the solid curve represents the effect of the aleatory uncertainties (those present in f_c' , f_y , P , I_e , ε_d , and ε_v) and the dispersion indicated by the confidence bounds represents the influence of the epistemic uncertainties (those present in the model parameters $\boldsymbol{\Theta}$). The confidence bounds are tighter than those in Gardoni *et al.* (2002) because the posterior variances of the model parameters are smaller as noted earlier.

Sensitivity Measures

Sensitivity analysis is used to see to which *parameter(s)* the reliability of RC columns is most sensitive. Sensitivity measures can be used for optimal design and resource allocation, and provide insight into the behavior of RC columns. To compute the sensitivity measures, I partition $\mathbf{x}$ in a vector of constant parameters $\mathbf{x}_c$ and a vector of

random variables $\mathbf{x}_p$, so that $\mathbf{x}$ can be written as $\mathbf{x} = (\mathbf{x}_c, \mathbf{x}_p)$. Also, let $f(\mathbf{x}_p, \boldsymbol{\Theta}_f)$ be the probability density function of the basic variables $\mathbf{x}_p$, where $\boldsymbol{\Theta}_f$ is a set of distribution parameters (e.g., means, standard deviations, correlation coefficients, or other parameters defining the distribution). The vector $(\mathbf{x}_c, \boldsymbol{\Theta}_f)$ denotes the set of all parameters of the problem. The solution of the reliability problem depends on the value of $(\mathbf{x}_c, \boldsymbol{\Theta}_f)$. I can find the *sensitivity* of the reliability index, $\nabla_{(\mathbf{x}_c, \boldsymbol{\Theta}_f)}\beta$, with respect to $(\mathbf{x}_c, \boldsymbol{\Theta}_f)$ following Hohenbichler and Rackwitz (1983).

Table 2-6. Sensitivity measures for deformation and shear failure modes

Parameter, $\mathbf{x}_c$ or $\boldsymbol{\Theta}_f$	Symbol	$\nabla_{(\mathbf{x}_c, \boldsymbol{\Theta}_f)}\beta$	
		Deformation failure mode†	Shear failure mode††
Diameter of transverse reinforcement	d_s	–0.064	0.308
Diameter of longitudinal reinforcement	d_b	0.019	0.087
Mean of compressive strength of concrete	$\mathrm{E}(f_c')$	0.009	–0.036
Spacing of transverse reinforcement	S	0.006	–0.027
Mean of Yield stress of longitudinal reinforcement	$\mathrm{E}(f_y)$	0.004	–0.004
Yield stress of transverse reinforcement	f_{yh}	0.003	0.004
Cover thickness of concrete	Cover	–0.002	–0.001
Gross diameter of column	D_g	–0.000	0.001
Mean of effective moment of inertia	$\mathrm{E}(I_e)$	0.000	0.000
Ultimate strength of longitudinal reinforcement	f_{su}	0.000	0.000

† Deformation failure mode computed at a drift ratio demand $d = 0.1$

†† Shear failure mode computed for a normalized shear demand $v = 0.7$

Once $\nabla_{(\mathbf{x}_c,\boldsymbol{\Theta}_f)}\beta$ is known, the gradient of the first-order reliability approximation of the failure probability is obtained by using the chain rule of the differentiation as

$$\nabla_{(\mathbf{x}_c,\boldsymbol{\Theta}_f)} p_1 = -\varphi(\beta)\nabla_{(\mathbf{x}_c,\boldsymbol{\Theta}_f)}\beta \tag{2-16}$$

where $\varphi(\cdot)$ is the standard normal probability density function. The form $\nabla_{(\mathbf{x}_c,\boldsymbol{\Theta}_f)}\beta$ (or $\nabla_{(\mathbf{x}_c,\boldsymbol{\Theta}_f)} p_1$) can be used to identify to which parameter the fragilities are most sensitive, guiding us in determining what to change to make a component or structure safer.

Table 2-6 shows the sensitivity measures for the deformation and shear failure modes. I see that a unit increase in the diameter of the transverse reinforcing bars d_s is most effective in increasing the deformation reliability (reducing the probability of failure) and shear reliability of the example RC column.

Importance Measures

I may have several random variables in a limit state function. Some random variables have a larger effect on the variance of the limit state function (and thus are more important) and some have a smaller effect (and thus are less important). Following Der Kiureghian and Ke (1995), I can define a *measure of importance* γ (Greek gamma) as

$$\gamma^T = \frac{\boldsymbol{\alpha}^T \mathbf{J}_{\mathbf{u}^*,\mathbf{z}^*}\mathbf{SD}'}{\left\|\boldsymbol{\alpha}^T \mathbf{J}_{\mathbf{u}^*,\mathbf{z}^*}\mathbf{SD}'\right\|} \tag{2-17}$$

where $\mathbf{z}$ is the vector of the random variables, $\mathbf{z} = (\mathbf{x}_p, \boldsymbol{\Theta})$ and $\mathbf{J}_{\mathbf{u}^*,\mathbf{z}^*}$ is the Jacobian of the probability transformation from the original space $\mathbf{z}$ to the standard normal space $\mathbf{u}$, with respect to the coordinates of the design point $\mathbf{z}^*$ (the most likely failure point). The

matrix $\mathbf{SD}'$ is the standard deviation matrix of equivalent normal variables $\mathbf{z}'$ defined by the linearized inverse transformation $\mathbf{z}' = \mathbf{z}^* + \mathbf{J}_{\mathbf{z}^*,\mathbf{u}^*}(\mathbf{u} - \mathbf{u}^*)$ at the design point. The elements of $\mathbf{SD}'$ are the square roots of the corresponding diagonal elements of the covariance matrix $\mathbf{\Sigma}' = \mathbf{J}_{\mathbf{z}^*,\mathbf{u}^*}\,\mathbf{J}^{\mathbf{T}}_{\mathbf{z}^*,\mathbf{u}^*}$ of the variables $\mathbf{z}'$.

Table 2-7. Importance measures for deformation failure mode computed at a drift ratio demand $d = 0.1$

Random Variable	Symbol	γ_i
Model error / σ_d	ε_d	–0.933
Model parameter for $h_{\delta,1}$	θ_{d1}	–0.241
Model parameter for $h_{\delta,11}$	θ_{d11}	–0.212
Yield stress of longitudinal reinforcement	f_y	–0.101
Standard deviation of deformation model error	σ_d	–0.076
Model parameter for $h_{\delta,7}$	θ_{d7}	–0.068
Compressive strength of concrete	f_c'	–0.029
Effective moment of inertia	I_e	0.000
Ultimate strength of longitudinal reinforcement	f_{su}	0.000

Table 2-7 shows the importance measures for the deformation failure mode. I see that the random variable ε_d is almost four times more important than the second most important random variable, θ_{d1}. Similarly, for the shear failure mode, ε_v is more than four times more important than the second most important one, θ_{v4} (Table 2-8).

Table 2-8. Importance measures for shear failure mode computed for $v = 0.7$

Random Variable	Symbol	γ_i
Model error / σ_v	ε_v	–0.945
Model parameter for $h_{v,4}$	θ_{v4}	–0.222
Model parameter for $h_{v,2}$	θ_{v2}	–0.147
Compressive strength of concrete	f_c'	0.123
Yield stress of longitudinal reinforcement	f_y	–0.087
Model parameter for $h_{\delta,1}$	θ_{d1}	0.073
Model parameter for $h_{\delta,11}$	θ_{d11}	0.065
Model parameter for $h_{\delta,7}$	θ_{d7}	0.021
Standard deviation of shear model error	σ_v	0.009
Effective moment of inertia	I_e	0.000
Ultimate strength of longitudinal reinforcement	f_{su}	0.000

Approximate Closed-form of the Fragility

I can use the fact that ε_d and ε_v are the most important random variables to develop approximate closed-form fragilities. The closed-form enables the computation of the fragility of RC columns without the need for specialized reliability software and without significant loss of accuracy.

Ignoring the uncertainty in the model parameters and using a point estimate $\hat{\boldsymbol{\Theta}}$ in place of $\boldsymbol{\Theta}$, Eq. (2-2) can be written as

$$C\left(\mathbf{x}, \hat{\boldsymbol{\Theta}}\right) = c\left(\mathbf{x}\right) + \gamma\left(\mathbf{x}, \boldsymbol{\theta}\right) + \sigma\varepsilon \tag{2-18}$$

further assuming that the measurable variables $\mathbf{x}$ are nonrandom, I can write

$$C\left(\mathbf{x}, \hat{\boldsymbol{\Theta}}\right) = \mu_C + \hat{\sigma}\varepsilon \tag{2-19}$$

where $\mu_C = \hat{c}(\mathbf{x}) + \gamma(\mathbf{x}, \hat{\boldsymbol{\theta}})$ is the mean of $C(\mathbf{x}, \hat{\boldsymbol{\Theta}})$. Since ε is a random variable with zero mean and unit variance, $C(\mathbf{x}, \hat{\boldsymbol{\Theta}})$ is normal with mean μ_C and variance $\hat{\sigma}^2$. A point estimate of the fragility can now be written as

$$\begin{aligned} \hat{F}(\mathbf{x}_s) = F(\mathbf{x}_s, \hat{\boldsymbol{\Theta}}) = \mathrm{P}\left[g(\mathbf{x}_r, \mathbf{x}_s, \hat{\boldsymbol{\Theta}}) \le 0 \,\middle|\, \mathbf{x}_s, \boldsymbol{\Theta} \right] = \\ \mathrm{P}\left[\{ C(\mathbf{x}_r, \mathbf{x}_s, \boldsymbol{\Theta}) - D(\mathbf{x}_r, \mathbf{x}_s) \} \le 0 \,\middle|\, \mathbf{x}_s, \hat{\boldsymbol{\Theta}} \right] = \\ = \Phi\left(-\frac{\mu_C - D(\mathbf{x}_r, \mathbf{x}_s)}{\hat{\sigma}} \right) = 1 - \Phi\left(\frac{\mu_C - D(\mathbf{x}_r, \mathbf{x}_s)}{\sigma} \right) \end{aligned} \tag{2-20}$$

Similarly, in case of q limit states, I can write

$$\begin{aligned} \hat{F}(\mathbf{x}_s) = F(\mathbf{x}_s, \hat{\boldsymbol{\Theta}}) = \mathrm{P}\left[\bigcup_{k=1}^{q} g_k(\mathbf{x}_r, \mathbf{x}_s, \hat{\boldsymbol{\Theta}}) \le 0 \,\middle|\, \mathbf{x}_s, \boldsymbol{\Theta} \right] = \\ \mathrm{P}\left[\bigcup_{k=1}^{q} \{ C_k(\mathbf{x}_r, \mathbf{x}_s, \boldsymbol{\Theta}) - D_k(\mathbf{x}_r, \mathbf{x}_s) \} \le 0 \,\middle|\, \mathbf{x}_s, \hat{\boldsymbol{\Theta}} \right] = 1 - \Phi_q(\mathbf{u}, \hat{\mathbf{R}}) \end{aligned} \tag{2-21}$$

where $\mathbf{u}$ is the vector with elements $u_i = [\mu_C - D(\mathbf{x}_r, \mathbf{x}_r)] / \hat{\sigma}$ and $\hat{\mathbf{R}}$ is its estimated correlation coefficient matrix. For the evaluation of $\Phi_q(\mathbf{u}, \hat{\mathbf{R}})$, several numerical methods have been developed (e.g., Ambartzumian *et al.* 1998). In the specific case of a bi-variate model, one can use the following single integral expression

$$\Phi_2(u_1, u_2, \hat{\rho}) = \Phi(u_1)\Phi(u_2) + \int_0^{\hat{\rho}} \varphi_2(u_1, u_2, \rho) d\rho \tag{2-22}$$

This expression can be easily solved numerically.

Fig. 2-8 compares the approximate closed-form of the uni-variate deformation fragility (solid lines) with the predictive fragility (dotted line). Similarly, Fig. 2-9 compares the closed-form approximation and the predictive fragility for the shear mode

of failure. I see that the closed-form fragilities are almost identical to the predictive fragilities. The closed-form fragility has an S-shape that is only marginally sharper than the predictive fragility (lower in the lower tail and higher in the upper tail). This behavior reflects the fact that the predictive fragility incorporates more uncertainties than the closed-form approximation where only ε is random. The closed-form approximation can be used as a very accurate approximation of the predictive fragility for practical purposes and does not require the use of reliability software.

Fig. 2-10 compares the approximate closed-form of the bi-variate deformation-shear fragility (solid line) with the predictive fragility (dashed line). Like the case of uni-variate deformation and shear fragilities, the closed-form approximation to the bi-variate fragility provides a close match to the predictive fragility.

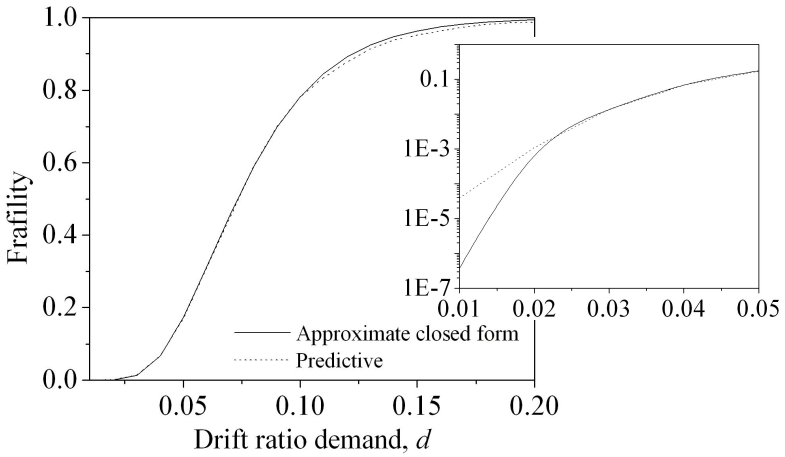

Fig. 2-8. Comparison between the approximate closed-form (solid line) and the predictive fragility (dotted line) in deformation

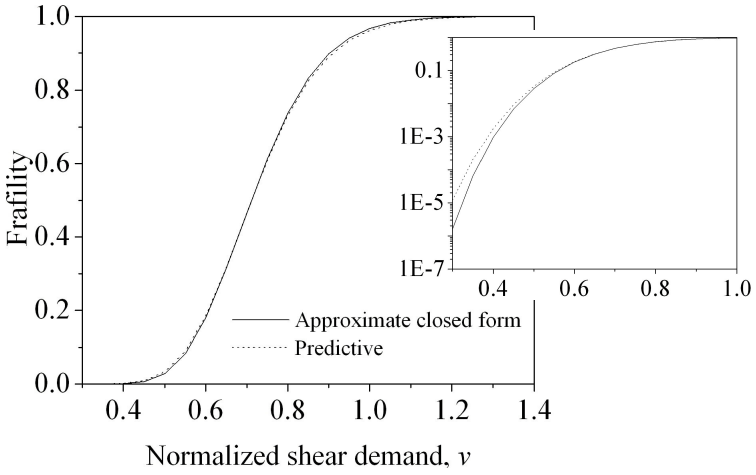

Fig. 2-9. Comparison between the approximate closed-form (solid line) and the predictive fragility (dotted line) in shear

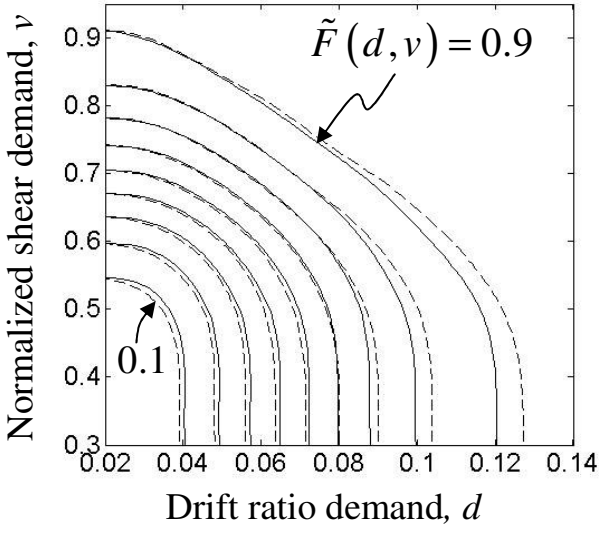

Fig. 2-10. Comparison between the approximate closed-form (solid line) and the predictive fragility (dashed line) in deformation-shear

Consistently with what was observed in the case of the uni-variate fragilities, the closed-form of the bi-variate fragility is marginally sharper (lower in the lower tail and higher in the upper tail) than the predictive fragility. This behavior reflects the fact that the predictive fragility incorporates more uncertainties than the closed-form approximation where only ε_d and ε_v are random.

Conclusions

This study presents a closed-form formulation to estimate the fragility of structural components. The formulation can be readily used in practice since it does not require the use of specialized reliability software. As an application, the formulation is used to estimate the conditional probability of failure of an example RC column for given shear and deformation demands. The example column has geometry and material properties that are representative of current construction in California (Naito, 2000). The closed-form fragilities are shown to be accurate when compared with more sophisticated estimates (e.g., predictive fragilities). This study also shows that the fragility of the example column is most sensitive to changes in the diameter of the transverse reinforcement.

A Bayesian procedure is presented to update existing probabilistic models with new data. The model updating process enables the incorporation of different types of information, including laboratory test data, field observations, and subjective engineering judgment, as they become available. As an application, deformation and shear capacity models are updated using a new set of data that include both equality and

lower bound data. Using additional data reduces the statistical uncertainty in the probabilistic models and increases their range of applicability. The updated capacity models are used in the closed-form fragility estimates to estimates the fragilities of the example column accounting for all available information.

CHAPTER III*

PROBABILISTIC CAPACITY MODELS AND SEISMIC FRAGILITY ESTIMATES FOR RC COLUMNS SUBJECT TO CORROSION

In this research, probabilistic drift and shear force capacity models are developed for corroding reinforced concrete (RC) columns. The developments represent a merger between a probabilistic model for chloride-induced corrosion, a time-dependent corrosion rate, and previously developed probabilistic models for drift and shear force capacity of pristine (undamaged) RC columns. Fragility estimates are obtained for an example corroding column by applying the developed models at given shear and drift demands. Model uncertainties in both the capacity and corrosion models are considered in the fragility estimation, in addition to uncertainties in environmental conditions, material properties, and structural geometry. Sensitivity analyses of the corroding RC column are carried out to identify the parameters to which the reliability of the example column is most sensitive. The developed models consider different combinations of chloride exposure condition, environmental oxygen availability, water-to-cement ratios, and curing conditions. They are applicable to both existing and new RC columns and may be employed for the prediction of service-life and life-cycle cost analysis of RC structures.

---

* Reprinted with permission from "Probabilistic Capacity Models and Seismic Fragility Estimates for RC Columns Subject to Corrosion" by Choe, D., Gardoni, P., Rosowsky, D., and Haukaas, T. Names, 2007. Reliability Engineering and System Safety, Special Issue, Copyright [2007] by RESS.

Introduction

Corrosion of reinforcement is detrimental to the serviceability and capacity of reinforced concrete (RC) structures. Corrosion is a long-term process that effectively weakens structural elements and increases their vulnerability to extreme loads (vehicles) and natural hazards. A structure that is originally designed to meet code specifications may not have the same margin of safety once the structure has undergone significant corrosion. Of particular significance to the developments in this research is the inevitable presence of uncertainties; the prediction of onset and progression of corrosion can only be made in a probabilistic manner. For example, the corrosion process is highly influenced by the material and environmental factors. To this end, a key objective in this chapter is to put forward structural capacity models that include the effects of deterioration, with appropriate consideration of uncertainties.

In recent decades, significant research efforts have been devoted to the quantification and inclusion of corrosion in design, construction and maintenance of RC structures. Tuutti (1982) and Liu and Weyers (1998) suggested deterministic corrosion models for RC reinforcement, while Thoft-Christensen *et al*. (1997) and Dura-Cretre (2000) presented probabilistic models for the deterioration process. Stewart and Rosowsky (1998), Vu and Stewart (2000), Enright and Frangopol (1998a,b) developed probabilistic corrosion models for bridge slabs, beams and girders by extending commonly employed RC capacity models. This research further extends these developments by constructing deterioration models that incorporate both probabilistic

models for the drift and shear capacity of RC columns and probabilistic models for the deterioration process.

Gardoni *et al.* (2002) and Choe *et al.* (2007a) developed probabilistic capacity models for pristine (not corroded) RC columns with circular cross section that properly account for all the prevailing uncertainties, including model error arising from potential inaccuracies in the model form and potentially missing variables, as well as measurement errors and statistical uncertainty. However, these models may not be appropriate once the structure begins deteriorating due to corrosion.

In this study, I incorporate information about material deterioration – employing a probabilistic corrosion model – into the probabilistic capacity models for RC columns developed by Gardoni *et al.* (2002) and Choe *et al.* (2007). The corrosion model is based on a probabilistic model for chloride induced corrosion (Dura-Crete, 2000) and a time-dependent corrosion rate function (Vu and Stewart 2000). The uncertainties in parameters and model inexactness (or model error) in both the material deterioration model and the structural capacity model are considered.

The developed probabilistic models are used to asses the time-varying reliability of an example column subject to different environmental and material conditions. The reliability (or the lack of) is expressed in terms of a fragility function where fragility is defined as the conditional probability of failure of the column for given demand variables. Sensitivity analysis is carried out to identify to which parameter(s) the reliability of the example column is most sensitive. The models developed in this

research may be used for the prediction of service-life of existing and new structures and life-cycle cost analysis for RC structures.

Probabilistic Model for Reinforcement Corrosion

There are three deterioration phases in the corrosion process of reinforcement steel (Liu and Weyers 1998). In the first phase, termed the *diffusion phase*, chloride ions diffuses to the surface of steel to initiate corrosion. The second phase, termed the *corrosion propagation phase*, comprise the time from initiation of corrosion to initiation of cracks in the concrete cover. The third phase, termed the *deterioration phase*, is the process that takes place after the initiation of cracks.

To determine the time to the initiation of corrosion, most diffusion models are based on the solution of the one-dimensional version of Fick's second law (Tuutti 1982). In a commonly employed solution the chloride concentration C at depth x and time t is expressed as

$$C(x,t) = C_s\left[1 - erf\left(\frac{x}{2\sqrt{Dt}}\right)\right] \tag{3-1}$$

where C_s is the chloride concentration on the surface, $erf(\cdot)$ is the error function, and D is the diffusion coefficient. The variable t is defined as the time from the moment of construction (whether in the present or in the past) to the specific time of interest in the future. It is assumed that the corrosion initiates at the time T_{corr} when the chloride concentration at the depth d_c of the reinforcement (cover depth) reaches the critical

chloride concentration, C_{cr}, that is $C(d_c, T_{corr}) = C_{cr}$. By solving $C(d_c, T_{corr}) = C_{cr}$ for T_{corr} and defining $D = k_e k_t k_c D_0 (t_0 / t)^n$, Dura-Crete (2000) provides the following probabilistic model for the time to onset of chloride induced corrosion, which considers uncertainties in measured parameters, environmental conditions, as well as model uncertainty:

$$T_{corr} = X_I \cdot \left[\frac{{d_c}^2}{4 k_e k_t k_c D_0 (t_0)^n} \left[erf^{-1}\left(1 - \frac{C_{cr}}{C_s}\right) \right]^{-2} \right]^{\frac{1}{1-n}} \tag{3-2}$$

where X_I is a model uncertainty coefficient to account for the idealization implied by Fick's second law, k_e is an environmental factor, k_t includes the influence of test methods to determine the empirical diffusion coefficient D_0, k_c is a parameter that accounts for the influence of curing, t_0 is the reference period for D_0, and n is the age factor. In this model, C_s is represented as the linear function $C_s = A_{cs}(w/b) + \varepsilon_{cs}$ of the variable water-to-binder ratio w/b, which is considered as one variable, where A_{cs} and ε_{cs} are model parameters. Appendix 1 provides the parameters in Eq. (3-2), A_{cs} and ε_{cs} for ordinary Portland cement. The probability distribution for these parameters is determined from experimental data considering different environments, water to cement ratios, and curing conditions (Dura-Crete 2000). Using Eq. (3-2), the probability that corrosion has initiated at time t can be written as

$$\mathrm{P}[T_{corr} \le t] = \mathrm{P}\left[g_{T_{corr}}(t, \mathbf{x}_T, \boldsymbol{\Theta}_T) \le 0 \,\middle|\, t \right] \tag{3-3}$$

where

$$g_{T_{corr}}(t, \mathbf{x}_T, \Theta_T) = T_{corr}(\mathbf{x}_T, \Theta_T) - t \tag{3-4}$$

where $\mathbf{x}_T = \{C_{cr}, d_c\}$ is a vector of measurable parameters, e.g., material and geometrical variables, and $\mathbf{\Theta}_T$ denotes a set of parameters introduced to fit the model to the observed data, i.e., $\mathbf{\Theta}_T = \{D_0, k_e, k_t, k_c, n, A_{cs}, \varepsilon_{cs}\}$.

Once corrosion is initiated, the load-carrying capacity of the reinforced concrete is altered. To estimate the loss of steel cross-section due to corrosion, I use the time-dependent corrosion rate function developed by Vu and Stewart (2000). It is suggested that the corrosion rate diminishes with time because corrosion products formed around the bar impede the diffusion of iron ions. The corrosion current density at time t is expressed as

$$i_{corr}(t) = 0.85\, i_{corr,0}\, (t - T_{corr})^{-0.29} \qquad t \geq T_{corr} \tag{3-5}$$

where $i_{corr,0}$ is the corrosion current density at the start of corrosion propagation; namely

$$i_{corr,0} = \frac{37.5(1 - w/c)^{-1.64}}{d_c} \qquad (\mu A / cm^2) \tag{3-6}$$

where w/c is the variable water-to-cement ratio, which is considered as one variable, and d_c is the previously defined cover depth.

Loss of load-carrying capacity due to corrosion in RC structures might be caused by reduction in the cross-section area of the reinforcing steel, loss of pullout resistance of the reinforcement bars, and cracking in the cover concrete. In this research, I limit the

scope to the consideration of loss of reinforcement area. This is justified by the experimental results reported by Wang and Liu (2004) and Fang *et al.* (2004), where it is shown that in the presence of confinement steel, which is the case under consideration, , the pullout resistance is not significantly affected by corrosion.

Probabilistic Capacity Models for Corroding RC Columns

The probabilistic capacity models presented herein for corroding RC columns represent a merger between the work by Gardoni *et al.* (2002) and Choe *et al.* (2007a) and the probabilistic diffusion model described above. A "model" in this study means a mathematical expression that relates one or more quantities of interest, e.g., capacities of structural components, to a set of measurable variables $\mathbf{x} = (x_1, x_2, \ldots)$, e.g., material properties, member dimensions, and imposed boundary conditions. In its general form, a probabilistic capacity model is written as

$$C_k = C_k\left(\mathbf{x}, \boldsymbol{\Theta}_k\right) \tag{3-7}$$

where C_k is the capacity quantity of interest, k indicates the mode of failure considered, e.g., drift or shear force, and $\boldsymbol{\Theta}_k$ is a set of random model parameters introduced to fit the model to observed data. The function $C_k(\mathbf{x}, \boldsymbol{\Theta}_k)$ may involve algebraic expressions, integrals, and differentials. Its form is ideally derived from first principles, e.g., the rules of mechanics, but other approaches are also feasible. For instance, Gardoni *et al.* (2002) established the form of $C_k(\mathbf{x}, \boldsymbol{\Theta}_k)$ by considering deterministic models extended with probabilistic model correction terms.

It is assume that the structural capacities do not vary prior to time T_{corr}, which is previously defined as the time at which the chloride concentration in the concrete reaches the critical level at the depth of the steel reinforcement. After the onset of corrosion, the diameter of the reinforcement steel is assumed to decrease. The variation of the diameter over time is expressed as

$$d_b(t,T_{corr}) = \begin{cases} d_{bi} & t \le T_{corr} \\ d_{bi} - 2\int_{T_{corr}}^{t} \lambda(t)dt & T_{corr} < t \le T_f \\ 0 & T_f < t \end{cases} \qquad (3\text{-}8)$$

where d_{bi} is the initial bar diameter at time $t = 0$, $\lambda(t)$ is the corrosion rate expressed as $\lambda(t) = 0.0116 i_{corr}(t)$, where $i_{corr}(t)$ is the corrosion current density at time t according to Eq. (3-5), and T_f is the time when $d_b(t)$, in theory, reaches zero. By considering Eq. (3-5) and Eq. (3-8) the degrading diameter becomes $d_b(t,T_{corr}) = d_{bi} - 0.0278 i_{corr,0}(t - T_{corr})^{0.71}$ for $T_{corr} < t \le T_f$. Hence, the time-varying bar diameter can be expressed as

$$d_b(t,T_{corr}) = \begin{cases} d_{bi} & t \le T_{corr} \\ d_b(t) = d_{bi} - \dfrac{1.0508\,(1 - w/c)^{-1.64}}{d}(t - T_{corr})^{0.71} & T_{corr} < t \le T_f \\ 0 & t > T_f \end{cases} \qquad (3\text{-}9)$$

where $T_f = T_{corr} + d_{bi}\{d/[1.0508\,(1 - w/c)^{-1.64}]\}^{1/0.71}$.

The reduced diameter $d_b(t,T_{corr})$ is used in the probabilistic drift and shear capacity models developed by Gardoni *et al.* (2002) and Choe *et al.* (2007a), where the

diameter was considered as the pristine one. As a special case of Eq. (3-7), the drift capacity model can be written as

$$\ln\left[d\left(\mathbf{x}(t,T_{corr}),\boldsymbol{\Theta}_d\right)\right]=\ln\left[\hat{d}\left(\mathbf{x}(t,T_{corr})\right)\right]+\gamma_d\left(\mathbf{x}(t,T_{corr}),\boldsymbol{\theta}_d\right)+\sigma_d\varepsilon \tag{3-10}$$

where $d=\Delta/H$ is the drift ratio capacity, Δ is the displacement capacity, H is the clear column height, $\boldsymbol{\Theta}_d=(\boldsymbol{\theta}_d,\sigma_d)$ denotes the set of model parameters in which $\boldsymbol{\theta}_d=(\theta_{d1},\theta_{d2},\theta_{d3})$, $\hat{d}(\mathbf{x}(t,T_{corr}))$ is a selected deterministic model, $\gamma_d(\mathbf{x}(t,T_{corr}),\boldsymbol{\theta}_d)$ represents a correction term defined to capture the bias inherent in the deterministic model, ε is a random variable with zero mean and unit variance, and σ_d represents the standard deviation of the model error.

Accounting for the deterioration process, the deterministic model is written as

$$\hat{d}\left(\mathbf{x}(t,T_{corr})\right)=\frac{1}{H}\left(\hat{\Delta}_y(t,T_{corr})+\hat{\Delta}_p(t,T_{corr})\right) \tag{3-11}$$

where $\hat{\Delta}_y(t,T_{corr})$ is the elastic component due to the onset of yield and $\hat{\Delta}_p(t,T_{corr})$ is the inelastic component due to the plastic flow for a single RC column. Both components include the effects of the loss of steel and the consequent deterioration of the moment capacity. The model for $\hat{\Delta}_y(t,T_{corr})$ is written as

$$\hat{\Delta}_y(t,T_{corr})=\hat{\Delta}_f(t,T_{corr})+\hat{\Delta}_{sh}(t,T_{corr})+\hat{\Delta}_{sl}(t,T_{corr}) \tag{3-12}$$

In this equation, $\hat{\Delta}_f(t,T_{corr})$ represents the flexural component based on a linear curvature distribution along the full column height and can be written as

$$\hat{\Delta}_f(t,T_{corr}) = \frac{1}{3}\phi_y(t,T_{corr}) l_{eff}^2(t,T_{corr}) \tag{3-13}$$

where $\phi_y(t,T_{corr})$ is the curvature at the idealized flexural strength point, $l_{eff}(t,T_{corr}) = H + YP(t,T_{corr})$ is the effective length of the column, in which $YP(t,T_{corr})$ denotes the depth of the yield penetration into the column base and is estimated as $YP(t,T_{corr}) = 0.022\, f_y\, d_b(t,T_{corr})$, where f_y is the yield stress of the longitudinal reinforcement. The shear component, $\hat{\Delta}_{sh}(t,T_{corr})$, due to shear distortion is written as

$$\hat{\Delta}_{sh}(t,T_{corr}) = \frac{V_y(t,T_{corr}) H}{G\, A_{ve}} \tag{3-14}$$

where $V_y(t,T_{corr})$ is the deteriorated shear strength at yield, G is the shear modulus of concrete, and A_{ve} is the effective shear area. The slip component, $\hat{\Delta}_{sl}(t,T_{corr})$, due to the local rotation at the base caused by slipping of the longitudinal bar reinforcement is

$$\hat{\Delta}_{sl}(t,T_{corr}) = \frac{\phi_y(t,T_{corr})\, f_y\, d_b(t,T_{corr})\, H}{8.64\sqrt{f_c'}} \tag{3-15}$$

where f_c' is the compressive strength of concrete.

The inelastic component $\hat{\Delta}_p(t,T_{corr})$ due to the plastic flow can be developed including the deterioration described above as follows:

$$\hat{\Delta}_p(t,T_{corr}) = \alpha_p\, H = \phi_p(t,T_{corr})\, l_p(t,T_{corr})\, H \tag{3-16}$$

where $l_p(t,T_{corr}) = 0.08H + YP(t,T_{corr}) \geq 0.044\, f_y\, d_b(t,T_{corr})$ is the equivalent plastic hinge length (Priestley *et al.*, 1996), in which f_y in the lower bound limit must be

expressed in units of MPa, and $\phi_p(t,T_{corr}) = \phi_u(t,T_{corr}) - \phi_y(t,T_{corr})$ is the plastic curvature, where $\phi_u(t,T_{corr})$ denotes the ultimate curvature.

The term $\gamma_d(\mathbf{x}(t,T_{corr}),\boldsymbol{\theta}_d)$ in Eq. (3-10) is a bias correction term and also includes the effects of corrosion. The bias correction term is expressed as

$$\gamma_d\left(\mathbf{x}\left(t,T_{corr}\right),\boldsymbol{\theta}_d\right) = \theta_{d1}\frac{4V_I\left(t,T_{corr}\right)}{\left(\pi D_g^2 f_t'\right)} + \theta_{d2}\rho_s\left(t,T_{corr}\right)\left(\frac{f_{yh}}{f_c'}\right)\left(\frac{D_c}{D_g}\right) + \theta_{d3}\varepsilon_{cu} \tag{3-17}$$

The first term in Eq. (3-17), $4V_I(t,T_{corr})/\pi D_g^2 f_t'$, represents the effect of the idealized elastic-perfectly plastic shear force, $V_I(t,T_{corr})$, D_g is the gross column diameter and f_t' is the tensile strength of concrete. The second term, $\rho_s(t,T_{corr})(f_{yh}/f_c')(D_c/D_g)$, captures the effect of confining transverse reinforcement and core size, where $\rho_s(t,T_{corr})$ is the volumetric transverse reinforcement ratio, f_{yh} is the yield stress of the transverse reinforcement, and D_c is the core column diameter. The third term, ε_{cu}, is the ultimate longitudinal compressive strain. The estimated parameters $\boldsymbol{\Theta}_d = (\boldsymbol{\theta}_d, \sigma_d)$ are considered as constant with time and are provided in Table 3-1.

Table 3-1. Posterior statistics of the parameters in the drift model

		St.	Correlation coefficient			
$\boldsymbol{\Theta}_d$	Mean	dev.	θ_{d1}	θ_{d2}	θ_{d3}	σ_d
θ_{d1}	0.675	0.105	1			
θ_{d2}	0.631	0.133	–0.27	1		
θ_{d3}	–57.5	10.1	–0.65	–0.39	1	
σ_d	0.400	0.045	0.39	–0.06	–0.13	1

Similarly, the shear capacity model is written as

$$\ln\left[v\left(\mathbf{x}(t,T_{corr}),\boldsymbol{\Theta}_v\right)\right]=\ln\left[\hat{v}\left(\mathbf{x}(t,T_{corr})\right)\right]+\gamma_v\left(\mathbf{x}(t,T_{corr}),\boldsymbol{\theta}_v\right)+\sigma_v\varepsilon \tag{3-18}$$

where $v=V/(A_g f_t')$ denotes the normalized shear capacity, where V is the shear capacity and A_g is the gross cross-sectional area. The vector $\boldsymbol{\Theta}_v=(\boldsymbol{\theta}_v,\sigma_v)$ denotes the set of model parameters, where $\boldsymbol{\theta}_v=(\theta_{v1},\theta_{v2})$, $\hat{v}(\mathbf{x}(t,T_{corr}))$ is a selected deterministic model, $\gamma_v(\mathbf{x}(t,T_{corr}),\boldsymbol{\theta}_v)$ represents the correction term, ε is a random variable with zero mean and unit variance, and σ_v represents the standard deviation of the model error.

Accounting for the deterioration process, $\hat{v}(\mathbf{x}(t,T_{corr}))$ can be written as

$$\hat{v}\left(\mathbf{x}\left(t,T_{corr}\right)\right)=\frac{\hat{V}_c\left(t,T_{corr}\right)+V_s\left(t,T_{corr}\right)}{A_g f_t'} \tag{3-19}$$

The first term, $\hat{V}_c(t,T_{corr})$, is the contribution from the concrete computed based on the model by Moehle *et al.* (2000, 2004) and the second term, $\hat{V}_s(t,T_{corr})$, is the contribution from the transverse steel based on a truss model and given by

$$\hat{V}_s\left(t,T_{corr}\right)=\frac{A_v\left(t,T_{corr}\right)f_{yh}D_e}{S} \tag{3-20}$$

where $A_v(t,T_{corr})$ is the total area in a layer of the transverse reinforcement in the direction of the shear force, D_e is the effective depth, and S is the spacing of transverse reinforcement.

The correction term $\gamma_v(\mathbf{x}(t,T_{corr}),\boldsymbol{\theta}_v)$ is expressed as

$$\gamma_v\left(\mathbf{x}\left(t,T_{corr}\right),\boldsymbol{\theta}_v\right)=\theta_{v1}\rho_l\left(t,T_{corr}\right)+\theta_{v2}\frac{A_v\left(t,T_{corr}\right)f_{yh}D_g}{\left(A_g f_t' S\right)} \tag{3-21}$$

where $\rho_l(t,T_{corr})$ is the contribution from the longitudinal steel, and $f_c'\ A_v(t,T_{corr})f_{yh}D_g/(A_g f_t' S)$ represents the contribution from the transverse steel. The estimated parameters $\boldsymbol{\Theta}_v=(\boldsymbol{\theta}_v,\sigma_v)$ are considered as constant with time and are provided in Table 3-2.

Table 3-2. Posterior statistics of the parameters in the shear model

		St.	Correlation coefficient		
$\boldsymbol{\Theta}_v$	Mean	dev.	θ_{v1}	θ_{v2}	σ_v
θ_{v1}	18.3	1.45	1		
θ_{v2}	–0.470	0.078	–0.87	1	
σ_v	0.185	0.018	–0.04	–0.02	1

Example Column

The numerical studies in this chapter are carried out with the OpenSees software (http://opensees.berkeley.edu) for an example column. OpenSees is a comprehensive, open-source, object-oriented finite element software that has previously been extended with reliability and response sensitivity capabilities (Moehle *et al.* 2004). In this study I employ OpenSees to obtain fragility estimates for the example column based on the probabilistic models presented above. The column is modeled by fiber-discretized cross-sections, where each fiber contains a uniaxial inelastic material model. In this

study, OpenSees is extended with implementations for corrosion initiation, corrosion rate, and loss of reinforcement area.

The example corroding column has geometry and material properties that are representative of currently constructed highway bridge columns in California (Naito 2000). Parameter values that enter in the probabilistic models for the corrosion rate at the time under consideration are provided in Table 3-3, as assessed by Dura-Crete (2000). For the example column I assume submerged exposure condition, i.e., the lower part of the column is permanently under the sea-water level. This choice is made for illustration purposes; it is stressed that the methodology is applicable to a wide range of environmental conditions with more or less severe deterioration of the shear and deformation capacity. The parameter values for the structural capacity models are from Choe *et al.* (2007a). The column has a nominal cover thickness of 59 mm, water-to-cement ratio equal to 0.50, pristine longitudinal reinforcement ratio $\rho_l = 1.99\%$, gross diameter $D_g = 1520$ mm, ratio of gross to core diameter $D_g / D_c = 1.07$, and clear height $H = 9140$ mm. To account for material variability, the compressive strength of concrete f_c' is assumed to be lognormally distributed with mean 35.8 MPa and 10% coefficient of variation (COV), the yield stress of longitudinal reinforcement f_y is assumed to be lognormal with mean 475 MPa and 5% COV, and the volumetric transverse reinforcement f_{yh} is assumed to be lognormal with mean 493 MPa and 5% COV. To account for variability in the axial load, P is assumed to be normally distributed with mean 4450 kN (corresponding to 7% of the axial capacity based on the gross cross-

sectional area) and 25% COV. Finally, to account for variability in construction and the effective moment of inertia, I_e is assumed to be lognormal with pristine mean 2.126×10^{11} mm^4 and 10% COV.

The top two diagrams in Fig. 3-1 show the degradation over time of the drift and shear capacity of the example RC column, respectively. Each plot shows a point estimate of the capacity, the mean capacity and the corresponding confidence band. The point estimate is obtained from Eq. (3-10) by ignoring all uncertainties and using the mean values of each random variable. The mean capacity and the confidence band are computed by sampling analysis considering different realizations of Eq. (3-10) based on the variability of each random variable. The confidence band is constructed as the mean capacity $\pm$ one standard deviation and reflects the model uncertainty. The third diagram from the top in Fig. 3-1 shows the loss of cross-sectional area of the reinforcement due to the propagation of corrosion. The bottom diagram in Fig. 3-1 shows the probability of corrosion initiation according to Eq. (3-2).

Table 3-3. Diffusion model parameter statistics

	d (mm)	k_e	k_c	k_t	D_0 (mm^2/yr)	n	C_{cr}	A_{cs}	ε_{cs}
Mean	59.0	1.33	2.40	0.832	473	0.362	1.60	10.3	0.000
St. dev.	17.7	0.22	0.700	0.024	43.2	0.245	0.100	0.714	0.580

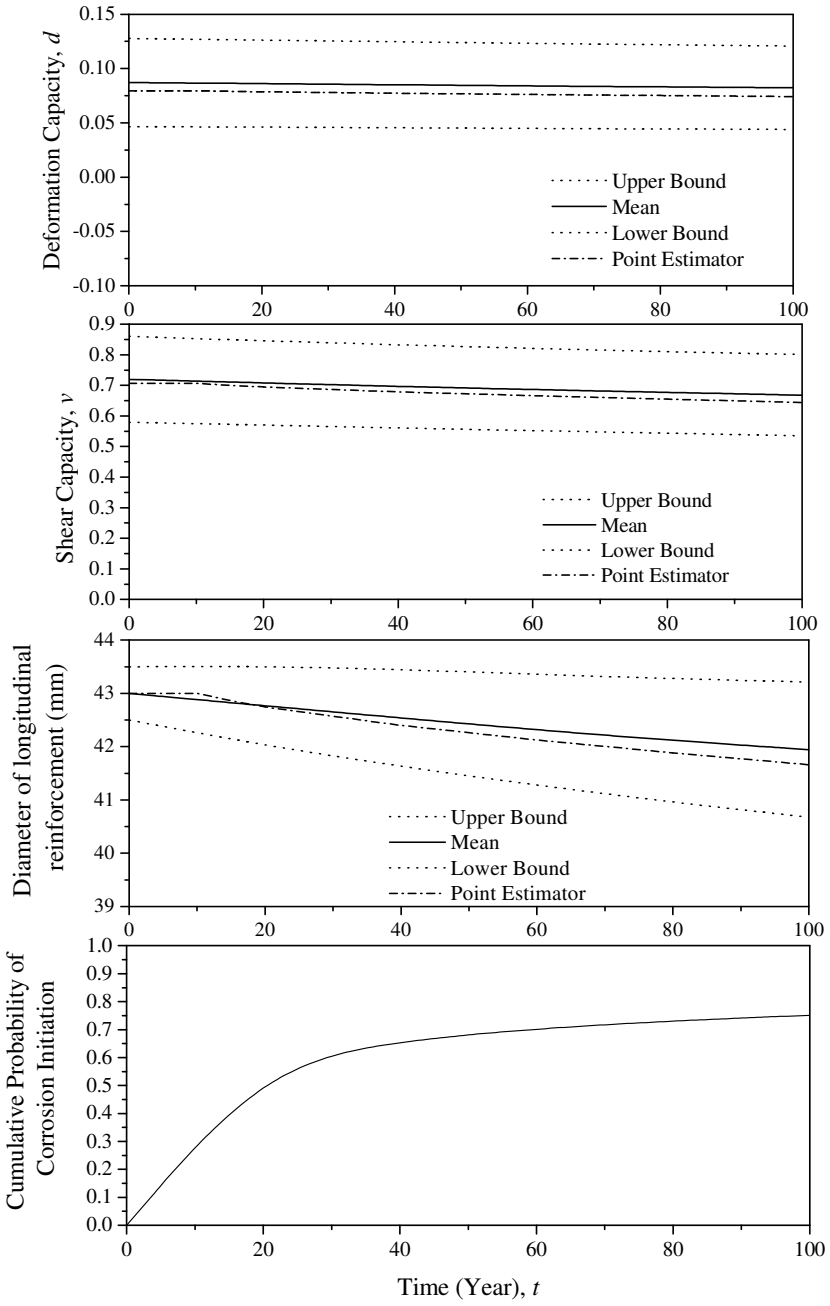

Fig. 3-1. Structural capacity deterioration, material deterioration, and probability of corrosion

Fragility Estimates

The probabilistic capacity models developed above enable estimating the fragility of corroding RC columns during their service-life. In particular, shear and drift fragilities are considered in this chapter. The fragility of a structural component is defined as the conditional probability of failure, given demand variable values. According to the conventional notation in structural reliability theory, e.g., Ditlevsen and Madsen (1996), a limit state function $g_k(\mathbf{x},\boldsymbol{\Theta}_k)$ is defined such that the event $\{g_k(\mathbf{x},\boldsymbol{\Theta}_k)\le 0\}$ denotes the failure of the *k*-th limit state by the structural component. In the probabilistic capacity models of corroding columns, the limit state functions are represented as $g_d(\mathbf{x}(t,T_{corr}),\boldsymbol{\Theta}_d)$ and $g_v(\mathbf{x}(t,T_{corr}),\boldsymbol{\Theta}_v)$ for the drift and shear capacity models, respectively. Note that $g_{T_{corr}}(t,\mathbf{x}_T,\boldsymbol{\Theta}_T)$ in Eq. (3-4) is the limit state function for corrosion initiation, not a limit state function for structural failure. The vector $\mathbf{x}$ of random variables is written as $\mathbf{x}=(\mathbf{x}_{\mathrm{r}},\mathbf{x}_{\mathrm{s}})$, where $\mathbf{x}_{\mathrm{r}}$ is a vector of material and geometry variables and $\mathbf{x}_{\mathrm{s}}$ is a vector of demand variables such as boundary forces and drifts. Considering the probabilistic model for corrosion initiation $T_{corr}(\mathbf{x}_T,\boldsymbol{\Theta}_T)$ and using the capacity models and diffusion model, $g_d(\mathbf{x}(t,T_{corr}),\boldsymbol{\Theta}_d)$ and $g_v(\mathbf{x}(t,T_{corr}),\boldsymbol{\Theta}_v)$ are formulated as

$$g_d\left(\mathbf{x}\left(t,T_{corr}\right),\boldsymbol{\Theta}_d\right)=C_d\left(\mathbf{x}\left(t,T_{corr}\right),\boldsymbol{\Theta}_d\right)-D_d \tag{3-22}$$

$$g_v\left(\mathbf{x}\left(t,T_{corr}\right),\boldsymbol{\Theta}_v\right)=C_v\left(\mathbf{x}\left(t,T_{corr}\right),\boldsymbol{\Theta}_v\right)-D_v \tag{3-23}$$

where T_{corr} is $T_{corr}(\mathbf{x}_T, \mathbf{\Theta}_T)$ from Eq. (3-3-2), $C_v(\mathbf{x}(t, T_{corr}), \mathbf{\Theta}_v)$ and $C_d(\mathbf{x}(t, T_{corr}), \mathbf{\Theta}_d)$ are the shear and drift capacities from Eqs. (3-10) and (3-18), and D_d and D_v denote the drift and shear demands. Note that D_d and D_v are part of $\mathbf{x}_s$.

The fragility of a structural component at time *t* is now written as

$$p_f(t) = F(t, \mathbf{x}_s, \mathbf{\Theta}_k, T_{corr}) = \mathrm{P}\left[\left\{g_k(\mathbf{x}_r(t, T_{corr}), \mathbf{x}_s, \mathbf{\Theta}_k) \le 0\right\} \mid t, \mathbf{x}_s, \mathbf{\Theta}_k, T_{corr}\right] \quad k = d, v \tag{3-24}$$

where $\mathrm{P}[A \mid \mathbf{x}_s]$ denotes the conditional probability of event *A* for the given values of variables $\mathbf{x}_s$. The uncertainty in the event for given $\mathbf{x}_s$ arises from the inherent randomness in the capacity variables $\mathbf{x}_r$, the inexact nature of the limit state model $g_k(\mathbf{x}(t, T_{corr}), \mathbf{\Theta}_k)$ (or its sub-models), and the uncertainty characterized by the model parameters $\mathbf{\Theta}_k$.

Predictive Estimates of Fragility

A "predictive" estimate of the fragility at time *t*, $\tilde{F}(t, \mathbf{x}_s)$, incorporates the uncertainties in the model parameters $\mathbf{\Theta}_k$ and T_{corr}, by characterizing $\mathbf{\Theta}_k$ and T_{corr} as random variables and taking the expectation of $F(t, \mathbf{x}_s, \mathbf{\Theta}_k, T_{corr})$ over the posterior distribution of $\mathbf{\Theta}_k$ and T_{corr}, i.e.,

$$\tilde{F}(t, \mathbf{x}_s, T_{corr}) = \int F(\mathbf{x}_s, \mathbf{\Theta}_k, T_{corr}) f(\mathbf{\Theta}_k) d\mathbf{\Theta}_k \tag{3-25}$$

$$\tilde{F}(t,\mathbf{x}_s) = \int F(t,\mathbf{x}_s,T_{corr}) f(T_{corr}) dT_{corr}$$
$$= \int \left\{ \int F(t,\mathbf{x}_s,\boldsymbol{\Theta}_k,T_{corr}) f(\boldsymbol{\Theta}_k) d\boldsymbol{\Theta}_k \right\} f(T_{corr}) dT_{corr} \quad (3\text{-}26)$$

where $f(\boldsymbol{\Theta}_k)$ and $f(T_{corr})$ are the probability density functions of $\boldsymbol{\Theta}_k$ and T_{corr}.

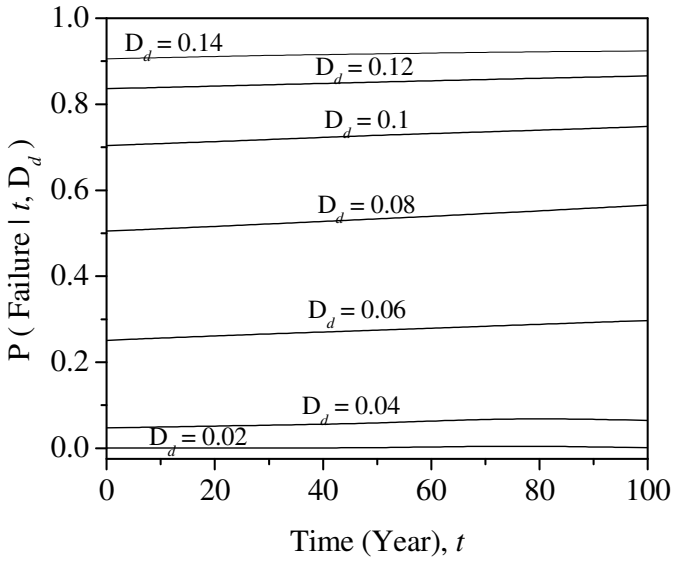

Fig. 3-2. Predictive fragility estimates for different drift demands

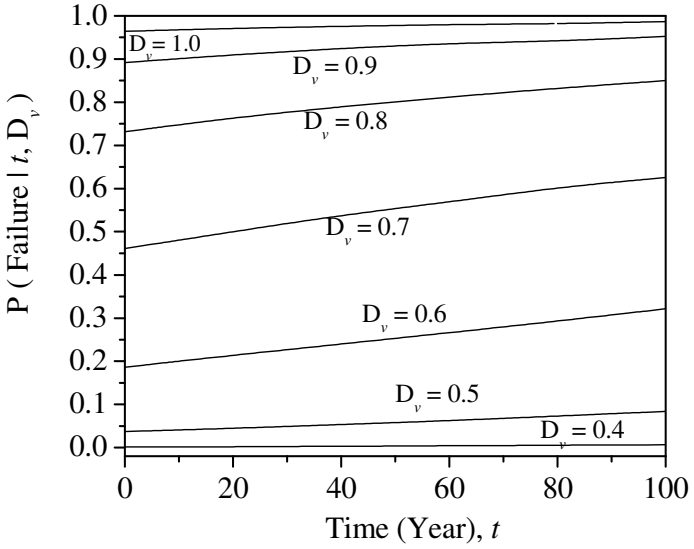

Fig. 3-3. Predictive fragility estimates for different shear demands

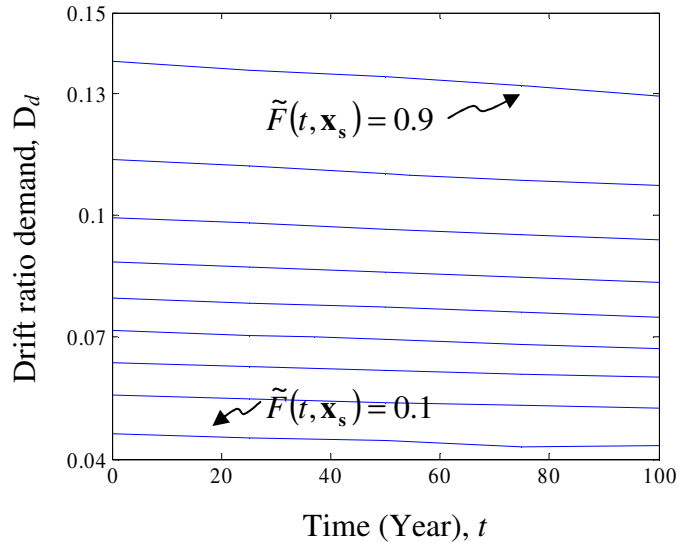

Fig. 3-4. Contour plot of predictive drift fragility

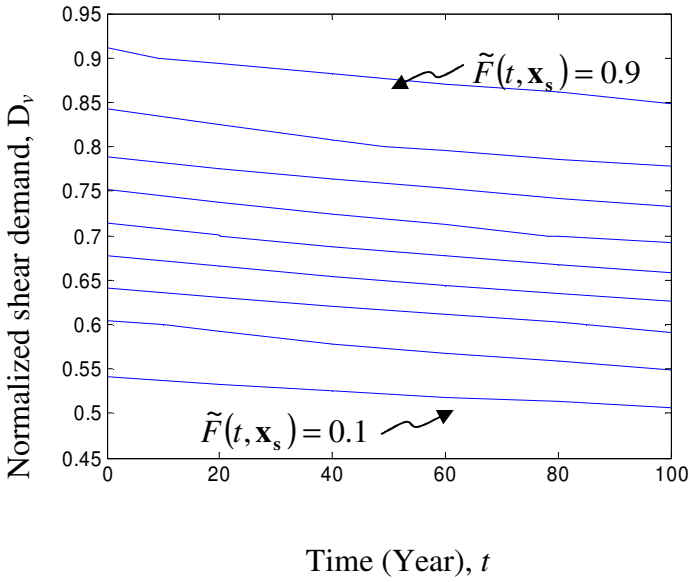

Fig. 3-5. Contour plot of predictive shear fragility

These fragility estimates incorporate the epistemic uncertainties in an average sense and the aleatory and epistemic uncertainties are no longer distinguished. Figs. 3-2 and 3-3 show predictive fragility estimates for varying drift and shear demands on the example column presented earlier as a function of time. Figs. 3-4 and 3-5 show the contour lines of the predictive fragility estimate as a function of time, and of drift and shear demands, respectively. Each contour line in this figure connects pairs of values of time t and drift demand D_d (Fig. 3-4) and time t and shear demand D_v (Fig. 3-5) that are associated with a given level of fragility in the range 0.1–0.9. Figs. 3-6 and 3-7 compare the predictive fragilities in Choe et al. (2007a) and the predictive fragilities based on probabilistic capacity models including the effect of corrosion for the drift and shear modes at time intervals of 25 years.

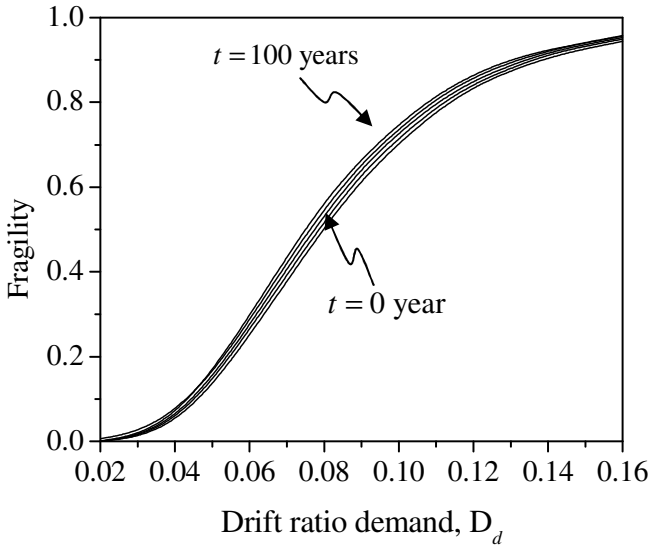

Fig. 3-6. Predictive fragility estimates of the example column for drift demand at intervals of 25 years

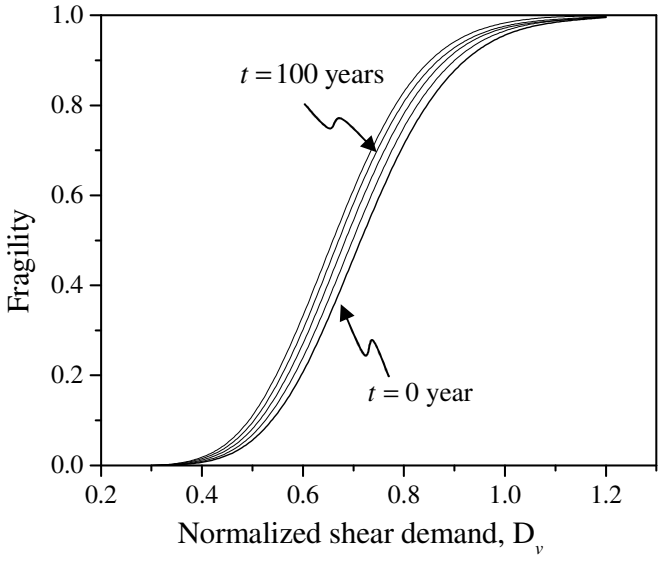

Fig. 3-7. Predictive fragility estimates of the example column for shear demand at intervals of 25 years

Sensitivity and Importance Measures

Sensitivity analysis is employed to determine to which parameter(s) the reliability of RC columns is most sensitive. Such results may provide physical insight and guidance in further data gathering and model development. To compute the sensitivity measures, I decompose $\mathbf{x}$ into a vector of constant parameters $\mathbf{x}_c$ and a vector of random variables $\mathbf{x}_p$, so that $\mathbf{x}$ can be written as $\mathbf{x} = (\mathbf{x}_c, \mathbf{x}_p)$. Also, let $f(\mathbf{x}_p, \boldsymbol{\Theta}_f)$ be the probability density function of the basic variables $\mathbf{x}_p$, where $\boldsymbol{\Theta}_f$ is a set of distribution parameters (e.g., means, standard deviations, correlation coefficients, or other

parameters defining the distribution). The vector $(\mathbf{x}_c, \boldsymbol{\Theta}_f)$ denotes the set of all parameters of the problem. The solution of the reliability problem depends on the value of $(\mathbf{x}_c, \boldsymbol{\Theta}_f)$. I find the *sensitivity of the reliability index*, $\nabla_{(\mathbf{x}_c, \boldsymbol{\Theta}_f)}\beta$, with respect to $(\mathbf{x}_c, \boldsymbol{\Theta}_f)$ following Hohenbichler and Rackwitz (1983) by conducting a first-order reliability analysis. Once $\nabla_{(\mathbf{x}_c, \boldsymbol{\Theta}_f)}\beta$ is known, the gradient of the first-order reliability approximation of the failure probability is obtained by using the chain rule of the differentiation as

$$\nabla_{(\mathbf{x}_c, \boldsymbol{\Theta}_f)} p_1 = -\varphi(\beta) \nabla_{(\mathbf{x}_c, \boldsymbol{\Theta}_f)}\beta \tag{3-27}$$

where $\varphi(\cdot)$ is the standard normal probability density function. The form $\nabla_{(\mathbf{x}_c, \boldsymbol{\Theta}_f)}\beta$ (or $\nabla_{(\mathbf{x}_c, \boldsymbol{\Theta}_f)} p_1$) can be used to identify to which parameter the fragilities are most sensitive, guiding us in determining what to change to make a component or structure safer.

Figs. 3-8 and 3-9 show the results of the sensitivity analysis for the drift mode, including the effect of corrosion. For brevity, only the drift mode is considered herein since, by design, it controls the probability of failure in case of a seismic event (Gardoni et al. 2002). The sensitivity with respect to the corrosion parameters (the parameters related to the corrosion initiation model) is seen to increase rapidly in the initial years since they regulate the beginning of the corrosion propagation phase. Once the corrosion phase has begun, their sensitivities reduce to close to zero. The opposite trend can be noticed for the sensitivities with respect to the parameters related to the structural capacity model. Their sensitivities increase in the first years when corrosion is not likely

to take place, decrease around the time of transition from the diffusion phase and the corrosion phase, and increase gradually back to the original values once the corrosion phase has begun. The measures presented above are useful as stand-alone measures of sensitivity. However, comparison between sensitivities is problematic because of different units.

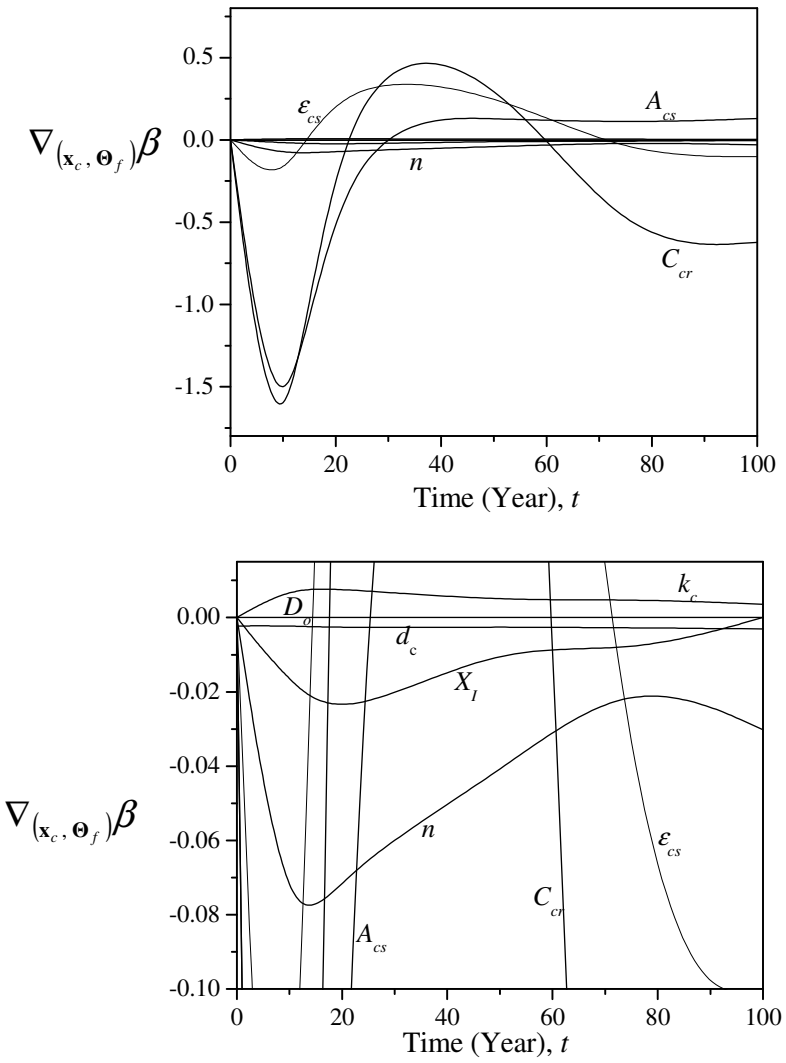

Fig. 3-8. Sensitivity measures for the drift failure mode of the diffusion model parameters (top) and close-up (bottom)

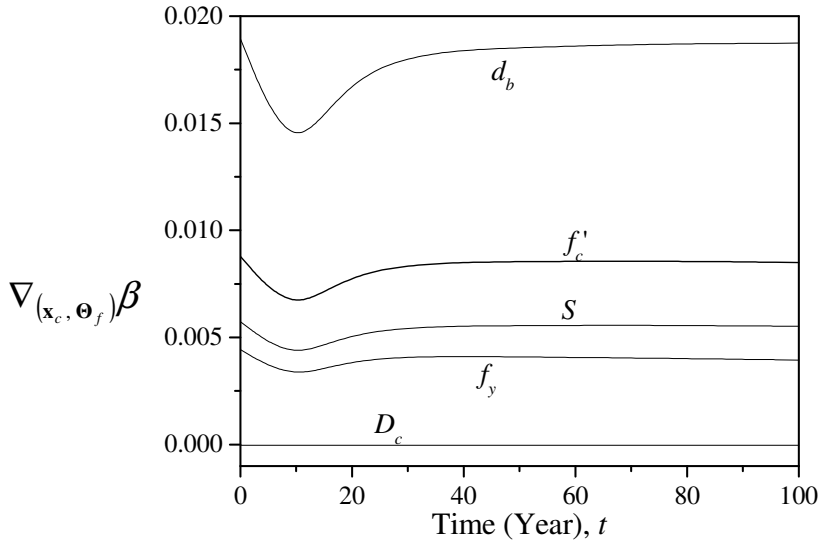

Fig. 3-9. Sensitivity measures for the drift failure mode of the structural parameters

In the limit state functions I have several random variables. Some random variables have a larger effect on the variance of the limit state function (and thus are more important) and some have a smaller effect (and thus are less important). Following Der Kiureghian and Ke [21], I define a *measure of importance* γ as

$$\gamma^T = \frac{\boldsymbol{\alpha}^T \mathbf{J}_{\mathbf{u}^*,\mathbf{z}^*} \mathbf{SD}'}{\left\| \boldsymbol{\alpha}^T \mathbf{J}_{\mathbf{u}^*,\mathbf{z}^*} \mathbf{SD}' \right\|} \tag{3-28}$$

where $\mathbf{z}$ is the vector of the random variables, $\mathbf{z} = (\mathbf{x}_p, \boldsymbol{\Theta})$ and $\mathbf{J}_{\mathbf{u}^*,\mathbf{z}^*}$ is the Jacobian of the probability transformation from the original space $\mathbf{z}$ to the standard normal space $\mathbf{u}$, with respect to the coordinates of the design point $\mathbf{z}^*$ (the most likely failure point). Matrix $\mathbf{SD}'$ is the standard deviation matrix of equivalent normal variables $\mathbf{z}'$ defined by the linearized inverse transformation $\mathbf{z}' = \mathbf{z}^* + \mathbf{J}_{\mathbf{z}^*,\mathbf{u}^*}(\mathbf{u} - \mathbf{u}^*)$ at the design point. The

elements of $\mathbf{SD}'$ are the square roots of the corresponding diagonal elements of the covariance matrix $\mathbf{\Sigma}' = \mathbf{J}_{\mathbf{z}^*,\mathbf{u}^*}\,\mathbf{J}^{\mathbf{T}}_{\mathbf{z}^*,\mathbf{u}^*}$ of the variables $\mathbf{z}'$.

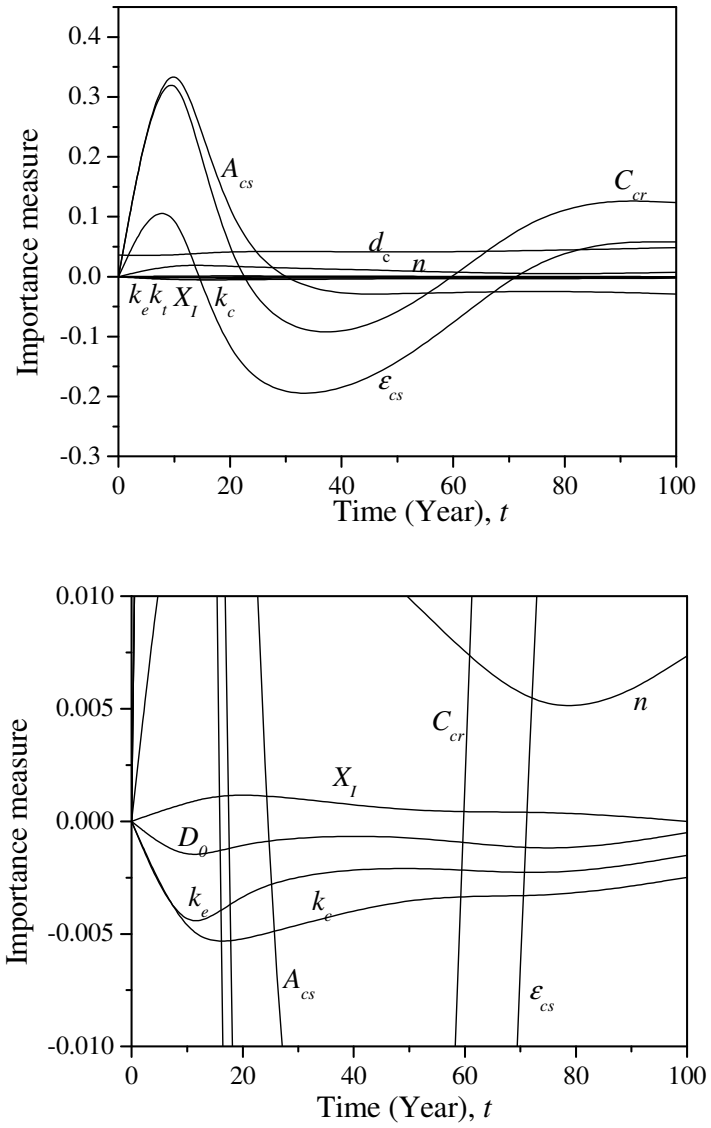

Fig. 3-10. Importance measures for the drift failure mode of the diffusion model random variables (top) and close-up (bottom)

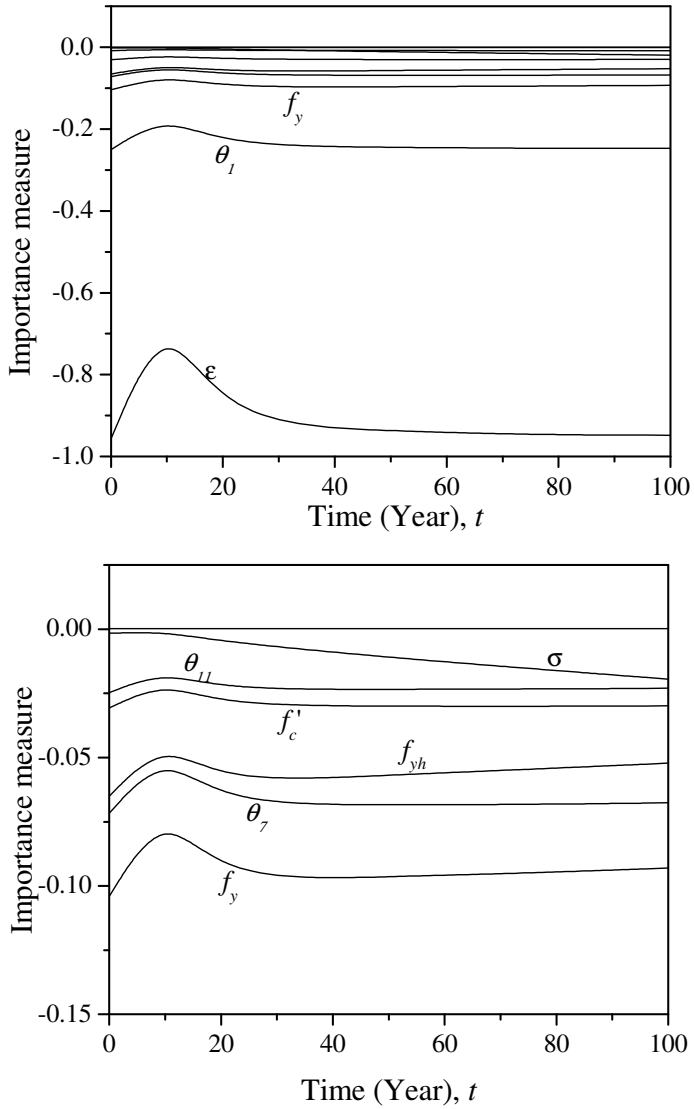

Fig. 3-11. Importance measures for the drift failure mode of the structural random variables (top) and close-up (bottom)

Figs. 3-10 and 3-11 show the importance measures for the drift failure modes with corrosion propagation. Fig. 3-10 suggests that C_{cr},, A_{cs} and ε_{cs} are the most important sources of uncertainty around the time of corrosion initiation. It is also

interesting to observe that the importance of the model uncertainty, σ, stays constant over the diffusion phase and increases with time thereafter (Fig. 3-11).

Conclusions

This chapter presents probabilistic capacity models for corroding reinforced concrete columns to estimate the fragility of deteriorated structural components. The models are applicable to existing and new columns that are subject to current or future deterioration and may be employed in service-life and life-cycle cost analyses. Fragility estimates for an example corroding column subjected to shear force and drift demands are developed using the models developed herein. The fragilities show that the shear force capacity degradation with corrosion is more rapid than the degradation of the drift capacity.

Sensitivity analysis for the example column indicates that the sensitivity with respect to the corrosion parameters (the parameters related to the corrosion initiation model) increases rapidly in the initial years of as they determine the beginning of the corrosion propagation phase. After the beginning of the corrosion phase their sensitivities reduce to close to zero. The opposite trend can be noticed for the sensitivities with respect to the parameters related to the structural capacity model. Their sensitivities increase in the first years, decrease around the time of transition from the diffusion phase and the corrosion phase, and they increasing gradually thereafter. Importance measures indicate that the model error of the structural capacity models are the most important random variable, as it is in the case of the pristine structure (Choe et al. 2007a). Parameter C_{cr} is the next most important random variable in the initial years,

while the importance of C_{cr} on the structural reliability diminishes after the corrosion propagation phase has begun.

CHAPTER IV

SEISMIC FRAGILITY ESTIMATES FOR REINFORCED CONCRETE BRIDGES SUBJECT TO CORROSION

In this research, novel probabilistic models for capacity and demand are merged to obtain fragility estimates for reinforced concrete bridges subject to corrosion. A probabilistic model for time-dependent chloride-induced corrosion is incorporated into previously developed probabilistic demand models for pristine bridge systems. Subsequently, the drift and shear force demand models are combined with previously developed capacity models for corroding bridge columns to obtain seismic fragility estimates. These estimates are applicable to the bridge systems with different combinations of chloride exposure condition, environmental oxygen availability, water-to-cement ratios, and curing conditions. Model uncertainties in the demand, capacity and corrosion models are considered, in addition to uncertainties in environmental conditions, material properties, and structural geometry. Sensitivity analyses of the deteriorating bridge are conducted to identify the components of the structure that contributes most to the reliability of the system in each failure mode. A single-bent bridge example typical of current California practice is presented to demonstrate the developed methodology.

Introduction

Corrosion of the reinforcement in reinforced concrete (RC) structures is a matter of increasing concern. Corrosion is a long-term process that effectively weakens structural elements and increases their vulnerability to extreme loads. The concerns include serviceability and safety limit-states, as well as economic costs due to maintenance and repair. In this chapter, particular attention is devoted to bridges subject to the seismic hazard. Due to the uncertainties in the corrosion process, the structural properties, and the demands on the structures due to an impending earthquake, it has been difficult to predict the seismic fragility of deteriorating RC bridges. The objectives of this chapter are: (1) to provide probabilistic demand models for RC bridge systems subject to earthquake ground motion, (2) to provide probabilistic capacity models that include time-dependent corrosion, (3) to estimate the ensuing seismic fragility, and (4) to identify the parameters, i.e., structural properties, environmental factors, and model parameters that have the highest influence on the seismic fragility estimates. It is emphasized that the utilized deterioration models incorporate uncertainties both in the structural properties and the material deterioration processes. This is significant because of the well-known presence of considerable uncertainty in these constituents.

Probabilistic capacity models for pristine (undamaged) RC columns are developed by Gardoni et al. (2002) and Choe et al. (2007a). The models, which are applicable to a wide array of RC columns with circular cross sections, account for uncertainties in a comprehensive manner. The uncertainties include model error arising

from inaccuracies in the model form and potentially missing variables, as well as measurement errors and statistical uncertainties. Choe et al. (2007b) incorporates deterioration into the probabilistic capacity models by employing a probabilistic corrosion model for the reinforcement (Dura-Crete 2000) and a time-dependent corrosion rate function (Vu and Stewart 2000).

Gardoni et al. (2002) developed probabilistic demand models by employing deterministic demand models used in practice as a starting point. Additional terms were included to explicitly describe the inherent systematic and random errors in the demand predictions. The developments included probabilistic models for drift and shear force demand of pristine RC bridge systems. In the present study, probabilistic demand models of deteriorating RC bridge systems are developed by incorporating the aforementioned probabilistic model for chloride-induced corrosion (Dura-Crete 2000) and the time-dependent corrosion rate function (Vu and Stewart 2000).

In this research, novel seismic fragility estimation and sensitivity analysis for deteriorating RC bridge systems are carried out. The work combines the new demand models for deteriorated RC bridge systems with the previously developed capacity models. A bridge design that is typical of current California practice is used to demonstrate the time-variant fragility assessment methodology. The fragility estimates consider different combinations of chloride exposure condition, environmental oxygen availability, water-to-cement ratios, and curing conditions. Model uncertainties in both the capacity and the corrosion models are considered, in addition to the uncertainties in the environmental conditions, material properties, and structural geometry. It is

emphasized that the models developed in this research are applicable to both existing and new RC bridges. Importantly, they may be used for the prediction of the service-life of existing and new structures as well as general-purpose life-cycle cost analysis for RC structures.

The five sections that are provided in this chapter cover – in this order – the corrosion modeling, the capacity modeling, the demand modeling, the fragility estimation methodology, and the parameter sensitivity studies. Novelties include the probabilistic modeling of the corrosion initiation time, the inclusion of corrosion both in the demand and the capacity models, the seismic fragility computation, and, importantly, parameter importance studies to provide physical insight into the effect of corrosion on RC bridge systems.

Corrosion Initiation Model

This study uses the probabilistic model of chloride-induced corrosion presented by Dura-Crete (2000) and the time-variant corrosion rate function by Vu and Stewart (2000) to predict the corrosion status of RC members. The corrosion model is extended to estimate the probability distribution of the corrosion initiation time. The model includes uncertainties in the structural parameters, environmental conditions, and model parameters. The original model for the corrosion initiation time reads

$$T_{corr} = X_I \cdot \left[\frac{d_c^{\,2}}{4 k_e k_t k_c D_0 (t_0)^n} \left[erf^{-1}\left(1 - \frac{C_{cr}}{C_s}\right) \right]^{-2} \right]^{\frac{1}{1-n}} \tag{4-1}$$

where d_c is the reinforcement cover depth, k_e is an environmental factor, k_t represents the influence of test methods to determine the empirical diffusion coefficient D_0, k_c is a parameter that accounts for the influence of curing, t_0 is the reference period for D_0, n is the age factor, X_1 is a model uncertainty coefficient to account for the idealization implied by Fick's second law, C_s is the chloride concentration on the surface, C_{cr} is the critical chloride concentration, and $erf(\cdot)$ is the error function. Dura-Crete (2000) provides the probability distributions for the parameters in Eq. (4-1). An application of the model in Eq. (4-1) is presented by Choe et al. (2007b). Of particular importance in this study is the availability of the cumulative distribution function (CDF) and the probability density function (PDF) for the corrosion initiation time:

$$\text{CDF: } F_{T_{corr}}(t_{corr}) = P[T_{corr} \le t_{corr}] \tag{4-2}$$

and

$$\text{PDF: } f_{T_{corr}}(t_{corr}) = \frac{\partial F_{T_{corr}}(t_{corr})}{\partial t_{corr}} \tag{4-3}$$

Given a realization of the corrosion initiation time, the deteriorated member properties, e.g. the corroded reinforcement area, is determined by the time-dependent corrosion rate function by Vu and Stewart (2000). For time instances less than T_{corr} the cross-section is assumed to match to the pristine cross-section. For time instances greater than T_{corr} the reinforcement bars are assumed to have a corroded dimension that is less than the original dimension, in accordance with Vu and Stewart (2000). The reduced

reinforcement area subsequently enters into the probabilistic capacity and demand models described in the following.

Probabilistic Capacity Models for Corroding Members

Gardoni et al. (2002) and Choe et al. (2007a) developed probabilistic capacity models for pristine RC columns. The general form of the probabilistic capacity models is

$$\mathbf{C} = \mathbf{C}(\mathbf{x}, \boldsymbol{\Theta}) \tag{4-4}$$

where $\mathbf{C} = (C_1, C_2, \cdots, C_k, \cdots, C_q)$, C_k is the capacity vector of interest, in which k indicates the mode of failure considered. The failure modes typically include drift and shear force. The vector $\mathbf{x} = (x_1, x_2, \ldots)$ is a set of measurable variables, e.g., material properties, member dimensions, and imposed boundary conditions. Finally, $\boldsymbol{\Theta} = (\boldsymbol{\Theta}_1, \boldsymbol{\Theta}_2, \cdots, \boldsymbol{\Theta}_k, \cdots, \boldsymbol{\Theta}_q)$ is a set of random model parameters introduced to fit the model to observed data.

Choe et al. (2007b) extended the aforementioned probabilistic capacity models for pristine RC columns to include corrosion. These models incorporate information about material deterioration to obtain the subsequent capacity degradations of the structure. The deterioration is estimated based on the probabilistic model for chloride induced corrosion outlined in the previous section.

A generic probabilistic capacity model for a corroding RC column at time t is now written as a function of time, t, as follows:

$$\mathbf{C}(t, \mathbf{x}_0, \boldsymbol{\Theta}) = \int_0^\infty \mathbf{C}(t, \mathbf{x}_0, \boldsymbol{\Theta} \mid T_{corr}) \cdot f_{T_{corr}}(t_{corr})\, dT_{corr} \tag{4-5}$$

where $\mathbf{x}_0$ is a set of measurable variables at the time of construction, $t = 0$, $\mathbf{C}(t, \mathbf{x}_0, \boldsymbol{\Theta} \mid T_{corr})$ is the conditional capacity for a given corrosion initiation time, and $f_{T_{corr}}(t_{corr})$ is the PDF from Eq. (4-3). The capacity $\mathbf{C}(t, \mathbf{x}_0, \boldsymbol{\Theta} \mid T_{corr})$ and the deteriorated member dimensions are calculated based on Choe et al. (2007b). The conditional capacity $\mathbf{C}(t, \mathbf{x}_0, \boldsymbol{\Theta} \mid T_{corr})$ during $t \le T_{corr}$ is assumed to be the same as the capacity at $t = 0$, denoted as $\mathbf{C}_0(\mathbf{x}_0, \boldsymbol{\Theta})$. Hence, Eq. (4-5) is rewritten as

$$\begin{aligned} \mathbf{C}(t, \mathbf{x}_0, \boldsymbol{\Theta}) &= \int_0^t \mathbf{C}(t, \mathbf{x}_0, \boldsymbol{\Theta} \mid T_{corr}) \cdot f_{T_{corr}}(t_{corr})\, dT_{corr} + \mathbf{C}_0(\mathbf{x}_0, \boldsymbol{\Theta}) \int_t^\infty f_{T_{corr}}(t_{corr})\, dT_{corr} \\ &= \int_0^t \mathbf{C}(t, \mathbf{x}_0, \boldsymbol{\Theta} \mid T_{corr}) \cdot f_{T_{corr}}(t_{corr})\, dT_{corr} + \mathbf{C}_0(\mathbf{x}_0, \boldsymbol{\Theta}) \left[1 - F_{T_{corr}}(t)\right] \end{aligned} \tag{4-6}$$

The probabilistic capacity models for the drift and shear failure mode are of particular interest in this study. In the following, the index δ denotes drift capacity and v denotes shear capacity. Hence, our attention is devoted to the capacity models $\mathbf{C} = (C_\delta, C_v)$. In accordance with the above notation, and introducing a logarithmic transformation, these models are denoted

$$C_\delta(t, \mathbf{x}_0, \boldsymbol{\Theta}_C \mid T_{corr}) = \ln\left[\delta(t, \mathbf{x}_0, \boldsymbol{\Theta}_C \mid T_{corr})\right] \tag{4-7}$$

$$C_v(t, \mathbf{x}_0, \boldsymbol{\Theta}_C \mid T_{corr}) = \ln\left[v(t, \mathbf{x}_0, \boldsymbol{\Theta}_C \mid T_{corr})\right] \tag{4-8}$$

where $\delta = \Delta / H$ is the drift capacity, in which Δ is the displacement capacity and H is the clear column height. $v = V / (A_g\, f_t^{'})$ is the normalized shear capacity, in which V is the shear capacity and A_g is the gross cross-sectional area. $\boldsymbol{\Theta}_C = (\boldsymbol{\theta}_{C\delta}, \boldsymbol{\theta}_{Cv}, \boldsymbol{\Sigma})$ is a set of random model parameters introduced to fit the models to observed data.

The generic form of the capacity models are

$$C_{\delta}(t,\mathbf{x}_0,\boldsymbol{\Theta}_C \mid T_{corr}) = \hat{c}_{\delta}(t,\mathbf{x}_0 \mid T_{corr}) + \gamma_{C\delta}(t,\mathbf{x}_0,\boldsymbol{\theta}_{C\delta} \mid T_{corr}) + \sigma_{C\delta}\varepsilon_{C\delta} \quad (4\text{-}9)$$

$$C_{v}(t,\mathbf{x}_0,\boldsymbol{\Theta}_C \mid T_{corr}) = \hat{c}_{v}(t,\mathbf{x}_0 \mid T_{corr}) + \gamma_{Cv}(t,\mathbf{x}_0,\boldsymbol{\theta}_{Cv} \mid T_{corr}) + \sigma_{Cv}\varepsilon_{Cv} \quad (4\text{-}10)$$

where $\hat{c}_{\delta}(t,\mathbf{x}_0 \mid T_{corr})$ and $\hat{c}_{v}(t,\mathbf{x}_0 \mid T_{corr})$] denote the selected deterministic capacity models, which are expressed as the natural logarithm of the deterministic drift and shear capacities, i.e., $\ln[\hat{\delta}(t,\mathbf{x}_0 \mid T_{corr})]$ and $\ln[\hat{v}(t,\mathbf{x}_0 \mid T_{corr})$, respectively. The deterministic model for drift capacity, $\hat{\delta}(t,\mathbf{x}_0 \mid T_{corr})$, includes the elastic component at the onset of yield as well as the inelastic component due to the plastic flow for a single corroded RC column. The elastic component of the drift considers (1) a flexural component based on a linear curvature distribution along the full column height, (2) a shear component of deformation due to shear distortion, and (3) a slip component; that is, the deformation due to the local rotation at the base caused by slipping of the longitudinal bar reinforcement. The quantities $\gamma_{C\delta}(t,\mathbf{x}_0,\boldsymbol{\theta}_{C\delta} \mid T_{corr})$ and $\gamma_{Cv}[t,\mathbf{x}_0,\boldsymbol{\theta}_{Cv} \mid T_{corr}]$ represent correction terms introduced to capture the bias inherent in the deterministic models. Further details on the capacity modeling are available in Choe et al. (2007b).

Probabilistic Demand Models for Deteriorated RC Bridges

Probabilistic Demand Models for Pristine Bridges

Gardoni et al. [6] developed probabilistic demand models for pristine RC bridge systems with components subject to multiple demands. Specifically, drift and shear demands were considered. As for the capacity models described in the previous section, the

demand models employ deterministic demand models used in practice, with additional terms that explicitly describe the inherent systematic and random errors. The model development incorporates nonlinear static push-over analysis followed by a nonlinear response spectrum analysis (Chopra and Goel 1999; Fajfar 2000).

The generic demand model for a bridge system consisting of s components, each subject to q different demands, is formulated as $s \times q$ multi-variate demand model. For a bridge system with s single-column bents, each subject to deformation and shear demand (δ and v), the demand models are written as

$$D_{i\delta}(\mathbf{x}_0, \boldsymbol{\Theta}_D) = \hat{d}_{i\delta}(\mathbf{x}_0) + \theta_{D\delta 1} + \theta_{D\delta 2}\hat{d}_{D\delta}(\mathbf{x}_0) + \sigma_{D\delta}\varepsilon_{i\delta} \qquad i = 1,...,s \qquad (4\text{-}11)$$

$$D_{iv}(\mathbf{x}_0, \boldsymbol{\Theta}_D) = \hat{d}_{iv}(\mathbf{x}_0) + \theta_{Dv1} + \theta_{Dv2}\hat{d}_{iv}(\mathbf{x}_0) + \theta_{Dv3}\hat{d}_{i\delta}(\mathbf{x}_0) + \sigma_{Dv}\varepsilon_{iv} \qquad i = 1,...,s \qquad (4\text{-}12)$$

where $D_{i\delta}(\mathbf{x}_0, \boldsymbol{\Theta}_D)$ and $D_{iv}(\mathbf{x}_0, \boldsymbol{\Theta}_D)$ are the natural logarithms of the predicted drift and shear demands for the *i*-th column of a bridge system, $\boldsymbol{\Theta}_D = (\boldsymbol{\theta}_{D\delta}, \boldsymbol{\theta}_{Dv}, \boldsymbol{\Sigma})$, where $\boldsymbol{\theta}_{D\delta} = (\theta_{D\delta 1}, \theta_{D\delta 2})$ and $\boldsymbol{\theta}_{Dv} = (\theta_{Dv1}, \theta_{Dv2}, \theta_{Dv3})$ are the sets of unknown model parameters, and $\hat{d}_{i\delta}(\mathbf{x}_0)$ and $\hat{d}_{iv}(\mathbf{x}_0)$ are the natural logarithms of the deterministic demand estimates for *i*-th column bent of the bridge system. Details and statistics for the unknown parameters are available in Gardoni et al. (2002).

Probabilistic Demand Model for Deteriorated Bridges

In this study, probabilistic demand models of corroded RC bridge are developed. This is achieved by integrating the previously described probabilistic model for chloride-induced corrosion with the probabilistic demand models described above.

To generalize the probabilistic demand models for deteriorated RC bridges, I derive similar formulations to those for the capacity models. The probabilistic demand models for a corroding RC column at a time instant t is written as a function of a set of measurable variables, $\mathbf{x}_0$, at the time of construction, and the set of unknown parameters $\boldsymbol{\Theta}_D$ as

$$\mathbf{D}(t,\mathbf{x}_0,\boldsymbol{\Theta}) = \int_0^\infty \mathbf{D}(t,\mathbf{x}_0,\boldsymbol{\Theta}_D \mid T_{corr}) \cdot f_{T_{corr}}(t_{corr})\, dT_{corr} \tag{4-13}$$

where $\mathbf{D}(t,\mathbf{x}_0,\boldsymbol{\Theta}_D \mid T_{corr})$ denotes the demand vector $\mathbf{D} = (D_\delta, D_v)$ for a given corrosion initiation time, and $f_{T_{corr}}(t_{corr})$ is the PDF defined in Eq. (4-3).

To investigate the influence of the corrosion process on the demands on RC bridge components I first assume that the demands are unaffected before the time t reaches the corrosion initiation time T_{corr}. By considerations similar to those previously carried out for the capacity models, the demand model at time t is written

$$\mathbf{D}(t,\mathbf{x}_0,\boldsymbol{\Theta}) = \mathbf{D}_0(\mathbf{x}_0,\boldsymbol{\Theta})\left[1 - F_{T_{corr}}(t)\right] + \int_0^t \mathbf{D}(t,\mathbf{x}_0,\boldsymbol{\Theta} \mid T_{corr}) \cdot f_{T_{corr}}(t_{corr})\, dT_{corr} \tag{4-14}$$

where $\mathbf{D}_0(\mathbf{x}_0,\boldsymbol{\Theta})$ is the demand for the pristine structure. To determine $\mathbf{D}(t,\mathbf{x}_0,\boldsymbol{\Theta} \mid T_{corr})$ in Eq. (4-14), I take the followings steps: (a) estimate the corrosion initiation time based on the model in Eq. (4-1); (b) calculate the deteriorated reinforcement area in the members; and (c) replace the pristine reinforcement with the deteriorated one in the analytical model of the bridge. Next steps (b) and (c) are described in detail.

In the computations outlined above the time-dependent corrosion rate developed by Vu and Stewart [5] is applied to predict the loss of steel cross-section area. The

corrosion rate is suggested to diminish with time because corrosion products formed around the bar impede the diffusion of iron ions. The corrosion current density at time t is expressed as

$$i_{corr}(t) = 0.85\, i_{corr,0}\, (t - T_{corr})^{-0.29}, \quad t \geq T_{corr} \tag{4-15}$$

where $i_{corr,0}$ denotes the corrosion current density at the initiation of corrosion propagation; namely

$$i_{corr,0} = \frac{37.5(1 - w/c)^{-1.64}}{d_c} \quad (\mu A / cm^2) \tag{4-16}$$

where *w*/*c* represents the variable water-to-cement ratio and d_c is cover depth which is a dimension from the surface of steel bar to the surface of concrete structure.

After the corrosion process initiates, the diameter of the reinforcement is assumed to decrease over time as (Choe et al. 2007b)

$$d_b(t \mid T_{corr}) = \begin{cases} d_{b0} & t \leq T_{corr} \\ d_{b0} - \dfrac{1.0508\,(1 - w/c)^{-1.64}}{d}(t - T_{corr})^{0.71} & T_{corr} < t \leq T_f \\ 0 & t > T_f \end{cases} \tag{4-17}$$

where d_{b0} is the diameter of the reinforcement at time $t = 0$, and T_f is the time when $d_b(t \mid T_{corr})$, in theory, reaches zero: $T_f = T_{corr} + d_{bi}\{d / [1.0508\,(1 - w/c)^{-1.64}]\}^{1/0.71}$.

Once the corroded member dimension at time *t* is calculated by Eq. (4-17), an analytical model of the RC bridge system having the new dimensions is constructed. Push-over analysis and nonlinear response spectrum analysis are performed with the new

analytical model – in the same manner as for the pristine structures – to determine the deterministic term in the demand models.

Using Eqs. (3-11) and (3-12) and the simplifications of these equations provided by Gardoni et al. (2002), the proposed demand models for the corroded RC bridge are expressed as

$$D_{i\delta}(t,\mathbf{x}_0,\boldsymbol{\Theta}_D \mid T_{corr}) = 0.61 + 3.90\theta_{D\delta 2} + (1+\theta_{D\delta 2})\hat{d}_{i\delta}(t,\mathbf{x}_0 \mid T_{corr}) + \sigma_{D\delta}\varepsilon_{i\delta} \quad i = 1,\ldots,s \tag{4-18}$$

$$\begin{aligned} D_{iv}(t,\mathbf{x}_0,\boldsymbol{\Theta}_D \mid T_{corr}) = {} & \hat{d}_{iv}(t,\mathbf{x}_0 \mid T_{corr}) + \theta_{Dv1} + \theta_{Dv2}\hat{d}_{iv}(t,\mathbf{x}_0 \mid T_{corr}) \\ & + \theta_{Dv3}\hat{d}_{i\delta}(t,\mathbf{x}_0 \mid T_{corr}) + \sigma_{Dv}\varepsilon_{iv} \qquad i = 1,\ldots,s \end{aligned} \tag{4-19}$$

where $D_{i\delta}(t,\mathbf{x}_0,\boldsymbol{\Theta}_D \mid T_{corr})$ and $D_{iv}(t,\mathbf{x}_0,\boldsymbol{\Theta}_D \mid T_{corr})$ are the natural logarithm of the predicted drift and shear demand on the *i*-th column of the RC bridge system at time *t*, given T_{corr}. The terms $\hat{d}_{i\delta}(t,\mathbf{x}_0 \mid T_{corr})$ and $\hat{d}_{iv}(t,\mathbf{x}_0 \mid T_{corr})$ are the natural logarithm of the deterministic drift and shear model at time *t*. The set of unknown model parameters $\boldsymbol{\Theta}_D$ is assumed not to vary with time. Estimation of the corroded member dimension is dependent on exposure condition, environmental oxygen availability, water-to-cement ratios, and curing conditions. Choe et al. (2007b) describes the procedure in detail.

The deterministic models, $\hat{d}_{i\delta}(t,\mathbf{x}_0 \mid T_{corr})$ and $\hat{d}_{iv}(t,\mathbf{x}_0 \mid T_{corr})$, are determined following Gardoni et al.(2002), where d_{b0} is replaced by $d_b(t \mid T_{corr})$. For any specific bridge, the deterioration of the structure at time *t* is estimated by using the case-specific environmental conditions and material properties.

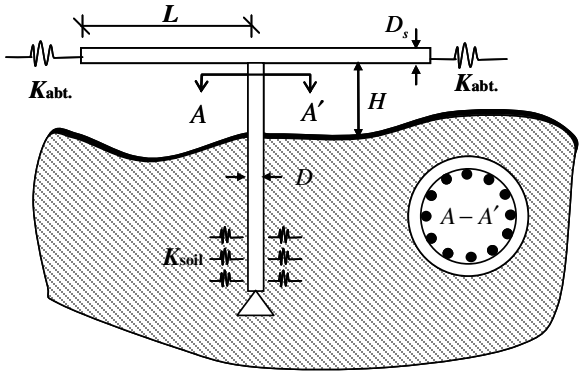

Fig. 4-1. Example single-bent over pass

Table 4-1. Variables for the pristine single-bent bridge.

Description	Parameter	Value/Distribution
Span length (right and left)	L [mm]	18,300
Span-to-column height ratio	L/H	2.4
Column-to-superstructure dimension ratio	D/D_s	0.75
Concrete nominal strength	f_c' [MPa]	LN(27.6, 2.76)
Reinforcement nominal yield strength	f_y [MPa]	LN(448.2, 22.4)
Initial longitudinal reinforcement ratio of column	ρ_{l0}	2.0%
Initial transverse reinforcement ratio of column	ρ_{s0}	0.7%
Soil stiffness based on NEHRP groups (FEMA-273, 1997)	K_{soil}	B
Additional bridge dead load (as a ratio of the dead weight)	r	N(0.1, 0.025)

Seismic Fragility Estimates

A seismic fragility study of an example RC bridge system is carried out to demonstrate the methodology and models presented above. The selected RC bridge is an highway overpass bridge with geometry and material properties that are representative of currently constructed highway bridges in California. The bridge is designed by Mackie

and Stojadinovic (2001) according to Caltrans' Bridge Design Specification and Seismic Design Criteria (2000). The single-bent bridge with Type I integral pile shaft foundations that extend the columns with the same cross-sections into the soil, as designed by Caltrans (2000), is shown in Fig. 4-1. The design parameters of interest for the considered bridge system are listed in Table 4-1. To estimate the corrosion initiation and propagation I assume that the bridge is constructed in a splash zone with water-to-cement ratio of the concrete material equal to 0.5, and that the zone is subjected to many humid-dry cycles.

Fig. 4-2 shows the capacity degradation and the demand shift of the example RC bridge system over time. The presented quantities are mean point estimates along with confidence bounds computed as $\pm$ 1 standard deviation of the model error, σ_{Dk}. The variations in the capacity and the demand in the drift failure mode are shown in the top plot. The variations in the capacity and the demand in the shear failure mode are show in the bottom plot. In a heuristic manner, the plots in Fig. 4-2 illustrates that the overlapping area between the capacity and the demand distributions increase, which implies that the fragility increases over time due to corrosion.

In this study, I develop a methodology for estimating seismic fragilities of deteriorated RC bridges having multiple failure modes. This is achieved by solving the reliability problem that incorporates both the structural capacities and the corresponding demands, given an earthquake ground motion. For this purpose, the OpenSees platform (McKenna and Fenves 2000) is extended to include the models for the corrosion initiation, the corrosion rate, and the loss of the section area of the reinforcement.

Moreover, the nonlinear push-over analyses for the deteriorated single-bent RC bridge, which produce the deterministic deformations and shear demands, are performed in the OpenSees software by extending it with an optimization algorithm. The Nelder-Mead Simplex Method (Nelder and Mead 1995) is used in this study as the optimization algorithm to find the bilinear force-displacement relation from the push-over curve of the structure.

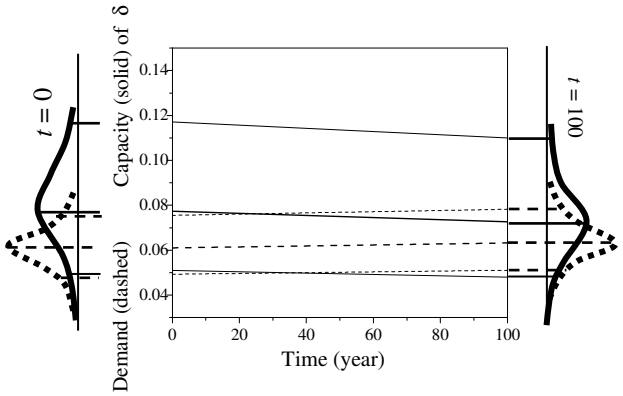

(a) Drift failure mode

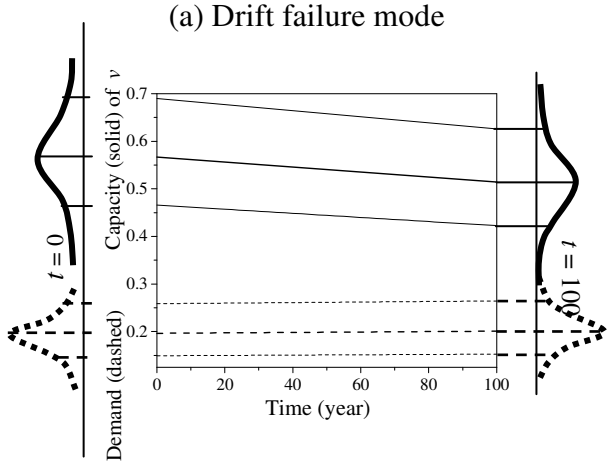

(b) Shear failure mode

Fig. 4-2. Capacity degradation (solid line) and demand increment (dash line) of RC bridge system, subject to an earthquake ground motion, due to corrosion, S_a =2.0

To account for uncertainties in the material properties I assume the following probability distributions: The compressive strength of concrete, f_c', has the lognormal distribution with mean 27.6 MPa and 10% coefficient of variation. The yield stress of the longitudinal reinforcement, f_y, has the lognormal distribution with mean 448.2 MPa and 5% coefficient of variation. To consider the variability in the axial load for the single-bent overpass I assume the additional bridge dead load has the normal distribution with mean equal to 10% of the dead weight and a 25% coefficient of variation. The parameter values that enter into the probabilistic models for the selected environmental and material conditions are provided in Table 4-2, in accordance with the values provided by Dura-Crete (2000). The initial value of the longitudinal reinforcement ratio is 2%, and the transverse reinforcement ratio is set to 0.7%.

Table 4-2. Diffusion model parameter statistics used to estimate the status of corrosion initiation

	d (mm)	k_e	k_c	k_t	D_0 (mm^2/yr)	n	C_{cr}	A_{cs}	ε_{cs}
Mean	38.1	0.924	2.40	0.832	473	0.362	0.900	7.76	0.000
St. dev.	11.4	0.155	0.700	0.024	43.2	0.245	0.150	1.36	1.11

Following Gardoni et al. (2002) the conditional probability of failure for the pristine structure is written in terms of a given spectral acceleration S_a as

$$F_0(S_a,\boldsymbol{\Theta}) = P\left[\bigcup_i \bigcup_k \{g_{0ik}(S_a,\mathbf{x}_0,\boldsymbol{\Theta}_k) \le 0\} \,\middle|\, S_a\right] \tag{4-20}$$

where

$$g_{0ik}(S_a,\mathbf{x}_0,\boldsymbol{\Theta}_k) = C_{0ik}(\mathbf{x}_0,\boldsymbol{\Theta}_{Ck}) - D_{0ik}(\mathbf{x}_0,\boldsymbol{\Theta}_{Dk} \mid S_a) \qquad k = \delta, v \quad i = 1, 2, \cdots \tag{4-21}$$

For the purpose of the present study, the fragility of the deteriorating RC bridge systems is expressed as

$$F(t,S_a,\boldsymbol{\Theta}) = P\left[\bigcup_i \bigcup_k \{g_{ik}(t,S_a,\mathbf{x}_0,\boldsymbol{\Theta}_k) \le 0\} \mid t, S_a\right] \tag{4-22}$$

where

$$g_{ik}(t,S_a,\mathbf{x}_0,\boldsymbol{\Theta}_k) = C_{ik}(t,\mathbf{x}_0,\boldsymbol{\Theta}_{Ck}) - D_{ik}(t,\mathbf{x}_0,\boldsymbol{\Theta}_{Dk} \mid S_a) \qquad k = \delta, v \quad i = 1, 2, \cdots \tag{4-23}$$

I observe the following relation between the limit state functions of the deteriorated and the pristine structures:

$$\begin{aligned} g_{ik}(t,S_a,\mathbf{x}_0,\boldsymbol{\Theta}_k) &= C_{ik}(t,\mathbf{x}_0,\boldsymbol{\Theta}_{Ck}) - D_{ik}(t,S_a,\mathbf{x}_0,\boldsymbol{\Theta}_{Dk} \mid S_a) \\ &= g_{0ik}(S_a,\mathbf{x}_0,\boldsymbol{\Theta}_k)\left[1 - F_{T_{corr}}\right] \\ &\quad + \int_0^t \left[C_{ik}(t,\mathbf{x}_0,\boldsymbol{\Theta}_{Ck} \mid T_{corr}) - D_{ik}(t,S_a,\mathbf{x}_0,\boldsymbol{\Theta}_{Dk} \mid T_{corr})\right] \cdot f_{T_{corr}}(t_{corr})\, dT_{corr} \end{aligned} \tag{4-24}$$

By incorporating the uncertainties in the model parameters $\boldsymbol{\Theta}$, a predictive estimate of fragility $\tilde{F}(t,S_a)$ is obtained. This is akin to taking the expected value of $F(t,S_a,\boldsymbol{\Theta})$ over the posterior distribution of $\boldsymbol{\Theta}$. Consequently, the fragility $\tilde{F}(t,S_a)$ of the deteriorated RC bridge system at time *t*, given an earthquake with intensity S_a, is

$$\tilde{F}(t,S_a) = \int F(t,S_a,\boldsymbol{\Theta}) f_{\Theta}(\boldsymbol{\Theta}) d\boldsymbol{\Theta} \tag{4-25}$$

where $F(t, S_a, \boldsymbol{\Theta})$ can be obtained from Eq. (4-22).

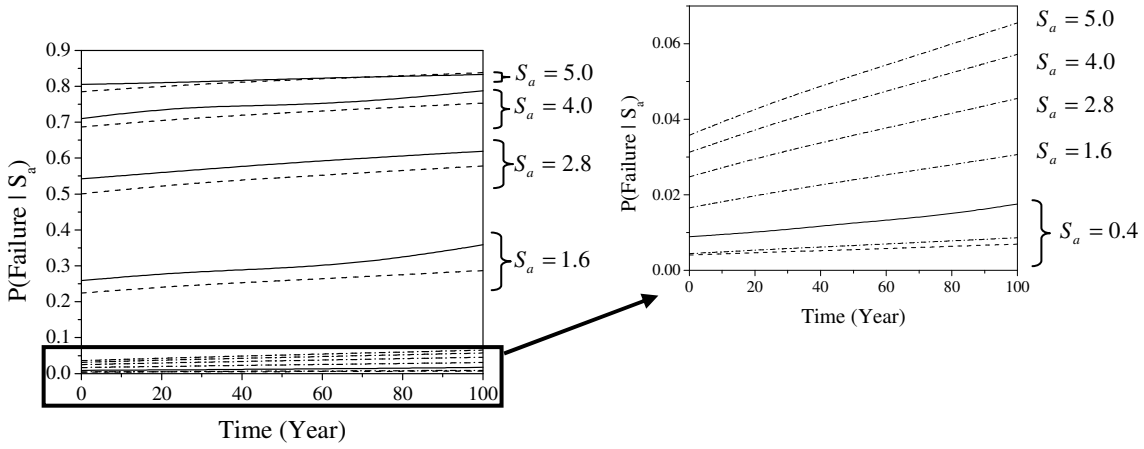

Fig. 4-3. Fragility estimates given S_a for drift (dashed), shear (dash-dotted), and drift and shear (solid) failure mode, with intervals 1.2 of S_a.

Fig. 4-3 shows the fragility estimates for the example single-bent bridge over time given a spectral acceleration S_a for the drift failure mode (dashed lines), the shear failure mode (dash-dotted lines), and the combined drift and shear failure mode (solid lines). Interestingly, I observe that the drift failure model dominates the fragility. This is consistent with the design approach used by Caltrans (1999). I also observe that the fragility increases with time due to the corrosion of the reinforcement. Fig. 4-4 provides the contour plot of the fragility surfaces as a function of time t and spectral acceleration S_a. The contour lines connect pairs of values of time *t* and S_a that are associated with a given level of fragility. The top plot in Fig. 4-4 shows the fragility contours for the drift failure mode (dashed lines) and for the combined drift and shear failure mode (solid

lines). The bottom plot in Fig. 4-4 shows the fragility contours for the shear failure mode. Fig. 4-5 compares the fragilities of the pristine and the deteriorated bridge using the developed probabilistic demand models. In the figure, the pristine bridge is compared with the bridge 100 years after construction. The fragilities reflect the capacity degradation and demand shift for the different failure modes. An increased fragility over time is again observed.

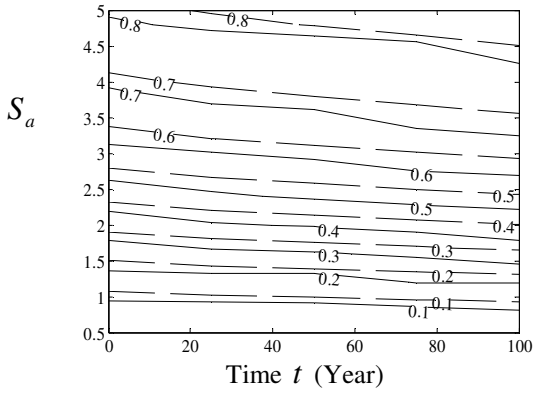

(a) Drift (dashed), and drift and shear (solid) failure mode

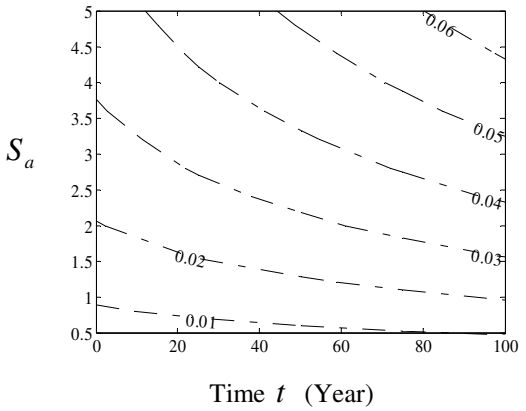

(b) Shear failure mode

Fig. 4-4. Contour plot of fragility $\tilde{F}(t, S_a)$

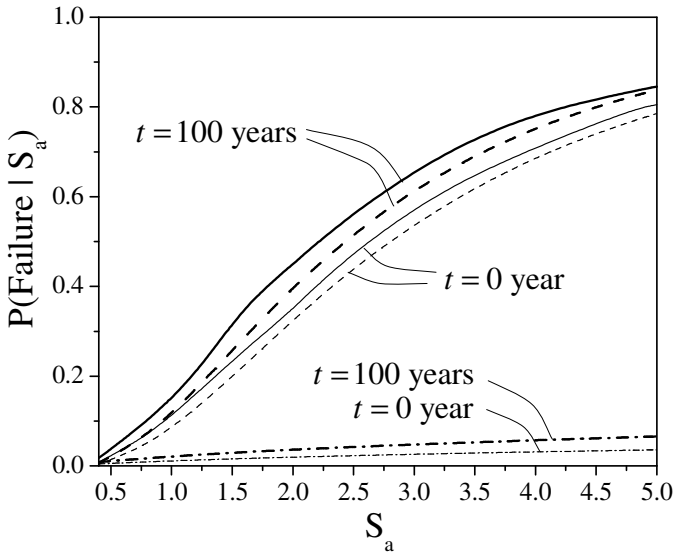

Fig. 4-5. Fragility estimates of example bridge system for drift (dashed), shear (dash-dotted), and drift and shear (solid) failure mode, with time interval 100 years.

Parameter Sensitivity Studies

The novel fragility estimates provided in this study are complemented with a parameter sensitivity study. It is argued that the utilization of sophisticated prediction models should generally be accompanied by such sensitivity studies to assess the confidence in the results, and to gain physical insight. From this viewpoint, the reliability analysis approach is particularly appealing. In fact, several parameter sensitivity and importance measures are available from traditional reliability sensitivity analysis. The distinction is made between sensitivity vectors – that essentially provide derivatives that may have different units and thus cannot be compared – and importance vectors, which have been

normalized to enable a parameter ranking. Importance vectors are in focus in this study. These may be employed in the decision making process for maintenance scheduling, as well as in a life-cycle cost analysis to determine where resources should be allocated to minimize the fragility of the structures in a network.

For the purpose of subsequent developments, the classical sensitivity of the reliability index is first introduced. It is expressed as $\nabla_{(\mathbf{x}_c,\boldsymbol{\Theta}_f)}\beta$, which is the derivative of the reliability index β with respect to $(\mathbf{x}_c,\boldsymbol{\Theta}_f)$, where $\mathbf{x}=(\mathbf{x}_c,\mathbf{x}_p)$. Here, $\mathbf{x}_c$ is the vector of deterministic parameters in the limit-state function, $\mathbf{x}_p$ is the vector of random variables, and $\boldsymbol{\Theta}_f$ is a set of distribution parameters; e.g., means, standard deviations, and correlation coefficients. In first-order reliability analysis (FORM), $\nabla_{(\mathbf{x}_c,\boldsymbol{\Theta}_f)}\beta$ is obtained according to the reliability sensitivity analysis developed by Hohenbichler and Rackwitz (1983) and Bjerager and Krenk (1989).

In this study the reliability index is considered to be a function of time: $\beta=\beta(t)$. In this case, the sensitivity is expressed as $\nabla_{(\mathbf{x}_f,\boldsymbol{\Theta}_f)}\beta(t)$, in which the derives of the FORM reliability approximation of the failure probability is obtained by the chain rule of the differentiation:

$$\nabla_{(\mathbf{x}_f,\boldsymbol{\Theta}_f)}p_1(t)=-\varphi\left[\beta(t)\right]\nabla_{(\mathbf{x}_f,\boldsymbol{\Theta}_f)}\beta(t) \tag{4-26}$$

where $\varphi(\cdot)$ is the standard normal PDF.

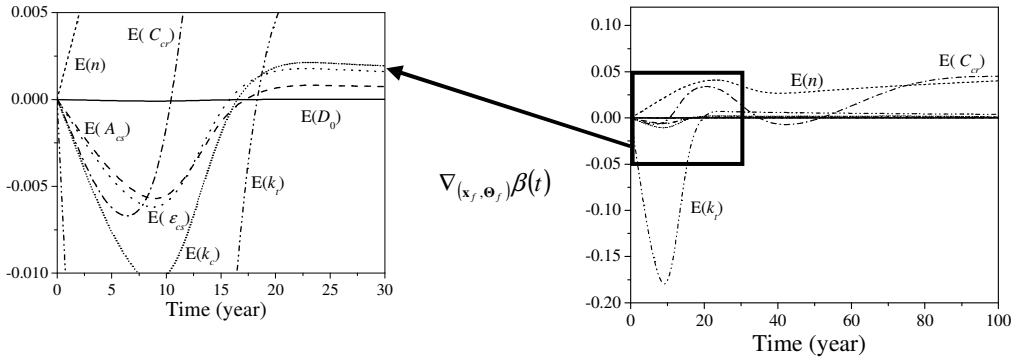

(a) Drift failure mode

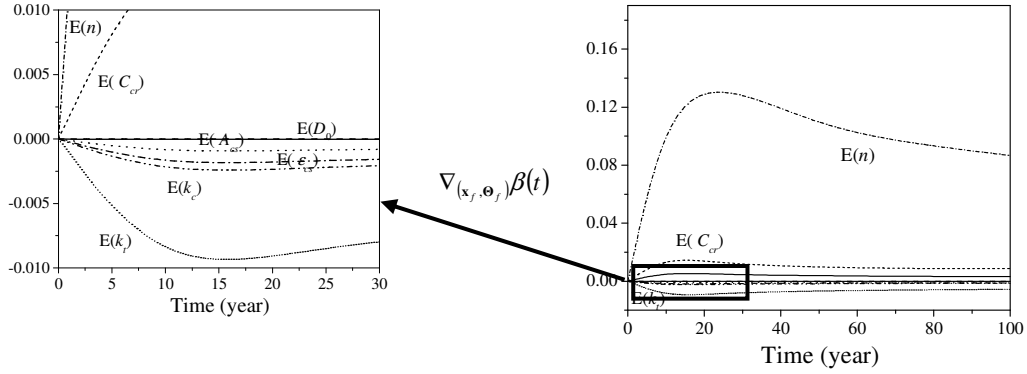

(b) Shear failure mode

Fig. 4-6. Sensitivity measures of the means of diffusion model parameters for the drift (top) and shear (bottom) failure mode, S_a =2.8

Although the components of the gradient $\nabla_{(\mathbf{x}_f,\boldsymbol{\Theta}_f)}\beta(t)$ (or $\nabla_{(\mathbf{x}_f,\boldsymbol{\Theta}_f)}p_1(t)$) have different units and thus cannot be employed for ranking of parameters, it is valuable to plot the sensitivity of the fragility to changes in various parameters. Fig. 4-6 shows the sensitivity over time, reflecting the effects of corrosion. In the first years, the sensitivity with respect to the corrosion parameters (the parameters related to the corrosion

initiation model) is shown to increase rapidly since they regulate the beginning of the corrosion propagation phase. Once the corrosion phase has begun, their sensitivities diminish. Moreover, the corrosion initiation is observed to have a more pronounced effect on the sensitivity measures for the drift failure mode than for the shear failure mode.

Fig. 4-7 illustrates the sensitivity with respect to the parameters related to the structural model. The parameters include the mean of several random variables, as well as several deterministic structural parameters. Different over-time variations are observed for the drift and shear failure mode. For the drift failure mode, the sensitivity of d_{sp0} keep increasing over time, having a soft peak at the transition from the diffusion phase to the corrosion phase. The sensitivity of d_{b0} is trended downward with a similar transition peak between the phases. In contrast, for the shear failure mode, the diameter size of the longitudinal reinforcement at initial construction (d_{b0}) becomes more and more sensitive as the corrosion develops. The trends observed in Fig. 4-7 are consistent with the form of the capacity model used in this study. Specifically, the effect of the longitudinal reinforcement on the shear capacity is included as a correction term in the capacity models developed by Gardoni et al. (2002). In that study, the significance of this term was assessed using 106 experimental observations through a Bayesian framework. In the presented study, the effect of the longitudinal reinforcement on the capacity is confirmed by its sensitivity for the deteriorated structure. Furthermore, the negative value of the sensitivity with respect to the spacing of the transverse

reinforcement, S, is observed. As expected, this implies that the fragility decreases when S increases.

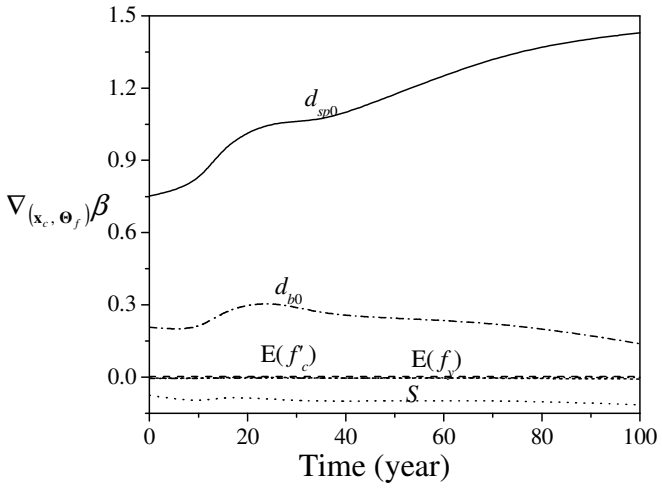

(a) Drift failure mode

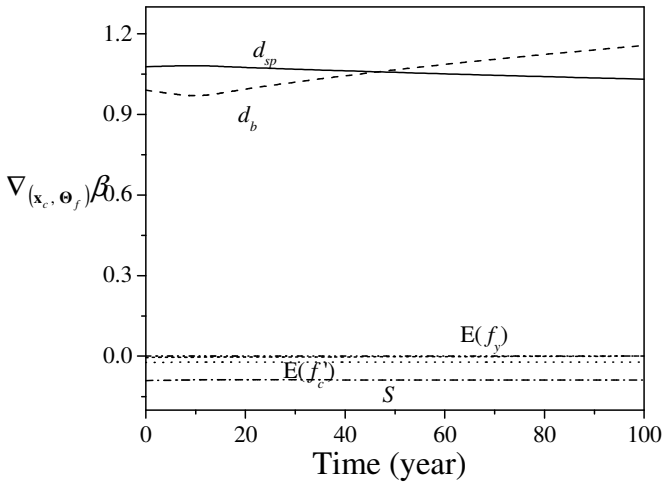

(b) Shear failure mode

Fig. 4-7. Sensitivity measures of the means of structural parameters for the drift (top) and shear (bottom) failure mode, S_a =2.8

As mentioned above, the sensitivity results cannot be used to rank the parameters according to their relative importance because of inhomogeneous units. To enable such rankings, the importance vector $\boldsymbol{\gamma}$ from Haukaas and Der Kiureghian (2005) is used. It reads

$$\boldsymbol{\gamma}^T = \frac{\boldsymbol{\alpha}^T \mathbf{J}_{\mathbf{u}^*,\mathbf{z}^*} \mathbf{SD}'}{\left\| \boldsymbol{\alpha}^T \mathbf{J}_{\mathbf{u}^*,\mathbf{z}^*} \mathbf{SD}' \right\|} \tag{4-27}$$

where $\mathbf{z}$ is the vector of the random variables, $\mathbf{z} = (\mathbf{x}_p, \boldsymbol{\Theta})$ and $\mathbf{J}_{\mathbf{u}^*,\mathbf{z}^*}$ is the Jacobian through which the probability is transformed from the original space $\mathbf{z}$ into the standard normal space $\mathbf{u}$, with respect to the coordinates of the most likely failure realization, $\mathbf{z}^*$. $\mathbf{SD}'$ is the standard deviation matrix of the equivalent normal variables $\mathbf{z}'$ which are defined by the linearized inverse transformation $\mathbf{z}' = \mathbf{z}^* + \mathbf{J}_{\mathbf{z}^*,\mathbf{u}^*}(\mathbf{u} - \mathbf{u}^*)$ at the most likely failure realization. The matrix $\mathbf{SD}'$ consists of the elements that are the square root of the corresponding diagonal elements of the covariance matrix $\boldsymbol{\Sigma}' = \mathbf{J}_{\mathbf{z}^*,\mathbf{u}^*} \mathbf{J}^{\mathbf{T}}_{\mathbf{z}^*,\mathbf{u}^*}$ of the variables $\mathbf{z}'$.

Fig. 4-8 shows the variation of the components of the importance vector $\boldsymbol{\gamma}$ for the random variables of the diffusion model. It is observed that the parameters related to the drift failure mode are highly significant for the corrosion initiation process, while those for the shear failure mode are less important. It is concluded that for the bridge under consideration the shear failure mode is less affected by corrosion compared with the drift failure mode. Fig. 4-9 presents the importance vector values associated with the random variables that represent the structural model. For the drift failure mode the

uncertainty in $\varepsilon_{D\delta}$ and $\varepsilon_{C\delta}$ are seen to be the most important. This agrees with the results in Choe et al.(2007a; 2007b). It is furthermore observed that the importance of the uncertainty in f_c' and f_y are more important for the corrosion process than those in $\boldsymbol{\Theta}$. The bottom plot in Fig. 4-9 is associated with the shear failure mode, in which it is observed that ε_{Dv} and ε_{Cv} represent the most important sources of uncertainty. It is also observed that the importance of θ_{Dv3}, which represents the effect of drift in the shear failure mode, increases as the corrosion propagates. This implies that the two failure modes are correlated and that this relationship is affected by corrosion.

Conclusions

The developments in this research include probabilistic demand models for deteriorating RC bridge systems for a given earthquake intensity, S_a. It is shown that the demands on the bridge increase as the deteriorating process unfolds. Furthermore, seismic fragility estimates are presented that reflects the effects of both capacity degradation and demand variation due to corrosion. The reliability analyses presented in this research involve multiple modes of failure; using the demand models developed in this research as well as previously developed capacity models. The models are applicable to existing and new columns that are subject to current or future deterioration. Importantly, they may be employed in service-life and life-cycle cost analyses. Uncertainties in the corrosion models, the capacity models, and the demand models are considered.

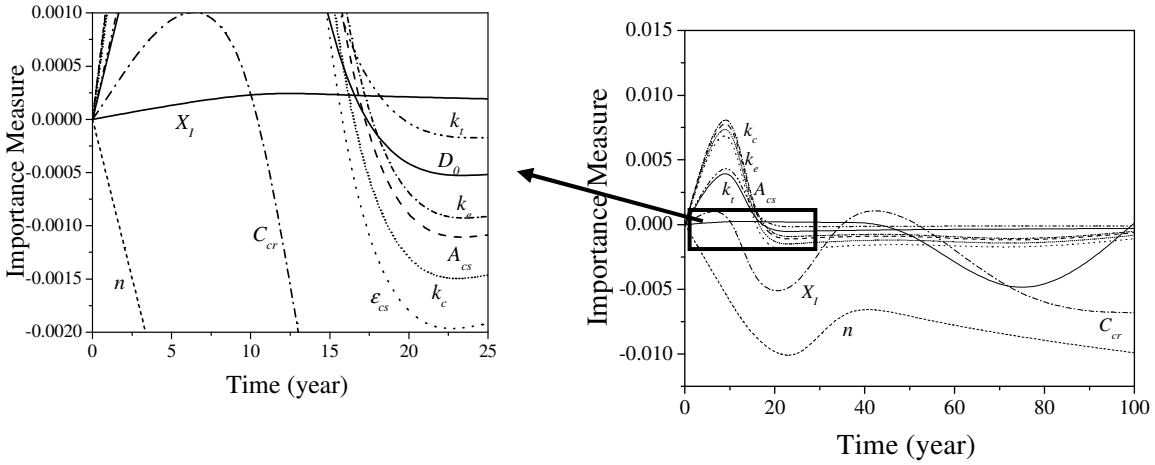

(a) Drift failure mode

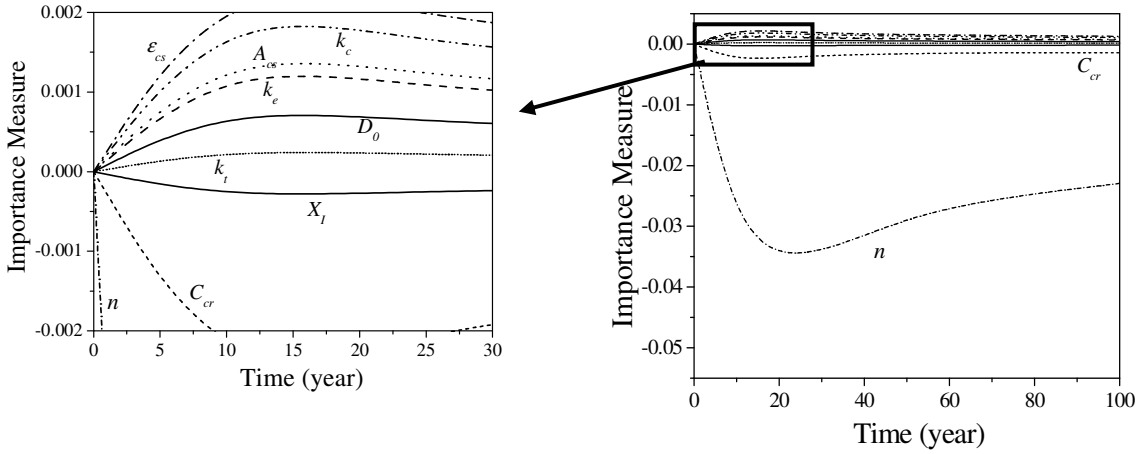

(b) Shear failure mode

Fig. 4-8. Importance measures of the diffusion model random variables parameters for the drift (top) and shear (bottom) failure mode, S_a =2.8

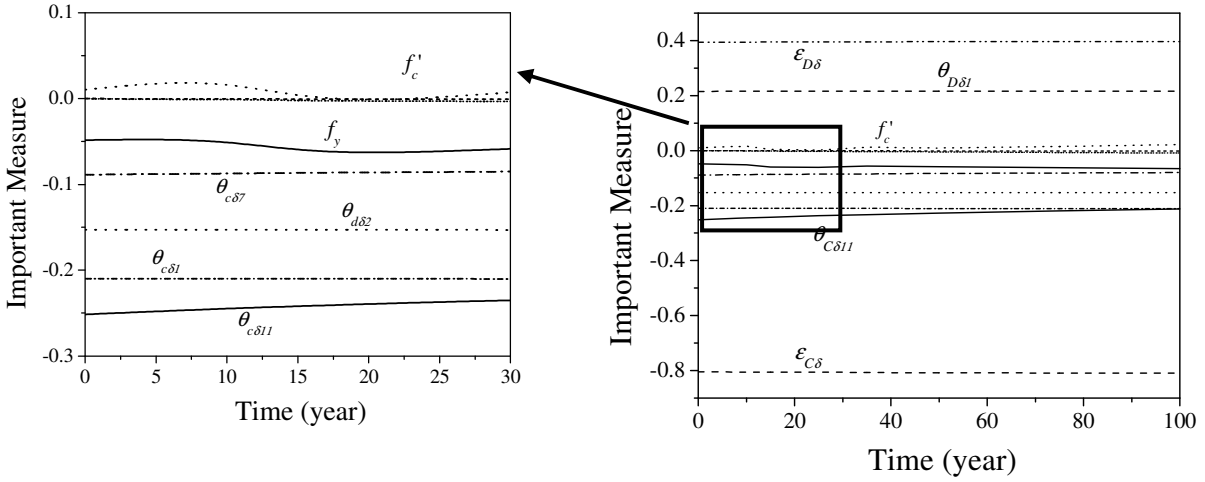

(a) Drift failure mode

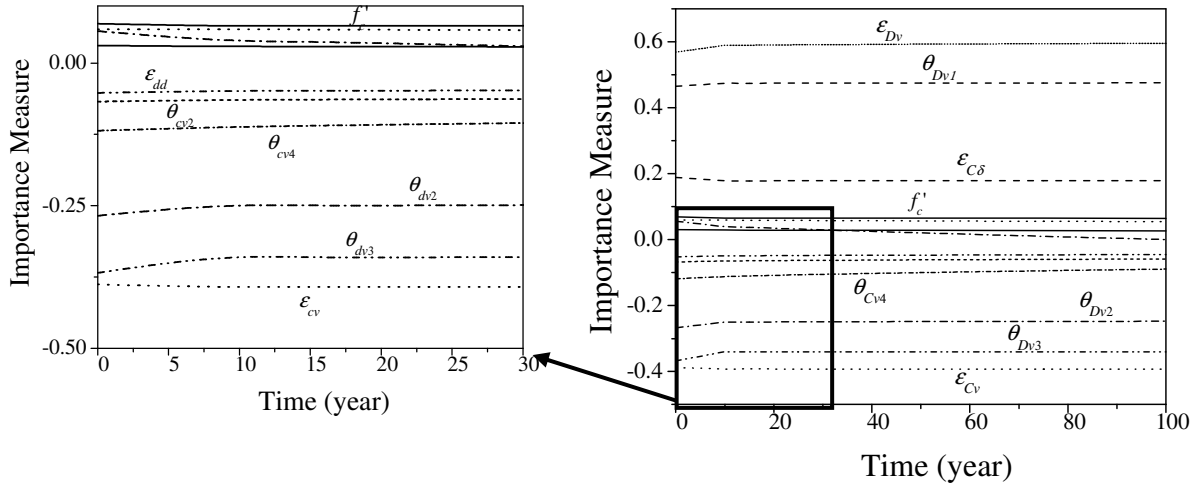

(b) Shear failure mode

Fig. 4-9. Importance measures of the structural random variables parameters for the drift (top) and shear (bottom) failure mode, S_a =2.8

The presented models and methodology are applied to an example bridge structure. Fragility estimates are obtained and a parameter sensitivity study is undertaken. Interestingly, it is observed that the presence of corrosion alters the

reliability sensitivities over time. For the pristine bridge it is observed that for both the drift and shear failure modes the transverse reinforcement carries significant importance. The results show that for the shear failure mode the sensitivity with respect to the longitudinal reinforcement keeps increasing over time, while that in the drift failure mode is decreasing. It is also observed that the importance of the randomness in the physical parameter are more influenced by corrosion than the importance of the model parameters.

CHAPTER V

FRAGILITY INCREMENT FUNCTIONS FOR CORRODING REINFORCED CONCRETE BRIDGE COLUMN

The increased deformation and shear fragilities of corroding reinforced concrete (RC) bridge columns are modeled as functions of time using fragility increment functions. These functions can be applied to various environmental and material conditions by means of controlling parameters that corresponds to the specific condition. For each model of failure, the fragility of a deteriorated column at any given time is obtained by simply multiplying the initial fragility of the pristine/undeteriorated column by the function developed in this research. The developed increment functions account for the effects of the time-dependent uncertainties that are present in the corrosion model as well as in the structural capacity models. The proposed formulation provides a useful tool in engineering practice in that the fragility of deteriorated columns is obtained without any extra reliability analysis once the fragility of the pristine column is known. The fragility increment functions are expressed as functions of time t and a given deformation or shear demand. Unknown parameters involved in the models are estimated using a Bayesian updating framework. A model selection is conducted during the assessment of the unknown parameters using the Akaike Information Criterion (AIC) and the Bayesian Information Criterion (BIC). For the estimation of the parameters, a set of data is obtained by FORM (First-Order Reliability Method) analysis using existing probabilistic capacity models for corroding RC bridge column. Example fragilities of a

deteriorated bridge column typical of current California's practice are presented to demonstrate the developed methodology. The increment functions suggested in this research can be used to assess the time-variant fragility for application to life-cycle cost analysis and risk analysis.

Introduction

A large number of the bridges in U.S. have been recorded as losing their structural capacity while providing transportation of people, products and vehicles. Of the approximately 600,000 bridges in the U.S., 343, 000 bridges are made of conventional or pre-stressed reinforced concrete (RC) and 15 % of the bridges are structurally deficient primarily due to corrosion of steel and steel reinforcement. Methods to predict remaining service life of a concrete structure or element subject to corrosion have been developed considering the material deterioration (Clifton and Knab 1989), the consequent loss of structural capacity, and the reduced reliability (Mori and Ellingwood 1993; Enright and Frangopol 1998a,b; Dura-Crete 2000; Vu and Stewart 2000). In particular, a significant effort has been made to adopt a probabilistic approach to account for the uncertainties involved in the mechanical and chemical properties of the deteriorating structure.

Several studies tried to assess the reliability of deteriorating bridges. In particular, Clifton and Knab (1989) suggested a deterioration function to model the material deterioration of underground concrete structures . The mathematical modeling is based on the chemistry and physics of the deterioration processes of concrete. Mori

and Ellingwood (1993) used the material deterioration function developed by Clifton and Knab (1989) and introduced a function that describes the loss of structural capacity to compute the time-varying reliability of RC bridges. However, while introducing the concept of a deterioration function, they did not assess its parameters. Enright and Frangopol (1998a) assessed a deterioration function for the loss of flexural strength due to corrosion for a specific set of environmental and material conditions. However, the formulation cannot be used for different environmental and material conditions and the parameters are specific to the considered structure. The developed model was used by Enright and Frangopol (1998b) to investigate the effects of the structural deterioration on the time-variant reliability of bridge beams. However, their formulation does not account for the increasing uncertainty over time that is accounted for in this research. Li and Melchers (2005) developed a deterioration function as a stochastic process with a mean function and a coefficient of variation function. While considering the increasing uncertainty of the capacity degradation over time, the reliability analysis neglected the increasing uncertainty. Furthermore, the function developed by Li and Melchers is still limited to specific material and environmental conditions.

For the practical use in engineering applications, it is desirable to have a capacity deterioration function that is general and can be used for different environmental conditions and material properties. Furthermore, the reliability should account the increasing uncertainty over time. Finally, using a degradation function, a reliability analysis has to be performed at each considered time using the newly calculated capacity to obtain the fragility of a deteriorating RC bridge.

In this research, I focus on RC bridge columns and I develop a fragility increment function that is generalized to different combination of material and environmental conditions, improving the previous efforts in terms of efficiency and accuracy. The increment function, $G_F(t)$, is defined as a ratio of the fragility of the deteriorating column at time t, $F(t)$, and the fragility of the prestine/undeteriorated column at the time of construction $F(0)$, that is $G_F(t) = F(t)/F(0)$. Using $G_F(t)$, the fragility of deteriorating structure is obtained as $F(t) = G_F(t)F(0)$. The fragility in this study is defined as the conditional probability of failure given a corresponding demand. The deformation and the shear failure modes are considered. The proposed function is expressed as a function of time t and the given deformation, D_δ, or shear , D_v, demands. While the previous studies focused on the ratio of capacity describing capacity deterioration, the proposed fragility increment describes directly the increase in the fragility. This approach reduces the computational cost by providing the fragility at any time of interest without any additional reliability analysis. Furthermore, the function $G_F(t)$ also accounts for the effects of the time-variant uncertainty.

The fragility increment function is modeled reflecting the mathematical properties of diagnostic fragility curves and satisfying the boundary conditions. Then, the unknown parameters involved in the models are estimated by a Bayesian approach. To select the most parsimonious and efficient model, a model selection process is used for the parameter estimation using the Akaike Information Criterion (AIC) (Akaike 1978a,b) and the Bayesian Information Criterion (BIC) (Schwarz 1978) as the selection

criteria. The data used to estimate the parameter distributions are obtained using the probabilistic capacity models for corroding RC columns developed by Choe et al. (2007). Fragilities of an example bridge column are obtained using the developed increment function, $G_F(t)$. A comparison shows that the fragilities obtained using $G_F(t)$ are in close agreement with those assessed carrying out a traditional reliability analysis.

The four sections that are provided in this chapter cover: (i) the concept of fragility increment function, (ii) the modeling of the increment function, which is conducted by modeling the fragility of pristine column, extending into the time-dependent fragility of deteriorated column, taking the friction of the fragilities, and testing the mathematical properties to satisfy boundary conditions, (iii) the parameter estimation, which includes the Bayesian updating parameter estimation and the model selection process using the criteria of AIC and BIC , and (iv) the results of the studies in previous section and the fragility estimation using the model developed in this study.

Fragility Increment Function

The fragility increment function, $G_F(t)$, is defined as a ratio between the fragility at time t, $F(t)$, and the fragility of the pristine column, $F(0)$. In general, the fragility of a pristine column can be written as the conditional probability $F = P\{C_0 - D \le 0 \mid D\}$, where C_0 is the structural capacity of the pristine column and D is a specified demand level. The time-variant fragility $F(t)$ of a deteriorating structure can then be written as

$F(t) = P\{C(t) - D \le 0 \mid D\}$, where $C(t)$ denotes the time-variant structural capacity of the deteriorating system.

A number of studies have been conducted to approximate $C(t)$ rather than focusing on $P(t)$, which is the quantity of ultimate interest and is the goal of this research. To estimate $F(t)$, previous studies have focused on modeling $C(t)$. In this case, the time-variant fragility can obtained by carrying out a reliability analysis at each time t. To obtain the time-variant capacity $C(t)$, a degradation function $G_C(t)$ is typically introduced and defined as a ratio between the time-variant capacity and the initial capacity, $G_C(t) = C(t)/C(0)$. Given $C(0)$, the capacity at any given time, $C(t)$, can be compute as $C(t) = G_C(t)C(0)$. The fragility can then be computed as $F(t) = P\{G_C(t)C(0) - D \le 0 \mid D\}$. Based on the previous research by Clifton and Knab (1989), Mori and Ellingwood (1993) introduced the degradation function $G_C(t) = 1 - \alpha_1 t^{\alpha_2}$, where α_1 and α_2 are two constant parameters, to assess the impact of the resistance degradation on the reliability. Similarly, Enright and Frangopol (1998a) used the formulation proposed by Mori and Ellingwood to assess the effects of structural degradation due to corrosion on the time-variant reliability of RC bridge beam. In their analysis, Enright and Frangopol assumed $\alpha_2 = 1$, which leads to a linear $G_C(t)$. They assessed the unknown parameter k using experimental data given one specific exposure condition and a specific set of material properties. As a further simplification, Enright and Frangopol assumed the value of the corrosion initiation time. These functions do not consider the actual environmental and material conditions that affect the corrosion

process. Enright and Frangopol (1998b) extended the original function to $G_C(t) = 1 - \alpha_1 t + \alpha_2 t^2$, where α_1 and α_2 are two constant parameters. However, the time-variant reliability neglected the uncertainty in $G_c(t)$. In addition to these limitations, while $G_C(t)$ provides a convenience way to compute $C(t)$, a reliability analysis is still needed to obtain the fragility $F(t)$ at every time t.

Neglecting the effects of the time-varying uncertainties present in the corrosion model and in the structural capacity models may cause an error in the fragility estimates as shown in Fig. 5-1. The top two plots in Fig. 5-1 display the capacity degradation with constant variance (left) and with the time-dependent variance considered in this study (right). The top-left plot shows a time-dependency in the mean capacities but the distribution around the means has a constant variance over time. However, in reality, the uncertainties keep growing with time due to the uncertainties in the corrosion process and result in wider ± 1 standard deviation bounds as shown in the top-right plot. Assuming that a given demand is less than the mean capacity, it is noted that the fragility in top-left diagram is underestimated because the growing model uncertainty is neglected. Conversely, if a given demand is higher than the mean capacity, not considering the time-dependency of the variance leads to an overestimated fragility. The two bottom plots in Fig. 5-1 present the fragility of a deteriorating structure for each case (on the left and considering constant or time-dependent uncertainty on the right.) The bottom-left plot shows the change over time of in the fragility curve in the case of constant variance. The fragility only shifts to the left. The bottom-right plot shows the change in the shape of the fragility curve that occurs when considering the increased

uncertainties. It is seen that there is a larger slope in the fragility (higher left tail and lower right tail) in addition to the shift to the left already discussed.

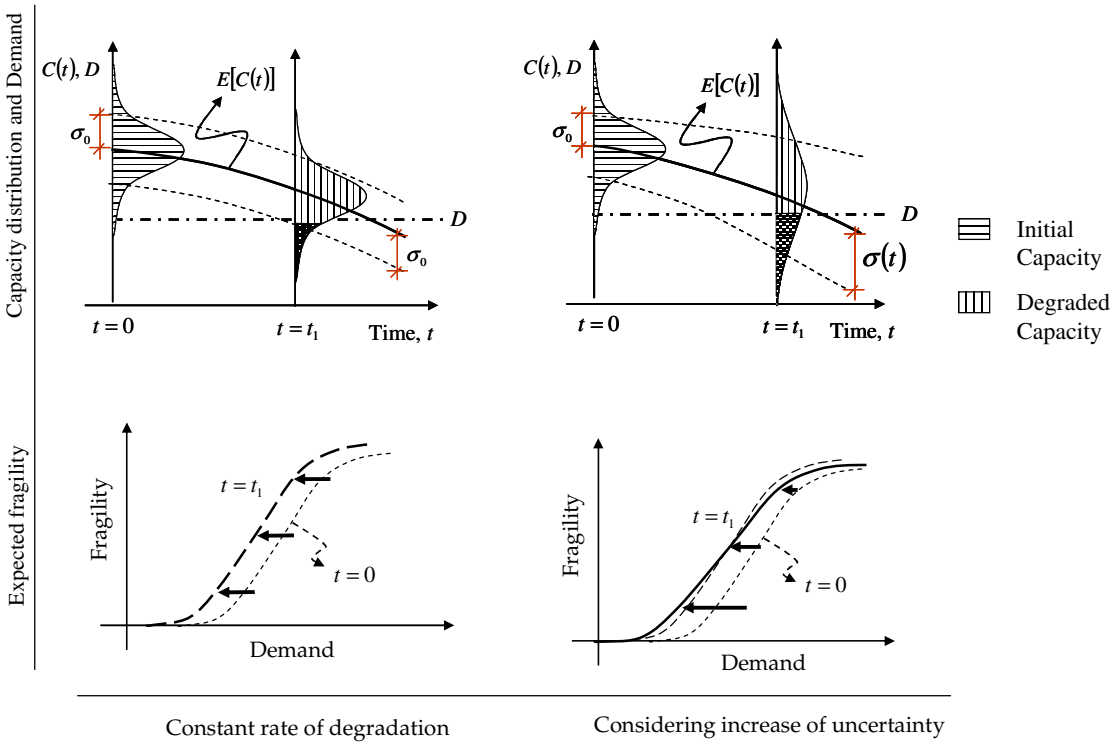

Fig. 5-1. The expected degradation in structural capacity (top) and fragility change (bottom)

In this research, I develop a fragility increment function expressed as a ratio of fragility at time t to the fragility of initial construction, $G_F(t) = F(t)/F(0)$. This function can be applied to various environmental and material conditions by means of controlling parameters that corresponds to the specific condition. The fragility of deteriorated columns at any given time is obtained by simply multiplying the initial fragility without extra reliability analyses, once the fragility at the initial construction is

known. Table 5-1 shows the range of environmental and material conditions that the function developed in this study is applicable to.

The proposed function $G_F(t)$ includes the effects of time-variant uncertainty by explicitly considering this effect in its mathematical formulation and by using sets of fragility data that are estimated considering the time-variant uncertainties contained in corrosion initiation and propagation models, and in the capacity model. The function developed in this research will be expressed as a function of time t and a given demand D.

Table 5-1. Range of the environmental and material conditions that the suggested functions are applicable to

w/c	Environmental Condition	Curing Condition	Humidity
0.4~0.5	Submerged Tidal Splash Atmospheric	1 day~28 days	Constantly saturated Constantly humid or many humid-dry cycles

Modeling

In this research I consider two modes of failure, deformation and shear. The fragility increment function for the k th failure mode is then expressed as

$$G_{F,k} = G_{F,k}\left(\mathbf{x}, t, D_k, \boldsymbol{\Theta}_k\right) \qquad k = \delta, v \tag{5-1}$$

where $k = \delta$ indicates the deformation failure mode and $k = v$ indicates the shear failure mode; $\mathbf{x}$ is the vector of environmental and material properties; D_k indicated the given

demand level; and $\boldsymbol{\Theta}_k$ denotes the sets of the unknown parameters introduced to fit the proposed models to fragility data.

In assessing the unknown parameters $\boldsymbol{\Theta}_k$, the model needs to satisfy the homoskedasticity and normality assumptions. That is the model standard deviation needs to be independent of t and D_k, and the model error needs to have the Normal distribution. These assumptions are approximately satisfied by employing a suitable transformation of each increment data. By investigating the possible transformations and diagnostic plots, I employ the logarithmic transformation. Eq. (5-1) is then rewritten as

$$\log\left[G_{F,k}\left(\mathbf{x},t,D_k,\boldsymbol{\Theta}_k\right)\right]=\log\left[\hat{G}_{F,k}\left(\mathbf{x},t,D_k,\boldsymbol{\theta}_k\right)\right]+\sigma_k\varepsilon \tag{5-2}$$

σ_k represents the standard deviation of the model error $\sigma_k\varepsilon$, ε is a Normally distributed random variable with zero mean and unit variance, and $\hat{G}_{F,k}$ is use to model $F_k(t)/F_k(0)$ as a function the environmental and material conditions, $\mathbf{x}$, and can be written as the ration between the models for the fragility of the deteriorating and the pristine fragilities, $\hat{F}_k(t)/\hat{F}_k(0)$.

Fragility of Pristine and Deteriorating RC Bridge Columns: $\hat{F}_{k0}(D_k)$ ***and*** $\hat{F}_k(t,D_k)$

The model in Eq. (2) is fitted using fragility data for pristine and deteriorating columns. The fragility data for pristine columns are obtained following Gardoni et al. (2002) and Choe et al. (2007a). The fragility data for deteriorating columns are obtained following Choe et al. (2007b) and considering different environmental and material conditions.

The reliability analyses to obtain the fragility data are carried out using a First Order Reliability Analysis (FORM) (Ditlevsen and Madsen 1996).

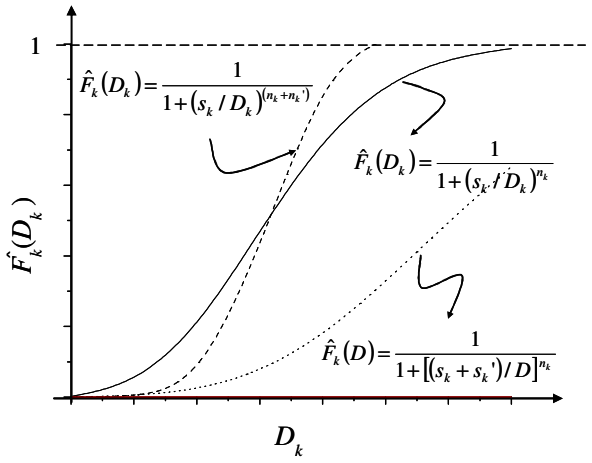

Fig. 5-2. Properties of the logistic function: original shape (solid line), change in shape due to an increment in s_k (dotted line) and change in shape due to an increment in n_k (dashed line).

The generated data show that the fragilities of pristine columns follow an S-shape. To model this shape, I considered several candidate functions. Based on its flexibility and simplicity, I selected the logistic function:

$$\hat{F}_k\left(D_k\right)=\frac{1}{1+\left(s_k/D_k\right)^{n_k}} \tag{5-3}$$

Fig. 5-2 displays the properties of the curve in Eq. (5-3). Based on the mathematical properties of this type of function, the parameter n_k controls only the slope of the curve and the parameter s_k characterizes both of the shift and slope of curve. The parameters

s_k and n_k can be obtained by regression using the fragility curves of pristine bridge column. Also the fragility of the deteriorating column follows an S-shape. Therefore, to model $\hat{F}_k(t, D_k)$ I develop correction terms for the parameters s_k and n_k of $\hat{F}_{k0}(D_k)$.

As discussed earlier, it is expected that fragility curves of the corroding columns have both a shift to the left and a change in slope. The shift along with the horizontal axis corresponds to the degradation of the mean capacity and the change of slope is caused by the effects of time-variant uncertainty. To capture these effects, I introduce two correction terms, $R_{s,k}$ and $R_{n,k}$. The controlling parameters s_k and n_k are the replaced by $s_k - R_{s,k}$ and $n_k - R_{n,k}$ respectively to write the fragility of deteriorating columns as

$$\hat{F}_k(t, D_k) = \frac{1}{1 + \left\{ \left[s_k - R_{s,k}(t) \right] / D_k \right\}^{n_k - R_{n,k}(t)}} \tag{5-4}$$

Since the parameter s_k is the only parameter to control the shift, $R_{s,k}$ describes the mean capacity degradation of the deteriorating column. To model $R_{s,k}$, I assume that the degradation of mean capacity is expressed as a function of the loss of steel diameter due to corrosion. Choe et al. (2007b) derived the expression $1.0508\left[(1 - w/c)/d\right]^{-1.64}(t - T_{corr})^{0.71}$ for the loss of the reinforcement diameter for $T_{corr} < t \le T_f$, where T_{corr} is the corrosion initiation time and T_f is the time when the diameter of reinforcement, in theory, reaches zero. This expression is based on the time-dependent corrosion rate function developed by Vu and Stewart (2000), where w/c is water-to-cement ratio, d is the concrete cover depth, and T_{corr} is the time to corrosion

initiation. Following Choe et al. (2007b), T_f is computed as $T_{corr} + d_{bi}\{d / [1.0508\,(1-w/c)^{-1.64}]\}^{1/0.71}$, where d_{bi} is the initial bar diameter at time $t = 0$. The correction term $R_{s,k}$ is then written as $R_{s,k}(t) = \theta_{k,1}\left[(1-w/c)/d\right]^{\theta_{k,2}}(t-T_{corr})^{\theta_{k,3}}$. Since a model for T_{corr} involves several other random variables, to simplify the equation, I introduce the expression of the time to initiation of the capacity degradation as $T_G = \theta_{k,4}\hat{T}_{corr}$ and replace T_{corr} with T_G, where $\hat{T}_{corr}$ is the point estimator of corrosion initiation time T_{corr} computed at the mean value of the input parameters and $\theta_{k,4}$ primarily accounts for the variability around $\hat{T}_{corr}$. However, due to the correlation between the parameters, $\theta_{k,4}$ might also reflect other sources of variability that influence $R_{s,k}(t)$. The correction term $R_{s,k}$ can be finally written as

$$R_{s,k}(t) = \begin{cases} \theta_{k,1}\left(\dfrac{1-w/c}{d}\right)^{\theta_{k,2}}\left(t-\theta_{k,4}\hat{T}_{corr}\right)^{\theta_{k,3}} & T_G < t \le T_f \\ R_{s,k}(T_f) & t > T_f \end{cases} \tag{5-5}$$

Since the parameter n_k controls the slope the logistic function, I used it to model the effect of the increasing uncertainty over time. The correction term $R_{n,k}$ is written as

$$R_{n,k}(t) = \theta_{5,k}\,t^{\theta_{6,k}} \tag{5-6}$$

Fragility Increment Functions: $\hat{G}_{F,k}(\mathbf{x},t,D_k,\boldsymbol{\theta}_k)$

According to the definition of the fragility increment function, the model $\hat{G}_{F,k} = \hat{F}_k(t)/\hat{F}_k(0)$ is modeled as

$$\hat{G}_{F,k}\left(\mathbf{x},t,D_k,\boldsymbol{\theta}_k\right)=\begin{cases}1 & t<T_G\\ \dfrac{1+\left(s_k/D\right)^{n_k}}{1+\left\{\left[s_k-R_{s,k}\left(t\right)\right]/D\right\}^{\left[n_k-R_{n,k}(t)\right]}} & t\geq T_G\end{cases} \tag{5-7}$$

Fig. 5-3(a) shows the shape of developed function in Eq. (5-7) in the 3-dimensional space of $D_k - t - \hat{G}_{F,k}(t,D_k)$. Figs. 5-3(b) and (c) compare the developed function (on the left) with calculated values using a set of example fragilities (on the right). The example fragility is obtained assuming the column is made of the concrete mixture $w/c = 0.5$ with 1 day of curing time and in submerged exposure condition, i.e., the lower part of the column is permanently under the sea-water level. For this illustration purpose, the deformation mode of failure was considered.

The curve projected onto the $t - \hat{G}_{F,k}(t,D_k)$ plane can be written as $\hat{G}_{F,k}(t)$ assuming a constant demand D (Fig. 5-3(b)). The asymptotic limit of $\hat{G}_{F,k}(t)$ for $t \to \infty$ is $L_k = 1 + (s_k / D_k)^{n_k}$. The curve agrees with the example data shown in right hand side.

Now, I look at the dependence of $\hat{G}_{F,k}$ on D_k. For each demand values $D_k = D_{k,1}, D_{k,2}, D_{k,3} \cdots$, the vertical upper limit L_k is written as $L_{k,1} = 1 + (s_k / D_{k,1})^{n_k}$, $L_{k,2} = 1 + (s_k / D_{k,2})^{n_k}$, $L_{k,3} = 1 + (s_k / D_{k,3})^{n_k}$. Therefore, the upper limit in the 3-D of $D_k - \hat{G}_{F,k}(D_k)$ plane can be written as $L_k(D_k) = 1 + (s_k / D_k)^{n_k}$ as shown in Fig. 5-3(c), comparing with the observed example data.

I introduce an additional parameter $\theta_{k,7}$ into Eq. (5-7) to capture a possible difference in the (functional) order of corrosion propagation and degradation of the structural capacity. Therefore the final suggested form is the following:

$$\hat{G}_{F,k}\left(\mathbf{x}, t, D_k, \boldsymbol{\theta}_k\right) = \begin{cases} 1 & t < T_G \\ \left[\dfrac{1 + \left(s_k / D\right)^{n_k}}{1 + \left\{ \left[s_k - R_{s,k}(t) \right] / D \right\}^{\left[n_k - R_{n,k}(t) \right]}} \right]^{\theta_k} & t \geq T_G \end{cases} \tag{5-8}$$

Parameter Estimation

The unknown parameters $\boldsymbol{\Theta}_k$ in the proposed models are assessed with a Bayesian approach using data generated following Choe et al. (2007b). In assessing $\boldsymbol{\Theta}_k$, a model selection process is carried out to identify unimportant terms in the proposed model and select a parsimonious one (with as few unknown parameter as possible). In this section, I describe how the data are generated, the Bayesian parameter estimation, and the model selection process.

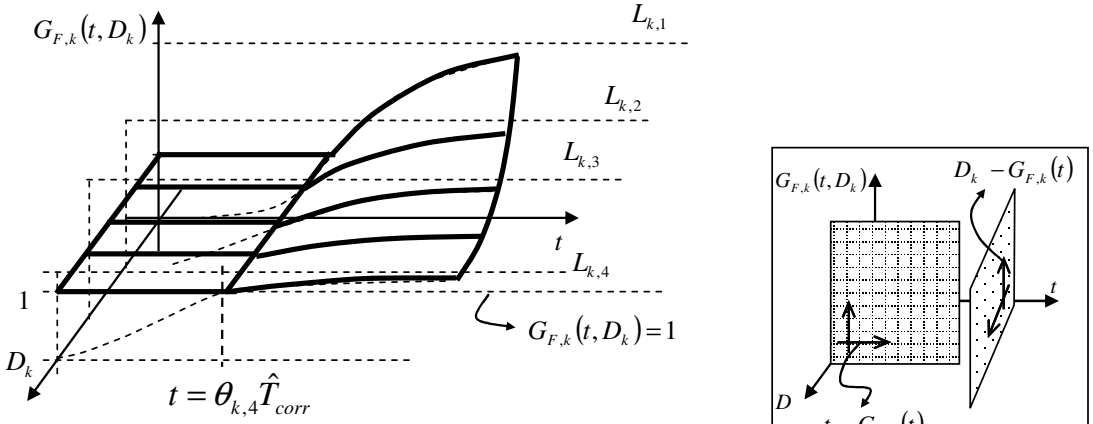

(a) Function Surface in $D_k - t - G_{F,k}(t)$

(b) $t - G_{F,k}(t)$

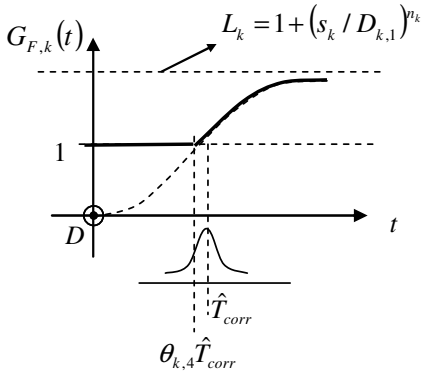

<Developed function >

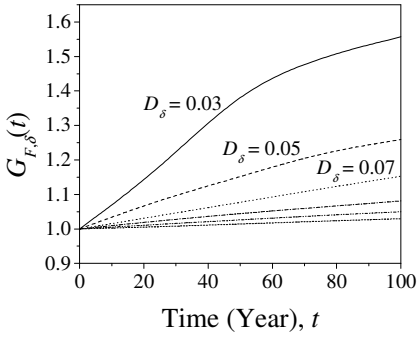

<Observed data>

(c) $D_k - G_{F,k}(D_k)$

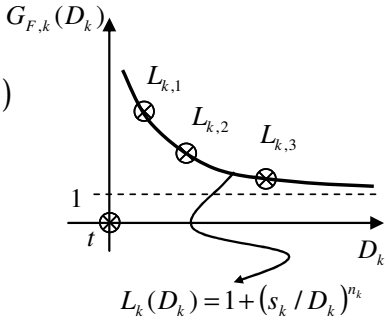

<Developed function >

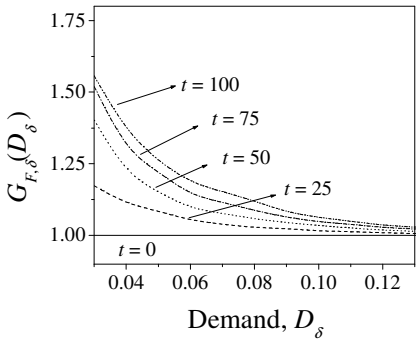

<Observed data>

Fig. 5-3. Mathematical property of developed function, $\hat{G}_{F,k}(t, D_k)$

Fragility Data for the Assessment of $\boldsymbol{\Theta}_k$

The model parameters $\boldsymbol{\Theta}_k$ are assessed using fragility data for pristine and deteriorating columns. The fragility data for pristine columns are obtained following Gardoni et al. (2002) and Choe et al. (2007a). The fragility data for deteriorating columns are obtained following Choe et al. (2007b) and considering the environmental and material conditions shown in Table 5-1 that include different combinations of chloride exposure conditions, environmental oxygen availabilities, water-to-cement ratios, and curing conditions. The reliability analyses to obtain the fragility data are carried out using a First Order Reliability Analysis (FORM). A total of 581 data points for each failure mode are considered and form the vector $\mathbf{G}_k$.

Choe et al. (2007b) developed a probabilistic capacity models for corroding RC columns considering the model uncertainties in both the capacity and corrosion models, in addition to the uncertainties in the environmental conditions, material properties, and structural geometry. The capacity at time t is written as

$$C_k\left(\mathbf{x},t,\boldsymbol{\Theta}_{C,k}\right)=\int_0^\infty C_k\left(\mathbf{x},t,\boldsymbol{\Theta}_{C,k}\left|T_{corr}\right.\right)\cdot f_{T_{corr}}\left(t_{corr}\right)dT_{corr} \qquad k=\delta,v \tag{5-9}$$

where $C_k(\mathbf{x},t,,\boldsymbol{\Theta}_{C,k}\,|\,T_{corr})$ is the capacity for failure mode k for a given corrosion initiation time, and $f_{T_{corr}}(t_{corr})$ is the probability density function (PDF) of the corrosion initiation time T_{corr}, written as (Dura-Crete 2000)

$$T_{corr} = X_I \cdot \left[\frac{d^2}{4k_e k_t k_c D_C (t_0)^n} \left[erf^{-1}\left(1 - \frac{C_{cr}}{C_s}\right) \right]^{-2} \right]^{\frac{1}{1-n_a}} \tag{5-10}$$

where d is the cover depth of the reinforcement, k_e is an environmental factor, k_t represents the influence of test methods to determine the empirical diffusion coefficient D_C, k_c denotes a parameter that accounts for the influence of curing, t_0 is the reference period for D_C, n_a is the age factor, X_I is a model uncertainty coefficient to account for the idealization implied in Fick's second law, C_s is the chloride concentration on the surface, C_{cr} is the critical chloride concentration, and $erf(\cdot)$ is the error function. This model is also used to obtain the time to degradation initiate $T_G = \theta_{k,4}\hat{T}_{corr}$ in Eqs. (5-6) and (5-8). Appendix 1 shows the mean value of each parameter corresponding to each material and exposure conditions.

Bayesian Updating Parameter Estimation

To estimate the unknown parameters $\boldsymbol{\Theta}_k$, I employ a Bayesian approach using of the updating rule (Box and Tiao 1992)

$$f(\boldsymbol{\Theta}_k) = \gamma L(\boldsymbol{\Theta}_k | \mathbf{G}_k)\, p(\boldsymbol{\Theta}_k) \tag{5-11}$$

where $p(\boldsymbol{\Theta}_k)$ is the prior distribution of $\boldsymbol{\Theta}_k$ that reflects our previous knowledge about $\boldsymbol{\Theta}_k$, $L(\boldsymbol{\Theta}_k | \mathbf{G}_k)$ is the likelihood function representing the objective information on $\boldsymbol{\Theta}_k$ in the fragility data $\mathbf{G}_k$, γ is a normalizing factor, and $f(\boldsymbol{\Theta}_k)$ is the posterior

distribution reflecting our updated knowledge on $\boldsymbol{\Theta}_k$. Since no prior information is available about $\boldsymbol{\Theta}_k$, I used a non-informative prior distribution employing formulas provided by Box and Tiao (1992).

Model Selection

Ideally, the fragility increment function $\hat{G}_{F,k}(\mathbf{x}, t, D_k, \boldsymbol{\theta}_k)$ should be accurate, unbiased, and easily implementable in practice. In addition, as a statistical consideration, a model should be parsimonious (as few parameters $\theta_{k,i}$ as possible) to avoid (1) loss of precision of the estimates of the parameters and of the overall model due to the inclusion of unimportant terms, and (2) overfitting the data.

All current model selection methods are categorized in two classes based on their statistical performance and objectives (Burnham 2002). The first class of the methods is based on the concept that no "true mode" exists because the truth is very complex. Therefore, the selection criteria for this class are aimed at estimating the approximate true model. Akaike Information Criterion (*AIC*) is one of the well known criteria in this class. It was developed to select a parsimonious model for the analysis of empirical data by Akaike (1978a,b). *AIC* provides a trade-offs between the model complexity and the quality of the fit of the data. The *AIC* can be written as

$$AIC = -2\log\left[L\left(\boldsymbol{\Theta}_k \middle| \mathbf{G}_k\right)\right] + 2N_P \tag{5-12}$$

where N_P is the number of unknown parameters included in $\boldsymbol{\Theta}_k$.

The second class of criteria has been developed based on the assumption that an exactly "true mode" exists. This assumption implies that the dimension (number of unknown parameter) and the true model form are fixed as the sample size increases. Under this assumption, these criteria provide consistent estimator of the model dimension, N_P. A consistent estimator is derived so that the probability to select the "true mode" approaches 1 when the sample size goes to infinity, $N_S \to \infty$. These criteria are refer to as "constant" or "dimension-constant" criteria. Schwarz (1978) provides a Bayesian argument for adopting the Bayesian Information Criterion (*BIC*), which is one of the best known "constant" criteria. The *BIC* penalizes the unknown parameters in terms of $N_P \log(N_S)$ that is in general a stronger penalty than the $2N_P$ used in *AIC*. The expression for *BIC* is written as

$$BIC = -2\log\left[L\left(\boldsymbol{\Theta}_k \middle| \mathbf{G}_k\right)\right] + N_p \log\left(N_S\right) \tag{5-13}$$

BIC is known to perform well especially for generated data and for large sample size of data (Burnham 2002). In this research, I use both *AIC* and *BIC* for the model selection. The selected model has the minimum values of *AIC* and *BIC*.

In addition to these selection criteria, I compute the mean absolute percentage error (*MAPE*) to have a more intuitive measure of the accuracy of the candidate models. The *MAPE* is the mean error in the model expressed as a percent of the FORM value. *MAPE* is written as:

$$MAPE = \frac{1}{N_S}\left[\sum_{i=1}^{N_S}\left(\frac{\left| \hat{G}_{F,k}(\mathbf{x},t,D_k,\boldsymbol{\theta}_k) - G_{F,k,i}\right|}{G_{F,k,i}} \right)\right]\times 100 \tag{5-14}$$

where $\hat{G}_{F,k}(\mathbf{x},t,D_k,\boldsymbol{\theta}_k)$ is the fragility increment using the developed function and $G_{F,k,i}$ is the fragility increment obtained by the observed data and $\hat{G}_{F,k}(\mathbf{x},t,D_k,\boldsymbol{\theta}_k)$ is the fragility increment by the developed function. The obtained results are discussed in the following section.

Results

In this section, I show the results of the parameter estimation and model selection. Five candidate models are presented and used in the selection process. The application of the fragility increment function is presented using an example bridge column with selected environment and material conditions.

Fragility Increment Functions

Table 5-2 displays the candidate models considered in this research. Model A is the full model presented in Eq. (5-8). Model B neglects the model correction $\theta_{k,7}$. Model C ignores both the effect of $\theta_{k,7}$ and the randomness in T_{corr} associated to $\theta_{k,4}$. Model D is generated from Model C neglecting the effect of the increasing model uncertainty with time (i.e., $\theta_{k,5}$ and $\theta_{k,6}$ are neglected). Model E neglects both the effects of the randomness of T_{corr}, $\theta_{k,4}$, and the mean capacity degradation ($\theta_{k,1}$, $\theta_{k,2}$, and $\theta_{k,3}$).

Table 5-2. Candidate models of fragility increment function.

Model	Parameters	Model: $\hat{G}_{F,k}(t,D)$ at $(t \geq T_G)$	Note
A	$\theta_{k,1},\theta_{k,2},\cdots\theta_{k,7},\sigma_k$	$\left[\frac{1+(s_k/D)^{n_k}}{1+\left\{\left[s_k-R_{s,k}(t)\right]/D\right\}^{\left[n_k-R_{n,k}(t)\right]}}\right]^{\theta_7}$	a,c
B	$\theta_{k,1},\theta_{k,2},\cdots\theta_{k,6},\sigma_k$	$\frac{1+(s_k/D)^{n_k}}{1+\left\{\left[s_k-R_{s,k}(t)\right]/D\right\}^{\left[n_k-R_{n,k}(t)\right]}}$	a,c
C	$\theta_{k,1},\theta_{k,2},\theta_{k,3},\theta_{k,5},\theta_{k,6},\sigma_k$	$\frac{1+(s_k/D)^{n_k}}{1+\left\{\left[s_k-R^*_{s,k}(t)\right]/D\right\}^{\left[n_k-R_{n,k}(t)\right]}}$	b,c
D	$\theta_{k,1},\theta_{k,2},\theta_{k,3},\sigma_k$	$\frac{1+(s_k/D)^{n_k}}{1+\left\{\left[s_k-R_{s,k}(t)\right]/D\right\}^{n_k}}$	a
E	$\theta_{k,5},\theta_{k,6},\sigma_k$	$\frac{1+(s_k/D)^{n_k}}{1+(s_k/D)^{\left[n_k-R_{n,k}(t)\right]}}$	b

a: $R_{s,k}(t)=\theta_{k,1}\left(\frac{1-wc}{d}\right)^{\theta_{k,2}}\left(t-\theta_{k,4}\hat{T}_{corr}\right)^{\theta_{k,3}}$

b: $R^*_{s,k}(t)=\theta_{k,1}\left(\frac{1-wc}{d}\right)^{\theta_{k,2}}\left(t-\hat{T}_{corr}\right)^{\theta_{k,3}}$

c: $R_{n,k}(t)=\theta_{k5}t^{\theta_{k6}}$

Table 5-3. Model selection criteria for candidate models

	Model	N_P	*AIC*	$\Delta_{i,AIC}$	*BIC*	$\Delta_{i,BIC}$	*MAPE*
$G_{F,\delta}(t,D_\delta)$	A	8	−1162	0	−1128	0	0.0130
	B	7	−1096	65	−1066	61	0.0144
	C	6	−1062	99	−1037	91	0.0146
	D	4	552	1714	569	1697	0.0631
	E	3	829	1992	842	1971	0.0868
$G_{F,v}(t,D_v)$	A	8	111	0	145	0	0.0320
	B	7	470	359	500	354	0.0353
	C	6	489	377	514	368	0.0578

Table 5-4. Posterior statistics of the parameters, $G_{F,\delta}$ (deformation failure mode)

	$\theta_{\delta,1}$	$\theta_{\delta,2}$	$\theta_{\delta,3}$	$\theta_{\delta,4}$	$\theta_{\delta,5}$	$\theta_{\delta,6}$	$\theta_{\delta,7}$	σ_{δ}
Mean	5.50E-09	–3.16	0.938	0.809	0.020	0.667	0.380	0.021
St. dev.	0.057	0.030	0.029	0.020	0.003	0.028	0.020	0.001
Correlation coefficients								
$\theta_{\delta,1}$	1.00	0.50	–0.29	0.34	–0.42	0.40	0.02	–0.24
$\theta_{\delta,2}$	0.50	1.00	0.60	0.20	0.059	–0.06	0.07	–0.41
$\theta_{\delta,3}$	–0.29	0.60	1.00	–0.11	0.33	–0.18	–0.40	-0.26
$\theta_{\delta,4}$	0.34	0.20	–0.11	1.00	–0.57	0.509	0.18	–0.25
$\theta_{\delta,5}$	–0.42	0.06	0.33	–0.57	1.00	–0.94	0.060	0.03
$\theta_{\delta,6}$	0.40	–0.06	–0.18	0.509	–0.94	1.00	–0.38	–0.06
$\theta_{\delta,7}$	0.02	0.07	–0.40	0.18	0.06	–0.38	1.00	0.04
σ_{δ}	–0.24	–0.41	–0.26	–0.25	0.03	–0.06	0.04	1.00

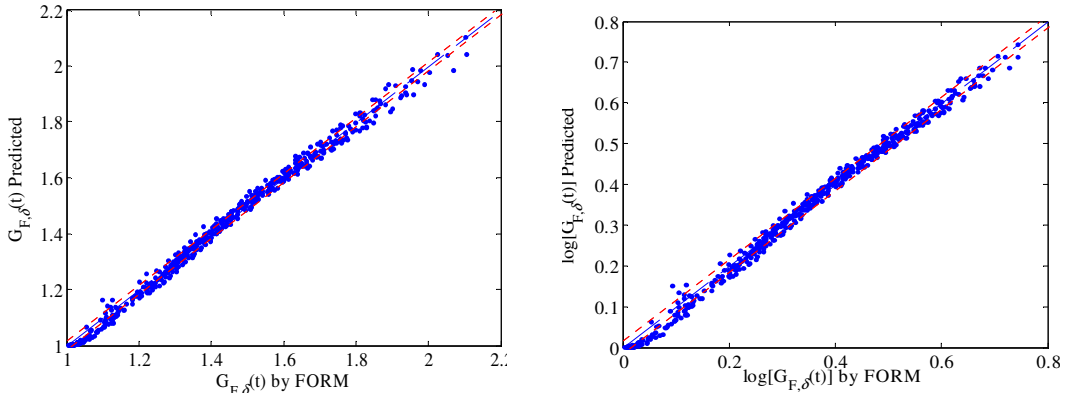

Fig. 5-4. Comparison between the predicted fraglity using the function developed and the results of FORM analysis : deformation failure (Model A)

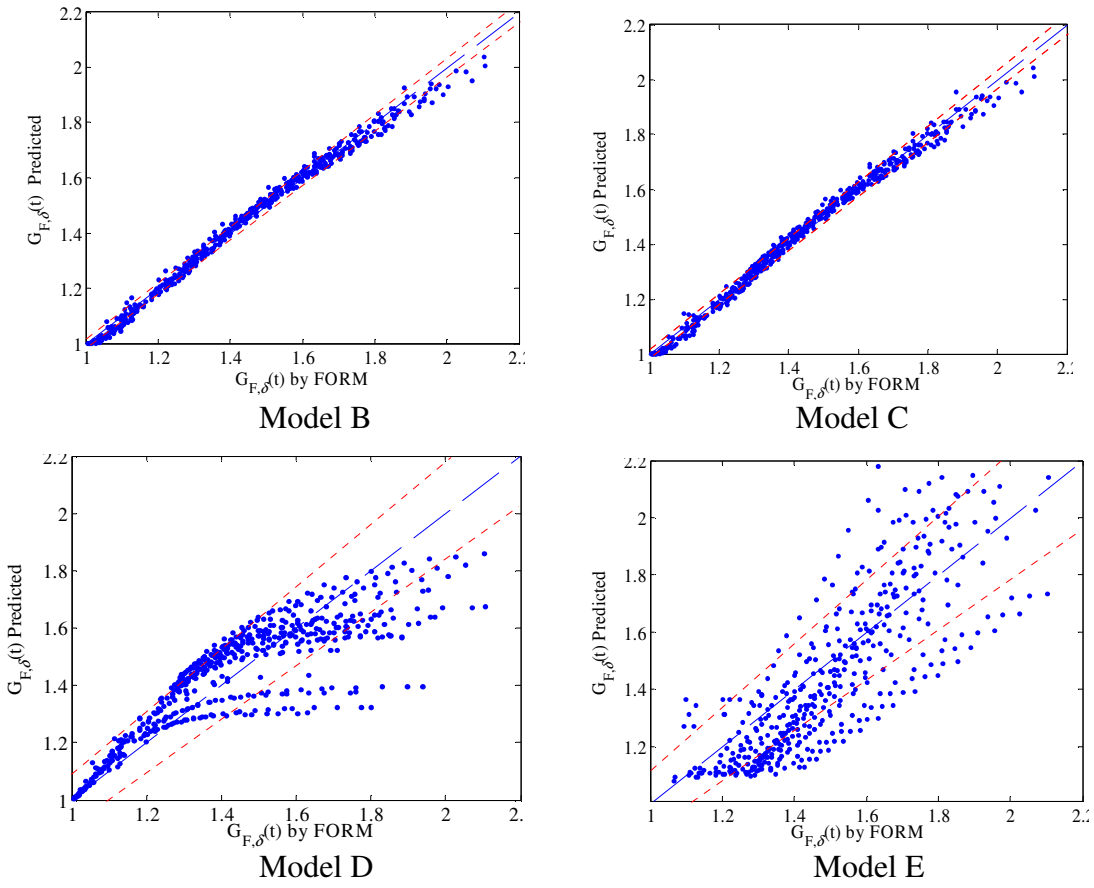

Fig. 5-5. Model selection process, deformation failure

Table 5-3 shows the values of *AIC*, *BIC* and *MAPE* for the candidate models. I introduce the relative measure of the criteria Δ_i. With i candidate models, differences, Δ_i, of *AIC* and of *BIC* are defined as $\Delta_{i,AIC} = AIC_i - AIC_{\min}$ and $\Delta_{i,BIC} = BIC_i - BIC_{\min}$ with respective.

For the deformation failure mode, I select Model *A* since it has the smallest AIC, BIC, and *MAPE* values (Table 5-3). Based on the *MAPE* value, on average Model *A* has

an error of 1.30% over 581 data points. Fig. 5-4 shows comparisons between the the median predicted inceremt function $\hat{G}_{F,\delta}(t, D_\delta)$ using the developed function and the results of FORM analysis in original space (left) and in log-scaled space (right), for the selected Model *A*. A perfect model would line up along the 1:1 line (dashed line). The figure also shows the +/− 1 standard deviation σ_k. Fig. 5-5 show the predictions based on Models *B*-*E*. Models *B* and *C* give a relatively good fit with a MAPE of 1.44% and 1.46%. However, they show a nonlinearity in the plot, which suggests that one or more parameters might be missing. Models *D* and *E* show a significantly worse fits than Model *A*, displaying both larger variances as well as nonlinearities in the residuals. Table 5- 4 lists the posterior distribution of parameters in the selected Model *A* for deformation failure mode.

Table 5-5. Posterior statistics of the parameters, $G_{F,v}$ (shear failure mode)

	$\theta_{v,1}$	$\theta_{v,2}$	$\theta_{v,3}$	$\theta_{v,4}$	$\theta_{v,5}$	$\theta_{v,6}$	$\theta_{v,7}$	σ_v
Mean	2.90E-05	−1.37	0.423	1.29	1.27	0.161	0.801	0.053
St. dev	1.45E-06	0.016	0.014	0.012	0.055	0.007	0.011	0.002
Correlation coefficients								
$\theta_{v,1}$	1.00	0.19	−0.37	0.29	−0.02	0.17	0.05	−0.01
$\theta_{v,2}$	0.19	1.00	0.82	−0.64	0.15	−0.48	0.07	−0.08
$\theta_{v,3}$	−0.37	0.82	1.00	−0.62	0.28	−0.64	0.06	−0.06
$\theta_{v,4}$	0.29	−0.64	−0.62	1.00	0.44	0.00	−0.21	0.07
$\theta_{v,5}$	−0.02	0.15	0.28	0.44	1.00	−0.89	−0.34	0.04
$\theta_{v,6}$	0.16	−0.48	−0.64	0.00	−0.89	1.00	0.28	−0.01
$\theta_{v,7}$	0.05	0.07	0.06	−0.21	−0.34	0.28	1.00	−0.05
σ_v	−0.01	−0.08	−0.06	0.07	0.04	−0.01	−0.05	1.00

As for the deformation failure mode, also for the shear mode of failure, Model *A* is selected as the preferable model based on *AIC, BIC* and *MAPE*. Fig. 5-6 show a comparison between the median predicted inceremt function $\hat{G}_{F,v}(t, D_v)$ based on selected Model *A* and the fragility increment function obtained using FORM analaysis. Fig. 5-7 shows the predicted values versus the FORM data for the rejected candidate models. Models *B* and *C* show a good fit but are not as accurate as Model *A*. The assessment of Models *D* and *E* does not reach convergence. The lack of convergence may be explained by the fact that Models *D* and *E* are too far from the true model. Table 5-5 lists the posterior statistics of parameters for Model *A* of shear failure.

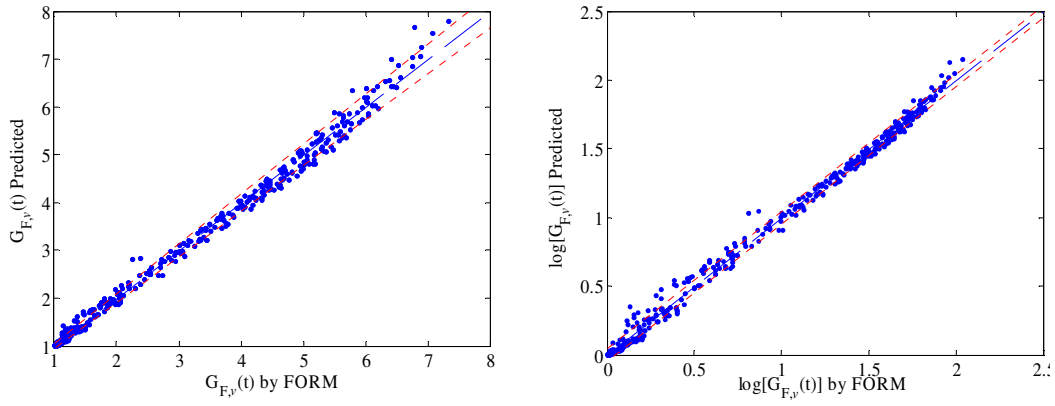

Fig. 5-6. Comparison between the predicted fraglity using the function developed and the results of FORM analysis : shear failure(Model A)

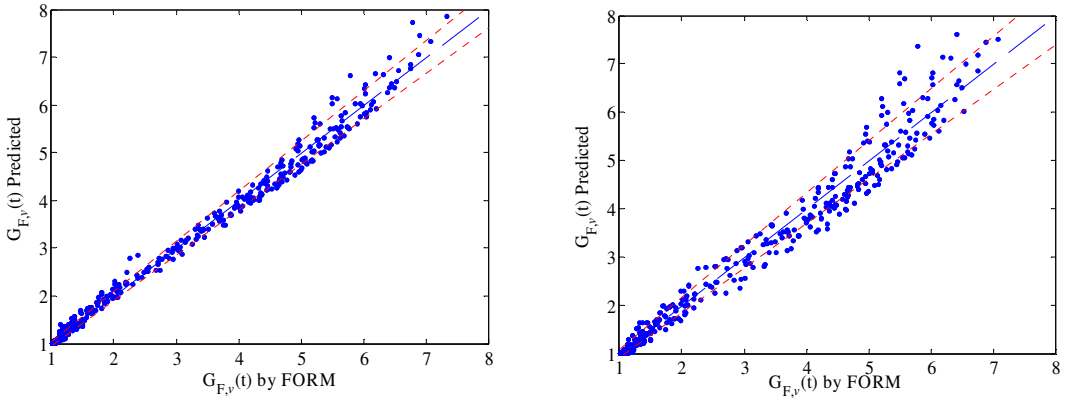

Fig. 5-7. Model selection process, shear failure

Fragility Estimation

The developed fragility increment functions $\hat{G}_{F,k}(\mathbf{x},t,D_k,\boldsymbol{\theta}_k)$ are used to obtain the fragility curves for an example RC column. I compare the predicted fragility with the results of FORM analysis. To compute the fragility at time t using $\hat{G}_{F,k}(\mathbf{x},t,D_k,\boldsymbol{\theta}_k)$, the required inputs are $\hat{F}_k(0)$, and the environmental and material conditions of the bridge column. The fragility $\hat{F}_k(0)$ is obtained by reliability analysis (in this case FORM analysis). The fragility of corroding column at time t is obtained as $F_k(t)=\hat{G}_{F,k}(\mathbf{x},t,D_k,\boldsymbol{\theta}_k)\times F_k(0)$. The fragility increment function $\hat{G}_{F,k}(\mathbf{x},t,D_k,\boldsymbol{\theta}_k)$ is compute using Eq. (5-8), where the correction terms $R_{s,k}$ and $R_{n,k}$ are compute using Eqs. (5-5) and (5-6).

The example corroding RC column has the material property and the geometry that are typical of currently constructed highway bridge columns in California (Naito 2000). To compute the pristine fragility $\hat{F}_k(0)$, the structural geometry and material properties are assumed as following: the column has a nominal cover thickness of 59 mm, pristine longitudinal reinforcement ratio $\rho_l = 0.0199$, gross diameter $D_g = 1520$ mm, ratio of gross to core diameter $D_g / D_c = 1.07$, and clear height $H = 9140$ mm. The yield stress of longitudinal reinforcement f_y is assumed to be a lognormal random variable with mean 475 MPa and 0.05 coefficient of variation (COV), the volumetric transverse reinforcement f_{yh} is assumed to be a lognormal random variable with mean 493 MPa and 0.05 COV, and the compressive strength of concrete f_c' is assumed to be a random variable lognormally distributed with mean 35.8 MPa and 0.1 COV.

To compute $\hat{G}_{F,k}(\mathbf{x}, t, D_k, \boldsymbol{\theta}_k)$, the column is assumed to be made of the concrete mixture with $w/c = 0.5$ with 1-day of curing time and is under constantly saturated atmospheric conditions and submerged exposure condition. These conditions are selected because they are the most extreme for corrosion. The parameters s_k and n_k are obtained by regression analysis using the initial fragility $\hat{F}_k(0)$. The estimated parameters are $n_k = 4.05$, $s_k = 0.0798$ for the deformation mode, and $n_k = 8.70$, $s_k = 0.711$ for the shear mode. The parameters $\boldsymbol{\theta}_k$ are listed in Tables 5-4 and 5-5 for deformation and shear modes, respectively.

Figs. 5-8 and 5-9 show the fragility of the example bridge column for drift and shear failure mode, respectively. The dotted line represents the fragility of the pristine column computed using FORM. The dashed line shows the fragility of the example column after 100 years. The solid line show the fragility computed with the developed fragility increment function, also at 100 years. Both for the deformation and shear failure modes, only negligibly differences can be seen between the fragilities computed using $\hat{G}_{F,k}(\mathbf{x}, t, D_k, \boldsymbol{\theta}_k)$ and using FORM, especially for lower demand values, which is the range of interest for civil engineering applications. For high demand values, using the developed increment functions provides a smaller estimate of the fragility than FORM analysis. This agrees with the results of the model fit shown in Figs. 5-4 and 5-6, where the values of $\hat{G}_{F,k}$ close to 1 tend to be smaller than the FORM data.

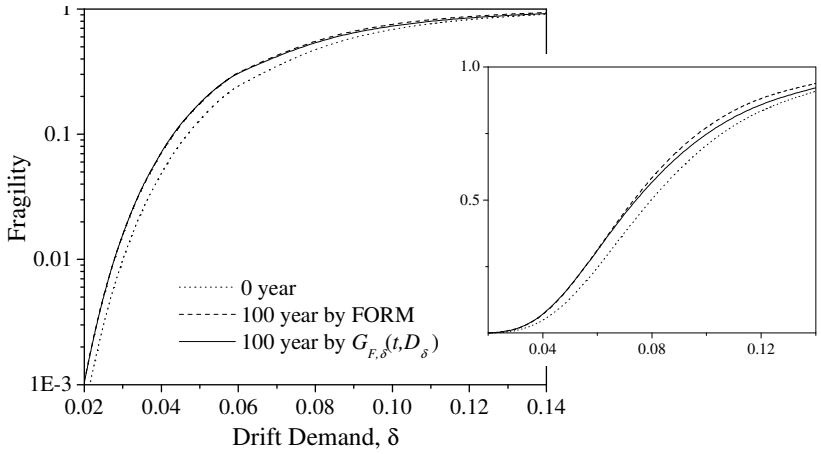

Fig. 5-8. Fragility of example submerged bridge column, $w/c = 0.5$, curing time 1 day and constantly humid atmospheric condition: deformation failure mode.

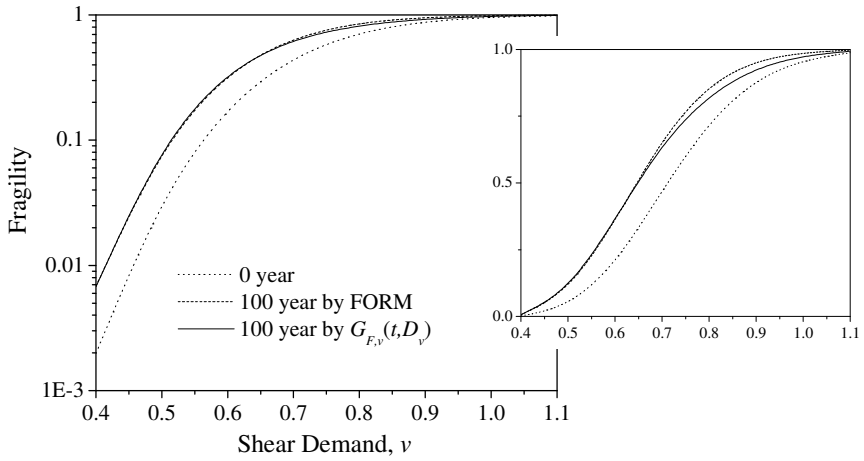

Fig. 5-9. Fragility of example submerged bridge column, $w/c = 0.5$, curing time 1 day and constantly humid atmospheric condition: shear failure mode.

Conclusion

Fragility increment functions are developed for determining the fragility of corroding RC bridge column. Deformation and shear failure models are considered. The developed increment functions provide estimates of the fragility at the time of interest without conducting a reliability analysis simply based on the fragility of the pristine/non-deteriorated bridge column. The increment functions are applicable to various environmental and material conditions. Their formulation satisfies the mathematical boundary conditions and the shape reflecting the sets of observed data. The formulation includes the effects of the capacity degradation as well as the time-variant uncertainty in corrosion process. A model selection process based on the Akaike Information Criterion

and the Bayesian Information Criterion is used to identify the most parsimonious model for the fragility increment function. The considered criteria show that it is important to account for both the capacity degradation and the effect of the increasing uncertainty over time. The developed models fit the data obtained by FORM analysis with a 1.30% and 3.20% average error for the deformation and shear modes, respectively. This research contributes to the assessment of accurate fragilities for corroding RC columns. The proposed approach reduces the computational cost compared to any reliability analysis. The function suggested in this research can be used to assess the time-variant fragility for application to life-cycle cost analysis and risk analysis.

CHAPTER VI

SUMMARY

My doctoral research has focused on the seismic reliability of deteriorating RC bridges. I employed a Bayesian methodology to develop probabilistic capacity models based on experimental data. To model the time-variant deterioration of the structural performance of RC bridges, probabilistic capacity and demand models for corroding bridges were developed. The probabilistic models objectively assessed the seismic fragilities of deteriorating bridges considering various environmental exposure conditions and the resulting corrosion-induced deterioration process. The models consider uncertainties in the measured parameters, the environmental conditions, as well as model uncertainty included in both structural and corrosion models. To facilitate the use in practice, the increased deformation and shear fragilities of corroding RC bridge columns were modeled using fragility increment functions as functions of time, environmental and material conditions. The models are applicable for various environmental and material conditions. The parameters in the fragility increment functions were estimated using a Bayesian updating framework.

I expect to extend the fragility increment function developed in this doctoral research to also consider seismic demands. In this case, the fragility increment will be modeled as a function of time, environmental and material conditions, and the earthquake spectral acceleration.

The results of this research can be of direct value to those making decisions about structural safety, condition assessment, residual life, and the ability of existing RC bridges to withstand future earthquakes.

REFERENCES

Akaike, H. (1978a). "A new look at the Bayes procedure." *Biometrika*, 65, 53–59.

Akaike, H. (1978b). "A Bayesian analysis of the minimum AIC procedure." *Annals of the Institute of Statistical Mathematics*, 30, 9–14.

Ambartzumian, R. V., Der Kiureghian, A. , Oganian, V. K., and Sukiasian, H. S. (1998). "Multinormal probability by sequential conditioned importance sampling: Theory and application." *Probab. Engrg. Mech.*, 13(4), 299-305.

Bjerager, P. and Krenk, S. (1989). "Parameter sensitivity in first order reliability theory." *Journal of Engineering Mechanics*, 115(7), 1577-1582.

Box, G. E. P., and Tiao, G. C. (1992). *Bayesian inference in statistical analysis,* Addison–Wesley, Reading, Mass.

Box, G.E.P., Cox, D. R. (1964). "An analysis of transformations with discussion." *Journal of the Royal Statistical Society*, Series B, 26, 211–252.

Burnham, K.P. (2002). *Model selection and multimodel inference: A practical information-theoretic approach*, 2nd ed., Springer, New York.

Caltrans (1999: ed. 1.1). *Seismic Design Criteria*, California Department of Transportation, Berkeley.

Choe, D., Gardoni, P., and Rosowsky, D. (2007a). "Closed-form fragility estimates parameter sensitivity and bayesian updating for RC columns." *Journal of Engineering Mechanics* ASCE, 133(7), 833-843.

Choe, D., Gardoni, P., Rosowsky, D., and Haukaas, T. (2007b). "Probabilistic capacity models and fragility estimates for corroding reinforced concrete columns." *Reliability Engineering and System Safety* (Special Issue), doi:10.1016/j.ress. 2006.12.015.

Chopra, A. K. and Goel, R. K. (1999). "*Capacity-demand-diagram methods for estimating seismic deformation of inelastic structures: SDF systems*." California: Report Number PEER-1999/02, Pacic Earthquake Engineering Research Center, University of California, Berkeley.

Clifton, J.R. , Knab, L.I. (1989). *Service life of concrete*, Division of Engineering, Office of Nuclear Regulatory Research, U.S. Nuclear Regulatory Commission, Gaithersburg, MD.

Der Kiureghian, A., and Ke, J.-B. (1995). "Finite-element based reliability analysis of frame structures." *Proceedings of ICOSSAR '85, 4th International Conference on Structural Safety and Reliability*, Kobe, Japan, 1, 395-404.

Ditlevsen, O., and Madsen, H. O. (1996). *Structural reliability methods*, Wiley, New York.

Dura-Crete (2000). *Statistical Quantification of the Variables in the Limit State Functions,* The European Union Brite EuRam 3 contract BRPR-CT95-0132 Project BE95-1347 Report no BE95-1347/R7 May 2000.

Enright, M.P., Frangopol, D.M. (1998a). "Service-life prediction of deteriorating concrete bridges." *Journal of Structural Engineering*, 124(3), 309-317.

Enright, M.P., Frangopol, D.M. (1998b). “Probabilistic analysis of resistance degradation of reinforced concrete bridge beams under corrosion.” *Engineering Structures*, 20(11), 960-971.

Fajfar, P. (2000). “A nonlinear analysis method for performance-based seismic design.” *Earthq. Spectra* 16(3): 573~592.

Fang C, Lundgren K, Chen L, Zhu C. (2004). "Corrosion influence on bond in reinforced concrete." *Cement and Concrete Research,* 34(11), 2159-2167.

FEMA. (1997). “Guidelines for the seismic rehabilitation of buildings.” *FEMA 273*, National Earthquake Hazard Reduction Program, Washington, D.C.

Gardoni, P. (2002). *Probabilistic models and fragility estimates for bridge components and systems*. Ph.D. Dissertation, University of California, Berkeley.

Gardoni, P., Der Kiureghian, A., and Mosalam, K. M. (2002). “Probabilistic capacity models and fragility estimates for RC columns based on experimental observations.” *J. Engrg. Mech., ASCE* 128(10), 1024-1038.

Guiasu, S. (1977). *Information theory with applications*. McGraw-Hill, New York, NY.

Haukaas, T. and Der Kiureghian, A. (2004). “Finite element reliability and sensitivity methods for performance-based earthquake engineering.” Report No. PEER 2003/14, Pacific Earthquake Engineering Research Center, University of California, Berkeley.

Haukaas, T. and Der Kiureghian, A. (2005). ”Parameter sensitivity and importance measures in nonlinear finite element reliability analysis.” *Journal of Engineering Mechanics*, 131(10), 1013-1026.

Hohenbichler, M., and Rackwitz, R. (1983). “First-order concepts in system reliability.” *Structural Safety*, 1(3), 177-188

Li, C.Q., Melchers, R.E. (2005). "Time-dependent risk assessment of structural deterioration caused by reinforcement corrosion." *ACI Structural Journal*, 102(5), 754-762.

Liu, Y., Weyers, R.E. (1998). “Modeling the time-to-corrosion cracking in chloride contaminated reinforced concrete structures.” *ACI Materials Journal* 95(6), 675-681.

Mackie, K. and Stojadinovic, B. (2001). “Probabilistic seismic demand model for California highway bridges.” *J. Bridge Engrg.* ASCE 6(6), 468~481.

McKenna, F. and Fenves, G. L. (2000). “An object-oriented software design for parallel structural analysis.” *Proceedings of the 2000 Structures Congress and Exposition Advanced Technology in Structural Engineering,* Philadelphia, PA.

Moehle, J.P., Lynn, A.C., Elwood, K., Sezen, H. (1998). “Gravity load collapse of reinforced concrete frames during earthquakes.” *Proceedings of the 1st U S - Japan Workshop on Performance-Based Design Methodology for Reinforced Concrete Building Structures*, Maui, Hawaii.

Moehle, J.P., Elwood, K., and Sezen, H. (2000). “Shear failure and axial load collapse of existing reinforced concrete columns.” *Proceedings, Second U.S.-Japan Workshop on Performance-Based Design Methodology for Reinforced Concrete Building Structures*, Sapporo, Japan, 241-255.

Moehle, J.P., Lynn, A.C., Elwood, K., and Sezen, H. (1999). “Gravity load collapse of reinforced concrete frames during earthquakes.” *Proceedings, First U.S.-Japan Workshop on Performance-Based Design Methodology for Reinforced Concrete Building Structures*. Maui, Hawaii, 175-189

Mori, Y., Ellingwood, B. (1993). “Reliability-based service-life assessment of aging concrete structures.” *Journal of Structural Engineering*, ASCE, 199(5), 1600-1621.

Naito, C.J. (2000). *Experimental and computational evaluation of reinforced concrete beam-column connections for seismic performance*, Ph. D. Dissertation, University of California Berkeley.

Priestley, M.J.N., Seible, F., and Calvi, G.M. (1996). *Seismic design and retrofit of bridges*, John Wiley & Sons, Inc., New York, NY.

Schwarz, G. (1978). “Estimating the dimension of a model.” *Annals of Statistics*, 6(2), 461-464.

Stewart, M.G., Rosowsky, D.V. (1998). "Structural safety and serviceability of concrete bridges subject to corrosion." *Journal of Infrastructure Systems ASCE,* 4(4):146–155.

Thoft-Christensen, P., Jensen, F.M., Middleton, C.R. (1997). *Blackmore A. assessment of the reliability of concrete slab bridges reliability and optimization of structural systems,* D.M. Frangopol, R.B. Corotis, and R. Rackwitz (eds) Pergamon, Oxford, 321-328.

Tuutti K. (1982). *Corrosion of steel in concrete*. Swedish Cement and Concrete Research Institute, Stockholm.

Vu, K.A.T. and Stewart, M.G. (2000). “Structural reliability of concrete bridges including improved chloride-induced corrosion models.” *Structural Safety*, 22(4), 313–333.

Wang, X., Liu, X. (2004). "Modeling bond strength of corroded reinforcement without stirrups." *Cement and Concrete Research,* 34(8), 1331-1339.

Yashinsky, M. and Ostrom, T. (2000). “Caltrans' new seismic design criteria for bridges.” *Earthq. Spectra* 16(1), 285~307.

APPENDIX

Parameter distribution of corrosion initiation model (Dura-Crete 2000)

D_o: Reference diffusion coefficient at t_0 =28_{day}

Condition	Distribution	Mean[mm^2/yr]	St. dev.[10^{-12} m^2/s]
w/c=0.4	Normal	220.9	25.4
w/c=0.45	Normal	315.6	32.5
w/c=0.5	Normal	473	43.2

n: Aging factor

Condition	Distribution	Mean	St. dev.	A	B
All	Beta	0.362	0.245	0	0.98

k_e: Environmental correction factor

Condition	Distribution	Mean	St. dev.
Submerged	Gamma	0.325	0.223
Tidal	Gamma	0.924	0.155
Splash	Gamma	0.265	0.045
Atmospheric	Gamma	0.676	0.114

k_c: Curing time correction factor

Condition	Distribution	Mean	St. dev.	A	B
curing 1day	Beta	2.4	0.7	1.0	4.0
curing 3day	Beta	1.5	0.3	1.0	4.0
curing 7day	Deterministic	1.0			
curing 28day	Beta	0.8	0.1	0.4	1.0

k_t : correction factor for tests

Condition	Distribution	Mean	St. dev.
All	Normal	0.832	0.024

C_{cs}: chloride surface concentration (linear function of A_{cs} and ε_{cs}, % by weight of binder)

Condition	Distribution	A_{cs}		ε_{cs}	
		Mean	St. dev.	Mean	St. dev.
Submerged	Normal	10.348	0.714	0	0.58
Tidal	Normal	7.758	1.36	0	1.105
Splash	Normal	7.758	1.36	0	1.105
Atmospheric	Normal	2.565	0.356	0	0.405

C_{cr}: critical chloride content (mass-% of binder)

	w/c ratio	Distribution	Mean	St. dev.

Constantly saturated	0.30	Normal	2.30	0.20
	0.40	Normal	2.10	0.20
	0.50	Normal	1.60	0.20
Constantly humid or many humid-dry cycles	0.30	Normal	0.50	0.10
	0.40	Normal	0.80	0.10
	0.50	Normal	0.90	0.15

X_I : modeling uncertainty

Condition	Distribution	Mean	St. dev.
All	Lognormal	1	0.05

VITA

Do-Eun Choe received her Bachelor of Engineering in Architectural Engineering, Inha University, Korea in 2000. She received her Master of Science degree in Architectural Engineering (Structural Engineering), Inha University, Korea in 2002. She entered the Zachry Department of Civil Engineering program at at Texas A&M University in September 2003 and received her Doctor of Philosophy degree in December 2007. Her research interests include structural reliability and modeling deteriorating RC bridge.

Ms. Choe may be reached by her email at dnchoe@gmail.com or mail to 8655 Jones Rd. #2227, Houston TX 77065.